

**THE STUDY AND CHARACTERIZATION OF THE NANO-  
ENCAPSULATION OF CLOTRIMAZOLE INTO N-PHTHANOYL  
CHITOSAN-g-mPEG SELF ASSEMBLY**




**A THESIS SUBMITTED IN PARTIAL FULFILLMENT  
OF THE REQUIREMENTS FOR  
THE DEGREE OF MASTER OF SCIENCE IN PHARMACY  
(PHARMACEUTICS)  
FACULTY OF GRADUATE STUDIES  
MAHIDOL UNIVERSITY  
2007**

**COPYRIGHT OF MAHIDOL UNIVERSITY**

Copyright by Mahidol University

Thesis  
Entitled

**THE STUDY AND CHARACTERIZATION OF THE NANO-  
ENCAPSULATION OF CLOTRIMAZOLE INTO N-PHTHANOYL  
CHITOSAN-g-mPEG SELF ASSEMBLY**



*Supa Kotcha*

Miss Supa Kotcha  
Candidate

*Korbtham Sathirakul*

Assoc. Prof. Korbtham Sathirakul,  
Ph.D. (Biopharmaceutics Pharmacokinetics)  
Major-Advisor

*Suwabun Chirachanchai*

Assoc. Prof. Suwabun Chirachanchai,  
Ph.D. (Applied Fine Chemistry)  
Co-Advisor

*M.R. Jisnuson Svasti*

Prof. M.R. Jisnuson Svasti,  
Ph.D.  
Dean  
Faculty of Graduate Studies

*Ampol Mitrevej*

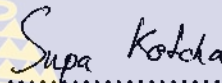
Prof. Ampol Mitrevej,  
Ph.D. (Pharmaceutics)  
Chair  
Master of Science in Pharmacy  
Programme in Clinical Pharmacy  
Faculty of Pharmacy

Thesis  
Entitled

**THE STUDY AND CHARACTERIZATION OF THE NANO-  
ENCAPSULATION OF CLOTRIMAZOLE INTO N-PHTHANOYL  
CHITOSAN-g-mPEG SELF ASSEMBLY**

was submitted to the Faculty of Graduate Studies, Mahidol University  
For the degree of Master of Science in Pharmacy (Pharmaceutics)

on  
May 25, 2007



.....

Miss Supa Kotcha  
Candidate



.....

Assist. Prof. Gaysorn Chansiri,  
Ph.D. (Pharmaceutics)  
Chair



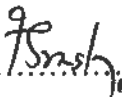
.....

Assoc. Prof. Suwabun Chirachanchai,  
Ph.D. (Applied Fine Chemistry)  
Member



.....

Assoc. Prof. Korbtham Sathirakul,  
Ph.D. (Biopharmaceutics Pharmacokinetics)  
Member



.....

Prof. M.R. Jisnuson Svasti,  
Ph.D.  
Dean  
Faculty of Graduate Studies  
Mahidol University



.....

Prof. Ampol Mitrevej,  
Ph.D. (Pharmaceutics)  
Dean  
Faculty of Pharmacy  
Mahidol University

## ACKNOWLEDGEMENTS

I would like to deeply thank the various people who, during the several months in which this endeavor lasted, provided me with useful and helpful assistance. Without their care and consideration, this thesis would likely not have matured.

First, I wish to express my deepest gratitude and appreciation to my major advisor, Associate Professor Dr. Korbtham Sathirakul for his valuable advice guidance, great attention, kindly support, creativity and assistance with consultant encouragement throughout the study. And for all his patience throughout an editing and cross-reviewing process which constitutes a rather difficult balancing act. Most importantly, his gracious given to me will always be recognized throughout my life. This thesis will never be accomplished without his.

Second, I am deeply grateful to Associate Professor Dr. Suwabun Chirachanchai, my co-advisors for his helpful guidance, suggestion, comment and recommendation. I am impressed by his kindness so much. And I am very thankful to Assistant Professor Dr. Gaysorn Chansiri for her advice and correction of this thesis and also for being member of my thesis committee.

Third, my special thanks give to Chantiga Choochottiros for her advising the technique of thermal analysis, NMR and available the copolymer throughout the experiment.

Fourth, I would like to thank The Petroleum and Petrochemical College, Chulalongkorn University, Bangkok, Thailand for the supporting instrument and equipments.

Fifth, I also acknowledge Faculty of Pharmacy, Mahidol University to the Institute of M.Sc. studies for providing good working facilities. I also would like to thanks to Mrs. Kanjana Timam and Mr. Rachata Nantasen for their supportive assistance during I was studing and doing the research.

Sixth, I would like to thank all my friends at the Faculty of Pharmacy, Mahidol University, at Faculty of Pharmacy for their friendship, kindly support and cheerfulness. I cannot list their names in this limited page; however, all of them will be in my mind forever. My greatest appreciation is extended to Banbung Hospital Chonburi and Dr. Jumpol Pobsuk for giving me a chance to study.

Seventh, I would like to thank Mae Mai for her kindness and supporting the house for living in Bangkok throughout the study.

Most importance, I would like to express the warmest gratefulness to my father, mother, sisters, brother and grandmother Yaijai for their love and full of cares which always cheered me up and assisted me to the success in my life.

Supa Kotcha

THE STUDY AND CHARACTERIZATION OF THE NANO-ENCAPSULATION OF CLOTRIMAZOLE INTO *N*-PHTHANOYL CHITOSAN-*g*-mPEG SELF ASSEMBLY

SUPA KOTCHA 4736932 PYPT/M

M.Sc. in Pharm. (PHARMACEUTICS)

THESIS ADVISORS: KORBTHAM SATHIRAKUL, Ph.D., SUWABUN CHIRACHANCHAI, Ph.D., GAYSORN CHANSIRI, Ph.D.

ABSTRACT

Oral candidiasis is an opportunistic infectious condition caused by *Candida albicans spp.* The pathology of the organ is located at the buccal mucosa of oropharyngeal. Among several antifungal drugs, clotrimazole (CLT) is cost-effective for treating oral candidiasis. The success of therapy depends on the performance of the formulation. An ideal formulation for local delivery of drugs into the buccal system should exhibit ease of delivery, a good retention at the application site and controlled release. Nanoparticles are one of strategies to improve the bioavailability of drugs because those carriers show sustained release. Also, because of their small size of nanoparticles tend to adhere more highly to mucous layers than larger particles. Chitosan and chitosan derivatives, biodegradable polymer, have been reported as effective bioadhesive delivery systems for prolonged contact time. *N*-phthaloyl chitosan-*g*-mPEG is a novel copolymer, previously concentrated by modification based on balancing of polarity on the chitosan chain in order to obtain novel derivatives. Which can self-assembly to be the spherical shape in aqueous solution. Now a days many copolymers are used to produce nanoparticles drug delivery. Thus, the feasibility of novel copolymer for drug delivery has been investigated. The various conditions of the preparation such as dialyzed medium, stirring time and percentage of initial drug loading to the copolymer were established. Underlying the using various dialyzed mediums, it was found that using 0.02 M PBS pH 7.4 aqueous solution could be achieve percentage of drug encapsulation efficiency (%DE) and drug loading (%DL) were  $25.51 \pm 1.06\%$  and  $11.57 \pm 0.76\%$ , respectively with uniform size 50-70 nm of spherical nanoparticles. Using distilled water as dialyzed medium, percentage of drug loading (%DL) of CLT-loaded nanoparticles were  $9.84 \pm 2.51\%$  with range size 150-300 nm and showed sustained drug release profile for 5 days with good reproducibility from batch to batch. This novel copolymer is suitable for a buccal hydrophobic drug delivery system. However, the prolonged contact time of this copolymer will be investigated in the future.

KEY WORDS : CLOTRIMAZOLE/ NANOPARTICLES/ CHITOSAN/  
DIALYSIS *N*-PHTHANOYL CHITOSAN-*g*-mPEG/  
BUCCAL/ DRUG DELIVERY

131 pp.

ศึกษาการห่อหุ้มและคุณลักษณะของโคไทรมาโซลที่ถูกห่อหุ้มโดย *N*-phthaloyl chitosan-g-mPEG ซึ่งสามารถรวมตัวกันเองได้อนุภาคระดับนาโนเมตร (THE STUDY AND CHARACTERIZATION OF THE NANO-ENCAPSULATION OF CLOTRIMAZOLE INTO *N*-PHTHALOYLCHITOSAN-g-mPEG SELF ASSEMBLY)

สุภา คชชา 4736932 PYPT/M

ภ.ม. (เภสัชการ)

คณะกรรมการควบคุมวิทยานิพนธ์: กอบรัชม ศถิรกุล Ph.D., สุวบุญ จิรชาญชัย, Ph.D.

#### บทคัดย่อ

โรคเชื้อราในช่องปากมักเกิดจากเชื้อกลุ่มแคนดิดา แอลบิแคน โดยเชื้อก่อพยาธิสภาพที่เยื่อภายในช่องปากรวมถึงเพดานปาก มียาด้านเชื้อราหลายชนิดที่ใช้ในโรคนี้ พบว่าโคไทรมาโซลเป็นยาที่มีราคาถูกและให้ผลการรักษาดีแต่อย่างไรก็ตามความสำเร็จในการรักษาขึ้นกับประสิทธิภาพของตำรับยาเป็นสำคัญ คุณสมบัติที่ดีของตำรับยาใช้เฉพาะที่ประกอบด้วยสามประการคือ สะดวกในการใช้ สัมผัสกับบริเวณที่เกิดโรคได้นาน และสามารถควบคุมการปลดปล่อยให้ยาดังกล่าวได้อย่างต่อเนื่อง การศึกษาพบว่าการทำยาให้อยู่ในตำรับที่มีขนาดเล็กระดับนาโนเมตรสามารถควบคุมการปลดปล่อยยาให้มีระยะเวลาอันประกอบด้วยอนุภาคที่มีขนาดเล็กระดับนาโนเมตรสามารถยึดเกาะกับเยื่อเมือกที่ปกคลุมเยื่อหุ้มผิวหนังได้นานกว่าอนุภาคที่มีขนาดใหญ่ โคไทรมาโซลหรืออนุพันธ์ของโคไทรมาโซลซึ่งเป็นโพลิเมอร์ที่สามารถย่อยสลายได้มีคุณสมบัติในการยึดเกาะกับเยื่อเมือกที่ดีและอยู่ได้นาน ทีมวิจัยก่อนหน้านี้ได้สังเคราะห์อนุพันธ์โคไทรมาโซลได้โพลิเมอร์ใหม่คือ *N*-phthaloyl chitosan-g-mPEG โดยพยายามให้เกิดสมดุลทางประจุไฟฟ้าของสายโคไทรมาโซลทำให้เมื่ออยู่ในน้ำจะรวมตัวกันเองเป็นอนุภาคทรงกลม ในปัจจุบันมีโพลิเมอร์หลายชนิดถูกนำมาทำเป็นตัวนำส่งยา ดังนั้นการศึกษาในครั้งนี้ต้องการดูความสามารถของโพลิเมอร์ในการเป็นตัวนำส่งยา โดยทดลองเตรียมตำรับด้วยวิธีต่างๆซึ่งแตกต่างกันได้แก่ ชนิดของน้ำที่ใช้เตรียม เวลาในการกวนและสัดส่วนของยาต่อโพลิเมอร์ แล้วติดตามผลของความสามารถที่เกิดขึ้นต่อลักษณะของตำรับ ผลการทดลองพบว่า ชนิดของน้ำที่ใช้เตรียมมีผลต่อปริมาณยาที่ถูกห่อหุ้ม โดยน้ำที่มีฟอสเฟสบัฟเฟอร์ความเข้มข้น 0.02 โมลต่อลิตรและมีค่าความเป็นด่างที่ 7.4 ทำให้ยาถูกห่อหุ้มได้มากที่สุดคือ 25.51±1.06%ของปริมาณยาที่ได้ตั้งต้นและ คิดเป็นยาโดยน้ำหนักต่อโพลิเมอร์เท่ากับ 11.57±0.7% มีขนาดของอนุภาคอยู่ในช่วง 50-70 นาโนเมตร แต่ถ้าน้ำกลั่นในการเตรียมพบว่ายาโดยน้ำหนักต่อโพลิเมอร์เท่ากับ 9.84±2.51 % และมีขนาดอนุภาคอยู่ในช่วง 250-300 นาโนเมตรและมีสามารถในการควบคุมการปลดปล่อยยาได้นานถึง 5 วัน อย่างไรก็ตามคุณสมบัติในการเกาะติดกับเยื่อเมือกของโพลิเมอร์จะทดสอบต่อไปในอนาคต

## CONTENTS

	<b>Page</b>
<b>ACKNOWLEDGEMENT</b>	iii
<b>ABSTRACT (ENGLISH)</b>	iv
<b>ABSTRACT (THAI)</b>	v
<b>LIST OF TABLES</b>	viii
<b>LIST OF FIGURES</b>	xiii
<b>LIST OF ABBREVIATIONS</b>	xiv
<b>CHAPTER</b>	
<b>I INTRODUCTION</b>	1
<b>II LITERATURE REVIEW</b>	3
A. Oral Candidiasis	3
B. Clotrimazole	4
Physical and chemical properties	4
Antifungal activity	7
Resistance	8
Pharmacokinetics	8
C. Buccal Route Delivery	9
Anatomy and biochemistry of oral mucosa	9
Physiological aspects	10
D. Polymeric Nanoparticles	14
Method to preparation of nanoparticles	14
E. Chitosan Nanoparticles	18
Properties of chitosan	18
Mechanism of the formation of chitosan nanoparticles	20
Application of chitosan derivatives nanoparticles	30
<b>III MATERIALS AND METHODS</b>	33

**CONTENTS (continued)**

	<b>Page</b>
<b>IV RESULTS AND DISCUSSION</b>	40
High Performance Liquid Chromatography Analysis and Validation Method	40
Preformulation Study	41
Characterization of CLT-Loaded Nanoparticles	46
Reproducibility of Method IV on Characteristic of CLT- Loaded <i>N</i> -Phathaoylchitosan-g-mPEG	81
Drug release profile of CLT-Loaded Nanoparticles	81
The Influence of Dialysis Method on Clotrimazole Encapsulation in to <i>N</i> -Phthanoyl-chitosan-g-mPEG.	89
<b>V CONCLUSION</b>	105
<b>REFERENCES</b>	108
<b>APPENDIX</b>	117
<b>BIOGRAPHY</b>	131

## LIST OF TABLES

Table		Page
1.	Antifungal drugs and costs for treatment of oropharyngeal candidiasis.	5
2.	Studies using chitosan based delivery systems for drug	31
3.	Average peak area versus concentration of clotrimazole standard solution and percentage of coefficient of variation (%CV)	44
4.	Average of peak area (n=5) with percentage of coefficient of variation for three days corresponding to 150 µg/ml standard solution.	45
5.	Represent characteristics of copolymer in various solvent	45
6.	Mean particle size of control and CLT-loaded nanoparticles were prepared by dialysis against distilled water with constant stirring.	50
7.	Polydispersity index of control and CLT-loaded nanoparticles were prepared by dialysis against distilled water with constant stirring.	50
8.	Percentage drug loading of CLT-loaded nanoparticles were prepared by dialysis against distilled water with constant stirring.	52
9.	Percentage drug encapsulation efficiency of CLT-loaded nanoparticles were prepared by dialysis against distilled water with constant stirring.	52
10.	Glass transition temperature ( $T_g$ ) and Melting point ( $T_m$ ) of CLT, bare nanoparticles and CLT-loaded nanoparticles, which were prepared by dialysis against distilled water with constant stirring.	53
11.	Residue solvent of bare nanoparticles and CLT-loaded nanoparticles, which were prepared by dialysis against distilled water with constant stirring.	53
12.	Mean particle size of control and CLT-loaded nanoparticles were prepared by dialysis against 0.02 M PBS pH 5.5 with constant stirring.	59

## LIST OF TABLES (continued)

<b>Table</b>	<b>Page</b>
13. Polydispersity index of control and CLT-loaded nanoparticles were prepared by dialysis against 0.02 M PBS pH 5.5 with constant stirring.	59
14. Percentage drug loading of CLT-loaded nanoparticles were prepared by dialysis against 0.02 M PBS pH 5.5 with constant stirring.	60
15. Percentage drug encapsulation efficiency of CLT-loaded nanoparticles were prepared by dialysis against 0.02 M PBS pH 5.5 with constant stirring.	60
16. Glass transition temperature ( $T_g$ ) and melting point ( $T_m$ ) of CLT, bare nanoparticles, CLT-loaded nanoparticles, which were prepared by dialysis against 0.02 M PBS pH 5.5 with constant stirring.	61
17. Residue solvent of bare nanoparticles and CLT-loaded nanoparticles, which were prepared by dialysis against 0.02 M PBS pH 5.5 with constant stirring.	61
18. Mean particle size of control and CLT-loaded nanoparticles were prepared by dialysis against 0.02 M PBS pH 7.4 with constant stirring.	65
19. Polydispersity index of control and CLT-loaded nanoparticles were prepared by dialysis against 0.02 M PBS pH 7.4 with constant stirring.	65
20. Percentage drug loading of CLT-loaded nanoparticles were prepared by dialysis against 0.02 M PBS pH 7.4 with constant stirring.	67
21. Percentage drug encapsulation efficiency of CLT-loaded nanoparticles were prepared by dialysis against 0.02 M PBS pH 7.4 with constant stirring.	67

## LIST OF TABLES (continued)

<b>Table</b>	<b>Page</b>
22. Glass transition temperatures ( $T_g$ ) and melting points ( $T_m$ ) of CLT, bare nanoparticles, CLT-loaded nanoparticles which were prepared by dialysis against 0.02 M PBS pH 7.4 with constant stirring.	68
23. Residue solvent of bare nanoparticles and CLT-loaded nanoparticles were prepared by dialysis against 0.02 M PBS pH 7.4 with constant stirring.	68
24. Mean particle size of control and CLT-loaded nanoparticles were prepared by dialysis against distilled water and non-used stirring in the first three hours.	72
25. Polydispersity index of control and CLT-loaded nanoparticles were prepared by dialysis against distilled water and non-used stirring in the first three hours.	72
26. Percentage drug loading of CLT-loaded nanoparticles were prepared by dialysis against distilled water with non-using stirring in the first three hours.	74
27. Percentage drug encapsulation efficiency of CLT-loaded nanoparticles were prepared by dialysis against distilled water with non-using stirring in the first three hours.	74
28. Glass transition temperatures ( $T_g$ ) and melting points( $T_m$ ) of CLT, bare nanoparticles, CLT-loaded nanoparticles, which were prepared by dialysis against distilled water and non-used stirring in the first three hours.	75
29. Residue solvent of bare nanoparticles, CLT-loaded nanoparticles were prepared by dialysis against distilled water and non-used stirring in the first three hours.	75

## LIST OF TABLES (continued)

Table	Page
30. The concentration of clotrimazole in nano-suspension was storage before 1 month	78
31. The concentration of clotrimazole in nano-suspension was storage after 1 month	78
32. Zeta potential value of control and CLT-loaded nano-suspension which were prepared by method I were dispersed and evaluated in SWI, 0.02 M PBS pH 5.5 and 0.02 M PBS pH 7.4.	78
33. Percentage drug loading (%DL) obtained from three batches of CLT-loaded nanoparticles which were prepared by method I.	84
34. Percentage drug encapsulation efficiency (%DE) obtained from three batches of CLT- loaded nanoparticles which were prepared by method I.	84
35. Mean particle size (nm) and polydispersity index with standard deviation obtained from three batches of CLT- loaded nanoparticles which were prepared by method I.	85
36. Represent percentage cumulative drug release, average percentage of cumulative drug release of positive control (clotrimazole standard solution 110 µg/ml, 2 ml) with standard deviation (n=2).	85
37. Percentage drug encapsulation efficiency corresponding to percentage of initial drug loading to the copolymer w/w (n=2).	91
38. Percentage drug loading corresponding to percentage of initial drug loading to the copolymer w/w (n=2).	92
39. Mean particle size of CLT loaded nanoparticles corresponding to percentage of initial clotrimazole loading to the copolymer w/w (n=6).	93

**LIST OF TABLES (continued)**

Table		Page
40.	Polydispersity index of CLT- loaded nanoparticles corresponding to percentage of initial clotrimazole loaded to the copolymer w/w (n=6).	94
41.	The percentage drug loading corresponding to dialyzed medium (n=4).	97
42.	The percentage drug encapsulation efficiency corresponding to dialyzed medium (n=4).	98
43.	Mean particle size of CLT-loaded nanoparticles corresponding to dialyzed medium. (n=12).	100
44.	Polydispersity index (PI) of CLT-loaded nanoparticles corresponding to dialyzed medium (n=12).	101
45.	Percentage drug encapsulation efficiency, percentage drug loading, mean particle size and polydispersity index corresponding to non-using stirring and using stirring with dialysis against distilled water (n=4).	104

## LIST OF FIGURES

Figure		Page
1.	Chemical structure of clotrimazole	6
2.	Schematic representation of physiology structure of buccal layer.	13
3.	Summary of the different methods to prepare nanosphere and nanocapsules from a polymer. w/o: water-in-oil, o/w: oil-in-water; w/o/w: water-in-oil-in-water.	17
4.	Structure of chitosan.	19
5.	Geometries of $\pi$ - $\pi$ complexes. A) Face-to-face stacking B) Edge-to-face stacking C) offset stacking.	26
6.	An $sp^2$ -hybridized atom in a $\pi$ -system.	27
7.	Electrostatic interactions between nonpolar $\pi$ system as a function of orientation.	29
8.	Structure of <i>N</i> -phthaloyl chitosan-g-mPEG.	32
9.	Chromatogram of buffer pH 7.4 with 50% methanol, medium for the experiment of drug release study.	42
10.	Chromatogram of extracted solution of non-drug loaded nanoparticles.	42
11.	Chromatogram of clotrimazole from drug release study	43
12.	Chromatogram of clotrimazole standard solution	43
13.	Standard curve and linear equation.	44
14.	Morphology of CLT-loaded nanoparticles with using 11.56 mg/ml of the copolymers and initial drug loaded 50% w/w.	47
15.	Morphology of CLT-loaded nanoparticles with using 3.0 mg/ml of the copolymers and initial drug loaded 50% w/w.	47

## LIST OF FIGURES (continued)

<b>Figure</b>	<b>Page</b>
16. A-C show morphology of CLT-loaded nanoparticles and D show bare nanoparticles were prepared by dialysis against distilled water with constant stirring.	49
17. Graph represent percentage weight loss of bare nanoparticles and CLT-loaded nanoparticles, which were prepared by dialysis against distilled water with constant stirring, corresponding to temperature with rate of heating was 10 °C/min.	54
18. A-C show morphology of CLT-loaded nanoparticles and D show bare nanoparticles were prepared by dialysis against 0.02M PBS pH 5.5 with constant stirring.	56
19. Aggregation particles was founded in CLT-loaded nano-suspensions which was prepared by dialysis against 0.02M PBS pH 5.5 with constant stirring.	57
20. Graph represent percentage weight loss of CLT-loaded nanoparticles which were prepared by dialysis against 0.02M PBS pH 5.5 with constant stirring, corresponding to temperature with rate of heating was 10 °C/min.	62
21. A-C show morphology of CLT-loaded nanoparticles and D show bare nanoparticles were prepared by dialysis against 0.02M PBS pH 7.4 with constant stirring.	64
22. Graph represent percentage weight loss of CLT-loaded nanoparticles and control, which were prepared by dialysis against 0.02M PBS pH 5.5 with constant stirring, corresponding to temperature with rate of heating was 10 °C/min.	69
23. A-C show morphology of CLT-loaded nanoparticles and D show bare nanoparticles were prepared by dialysis against distilled water and non-use stirring in the first three hours of dialysis time.	71

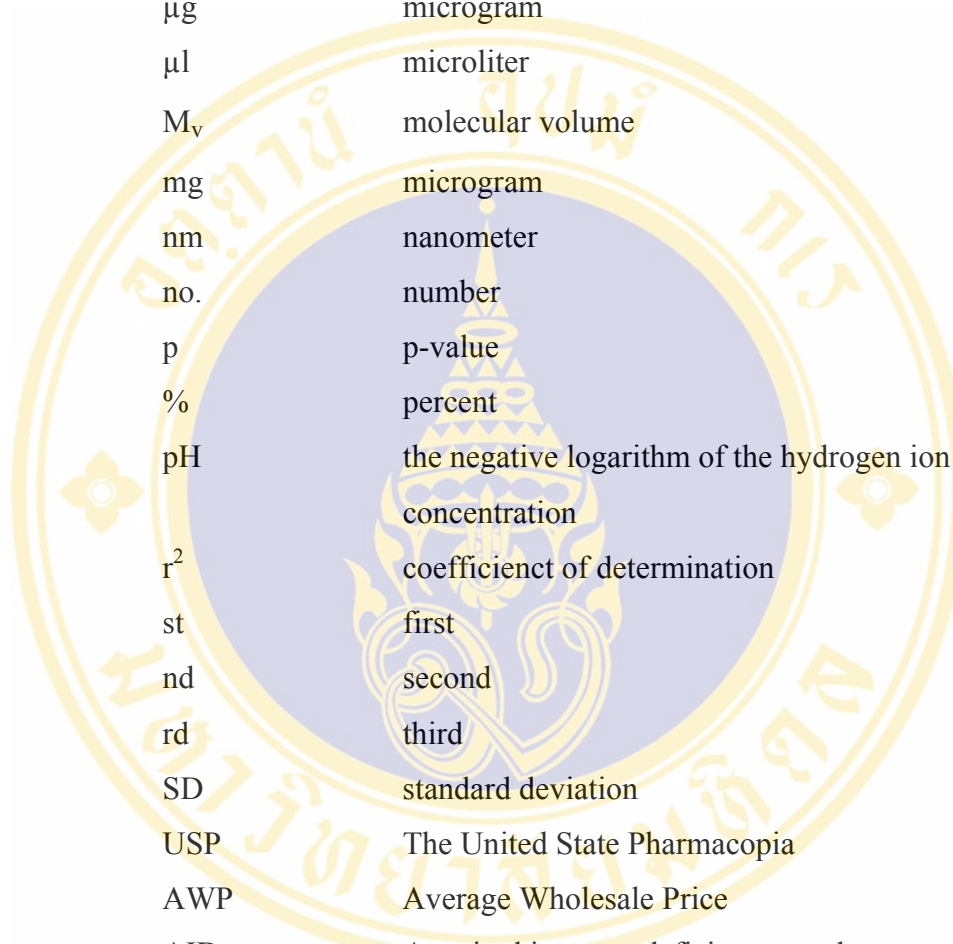
## LIST OF FIGURES (continued)

Figure		Page
24.	Graph represent percentage weight loss of CLT-loaded nanoparticles and bare nanoparticles, which were prepared by dialysis against distilled water and non-used stirring in the first three hours, corresponding to temperature with rate of heating was 10 °C/min.	76
25.	Schematic illustrated of CLT-loaded nanoparticle	80
26.	A-C represent morphology of clotrimazole-loaded nanoparticles from batch 1-3 which was prepared by against distilled water with non-used stirring constant in the first three hours.	83
27.	Average of cumulative drug release $\pm$ SD of positive control (n=2).	86
28.	Drug release profile of CLT-loaded nanoparticles obtained from three batches (n=5)	86
29.	Average percentage of cumulative drug release $\pm$ SD of CLT-loaded nanoparticles release profile (n=5).	87
30.	The average percentage of cumulative drug release $\pm$ SD of CLT-loaded nanoparticles (n=5) and the average percentage of cumulative drug release $\pm$ SD of positive control (n=2).	88
31.	Percentage of clotrimazole encapsulation efficiency corresponding to percentage of initial clotrimazole loading to the copolymer w/w (n=2).	91
32.	Percentage of clotrimazole loaded in nanoparticles corresponding to percentage of initial clotrimazole loading to the copolymer w/w (n=2).	92
33.	Mean particle size corresponding to percentage of initial clotrimazole loading to the copolymer w/w (n=2).	93
34.	Polydispersity index corresponding to percentage of initial clotrimazole loading to the copolymer w/w (n=2).	94
35.	3% W/W initial drug loaded to polymer	95

**LIST OF FIGURES (continued)**

<b>Figure</b>		<b>Page</b>
36.	15% W/W initial drug loaded to polymer	95
37.	50% W/W initial drug loaded to polymer	95
38.	100% W/W initial drug loaded to polymer	95
39.	The percentage drug loading corresponding to dialyzed medium, 0.02 M PBS pH 7.4, pH 5.5 and distilled water, respectively (n=4).	97
40.	The percentage drug encapsulation efficiency corresponding to dialyzed medium using 0.02 M PBS pH 7.4, pH 5.5 and distilled water, respectively (n=4).	98
41.	Mean particle size corresponding to dialyzed medium, 0.02 M PBS pH 7.4, pH 5.5 and distilled water, respectively (n=12).	100
42.	Polydispersity index corresponding to dialyzed medium, 0.02 M PBS pH 7.4, pH 5.5 and distilled water, respectively (n=12).	101
43.	A-C showed morphology of drug-loaded nanoparticles which using distilled water, 0.02 M PBS pH 5.5, 0.02 M PBS pH 7.4 as dialyzed medium, respectively with constant stirring.	102

## LIST OF ABBREVIATIONS



$\mu\text{g}$	microgram
$\mu\text{l}$	microliter
$M_v$	molecular volume
mg	microgram
nm	nanometer
no.	number
p	p-value
%	percent
pH	the negative logarithm of the hydrogen ion concentration
$r^2$	coefficient of determination
st	first
nd	second
rd	third
SD	standard deviation
USP	The United State Pharmacopia
AWP	Average Wholesale Price
AID	Acquired immune deficiency syndrome
HIV	Human immunodeficiency virus
HPLC	high performance chromatography
Hr	hour
ANOVA	analysis of variance
CLT	clotrimazole
PLC-g-mPEG	<i>N</i> -phthanoyl chitosan-graft-methoxy poly (ethylene glycol) methyl ether
DMF	<i>N, N</i> -dimethylformamide

## CHAPTER I

### INTRODUCTION

Oral candidiasis is an opportunistic infectious condition caused by *Candida albicans* spp. The pathological organ is located in the buccal mucosa of oropharyngeal (1). The disease can be treated by antifungal drugs such as clotrimazole. Clotrimazole (CLT) is a cost-effective drug for treatment oral candidiasis (2). However, because of hydrophobicity of clotrimazole, this property of drug is an important barrier for passing hydrophilic mucous membrane which covers on the buccal mucosa. Several strategies have been explored in the development for buccal drug delivery including biodegradable nanoparticles which have drawn a considerable interest.

Recent studies demonstrated the benefit of the colloidal carriers such as nanoparticle and liposome (3-9). Those were reported to be a promising way to improve the bioavailability of drugs and macromolecules in term of sustained release (5, 9). Moreover, the study on the effect of particle size on muco-adhesive properties from polystyrene latex, poly (isobutyl cyanoacrylate) nanospheres, and polylactic acid microspheres in the gastrointestinal tract of rats were found that the smaller particle tended to adhere more higher to mucous layers than larger particles (10). The sustained release and muco-adhesive properties of chitosan and chitosan derivatives nanoparticles are the appropriate tools for the buccal hydrophobic drug delivery system (11-19). Several types of polymer have been used to prepare nanoparticles. Focusing on chitosan and chitosan derivatives, they are the interesting polymers to produce the nanoparticles for buccal drug delivery.

*N*-phthaloyl chitosan-*g*-mPEG is the novel chitosan derivatives copolymer, which was modified by balancing the polarity of the chitosan chain. It can self-assembly to be the spherical nanoparticles in aqueous solution (20). In this study, the chitosan with 90% deacetylation,  $M_v$  of  $1.7 \times 10^5$  and 5,000 Da mPEG

were used to synthesis *N*-phthaloyl chitosan grafted poly (ethylene glycol) methyl ether (PLC-g-m PEG). Chitosan nanoparticles can be prepared by various methods such as salting out, chemical cross-linking and dialysis method (21, 22).

The dialysis method was selected to prepare clotrimazole-loaded PLC-g-m PEG. Based on the characteristics of both clotrimazole and copolymer, those are not readily soluble in water but completely dissolved in DMF (20).

Two objectives for this experiment were studied as followed ;

1. Feasibility of PLC-g-mPEG that can be the carrier of clotrimazole for buccal delivery system.
2. To understand the influence of dialysis method on the characteristics of CLT-loaded nanoparticles such as morphology, drug encapsulation efficiency, drug loading level and drug release pattern.

## CHAPTER II

### LITERATURE REVIEW

#### A. Oral Candidiasis

A Candidiasis is an opportunistic infectious condition caused by a ubiquitous saprophytic fungi of the genus *Candida*, which included eight species of fungi, the most common of which is *Candida albicans*. Candidiasis is usually limited to the skin and mucous membranes. Common clinical types of mucocutaneous candidiasis include oropharyngeal (affecting the oral cavity and/or pharynx), vulvovaginal (affecting the vaginal and vulvar mucosa), paronychia (affecting the nail beds and folds), interdigital (usually affecting the skin in between the fingers) and intertriginous (affecting the skin of the submammary areas or the groin and/or scrotum). Systemic invasive, infections of candidiasis can occur, especially in those patients with severe immunosuppression such as HIV patient. The gastrointestinal tract, trachea, lungs, liver, kidneys and central nervous system are all potential sites for infection in disseminated systemic candidiasis and may result in septicemia, meningitis, hepatosplenic disease, and endocarditis.

Oral candidiasis is predominately caused by *Candida albicans*, although other related *Candida* species may be involved. *Candida* is commensal organism and part of the normal oral flora in about 30%-50% of the population, and is capable of producing opportunistic infections within the oral cavity when appropriate predisposing factors exist (1). Oral candidiasis is one of the most common, treatable oral mucosal infections seen in persons with human immunodeficiency virus (HIV) infection or acquired immune deficiency syndrome (AIDS). Oral candidiasis can be a frequent and significant source of oral discomfort, pain, loss of taste, and aversion to food. For some patients with HIV/AIDS, it may also lead to secondary complications, such as esophageal candidiasis. For these reasons, antifungal prophylaxis may be justified in some high-risk patients (23). Table 1 lists the 6 antifungal drug preparations approved for marketing in the United States by the Food and Drug

Administration to manage mucosal fungal disease, as well as the average wholesale price associated with a recommended course of treatment for oral candidiasis (24).

A wide variety of agents are effective for the treatment of candidiasis (Table 1). Important factors that determine clinical response, besides the choice of antifungal agent, include the extent and severity of disease, patient adherence, the pharmacokinetic properties of the drug and safety. In terms of safety topical product is the first choice because of the lower side effect compared with the systemic product. Several topically antifungal agents-including nystatin (a polyene antifungal), clotrimazole (a topical imidazole), and amphotericin B oral suspension can be used to treat oral candidiasis. Clotrimazole seems to be cost-effectiveness to treat oral candidiasis because clotrimazole is available as a spray, solution, and troche for oral use, few side effects at normal therapeutic doses because of their lack of gastrointestinal absorption and low cost. However the traditional clotrimazole formulations must be used for several times per day to administrations. In addition, for the topical agents, successful therapy depends on adequate contact time (2 minutes) between the agent and the oral mucosa. Treatment duration varies from 7 to 14 days, with therapy minimally continued for 2 to 3 days beyond the last clinical signs and symptoms. Thus, if the topical formulation of clotrimazole have sustained release property causing one or twice time per day and have enough therapeutic dose which may be improve patients compliance that is the benefit to the AIDs or HIV patients for prophylaxis therapy.

**Table 1.** Antifungal drugs and costs for treatment of oropharyngeal candidiasis (24)

Generic name	Proprietary name	Formulation	2000 AWP/quantity	Typical treatment course
Amphotericin B	Fungizone	100 mg/mL oral suspension	\$70.56/56 mL	Rx: 100 mg QID for 14 d
Clotrimazole	Mycelex	10-mg troche	\$62.43/50	Rx: 10 mg 5×/d for 10 d
Fluconazole	Diffucan	100-mg tablet	\$112.03/15	Rx: 200 mg stat and 100 mg QD for 14 d
Itraconazole	Sporanox	10 mg/mL oral solution	\$122.16/140 mL	Rx: 100 mg QD for 14 d
		40 mg/mL oral solution	\$110.95/35 mL	Rx: 100 mg QD for 14 d
		100-mg capsule	\$198.00/28	Rx: 200 mg QD for 14 d
		10 mg/mL oral solution	\$207.48/280 mL	Rx: 200 mg QD for 14 d
Ketoconazole	Nizoral	200-mg tablet	\$52.66/15	Rx: 400 mg stat and 200 mg QD for 14 d
Nystatin	Mycostatin	100,000 u/mL oral suspension	\$69.85/200 mL	Rx: 500,000 U QID for 10 d
		200,000 u/oral pastille	\$52.33/50	Rx: 200,000 U 5×/d for 10 d
		500,000 u/oral tablet	\$27.48/40	Rx: 500,000 U QID for 10 d
		100,000 u/vaginal tablet	\$38.04/56	Rx: 100,000 U QID for 14 d

AWP, Average wholesale cost.

Adapted from Medical Economics . Drug Topics Red Book . Montvale, NJ: Medical Economics Company, Inc; 2000.

## B. Clotrimazole (25)

### 1. Physical and chemical properties

Clotrimazole (bis-phenyl-(2-chloro-phenyl)-1-imidazolymethane)(Figure 1) has a molecular weight of 344.8, is a colorless crystalline substance with a melting point of 143-144 °C, and is practically insoluble in water (0.49 µg/ml). It is soluble in a wide range of organic solvent, including polyethylene glycol, alcohol, chloroform, dimethylformamide, dimethylsulphoxide. The pure substance is hygroscopic, and is best stored in the dark in a desiccator, under which condition it appears stable indefinitely; concentrated solution stored at 4°C in dark have been found to be stable for years. Dilution into aqueous vehicles results in opalescent fluids, but providing the pH is more alkaline than 7.0 the dilution retains full antifungal potency because clotrimazole slowly hydrolyses in acid medium.

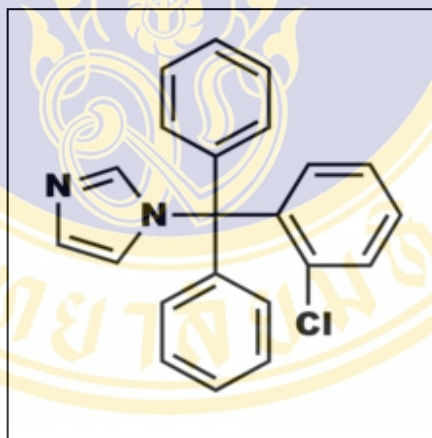


**Figure 1.** Chemical structure of clotrimazole (25)

## 2. Antifungal activity (25)

The inhibitory level for inhibited the growth of almost all fungi of clinical interest is below 2 mg/l.; Another report found an MIC of 3 mg/l or less. Clotrimazole has also some antibacterial activity for strain of *Staph. Aureus spp.*, *Strep. Pyogens*, *Proteus spp.*, *Salmonella spp.*, *Trichomonas spp.* and *Naegleria fowleri*. For amoebicidal activity usually well bellow 1 mg/l. It have the report suggested that systemic administration of the drug is effective in acute human toxoplasmosis, although no in vitro evidence of sensitivity of the protozoon to clotrimazole has yet appeared.

## 3. Mode of Action

Most of what is known about the mode of action this imidazole revealed that the drug inhibited the synthesis of various cellular constituents, especially protein and RNA, although DNA, lipid, and cell-wall polysaccharides were also affected; further studies with cell-free incorporating systems involving amino acid showed that the drug did not act directly on the mechanism of protein synthesis. It was suggested that an interaction occurred with the phospholipid layer of the cell membranes, causing changes in membrane permeability, and minimal cidal concentrations of clotrimazole greatly accelerated the leakage of intracellular phosphorus and potassium, with efflux into the surrounding medium; confirm by  $^{32}\text{P}$ -labeled compounds and of  $^{42}\text{K}$ . This occurred very soon after addition of the drug to growing cultures of *C. albican* and results showed that damage to the cell membranes of *C. albicans* by clotrimazole depended on two variables: drug concentration and length of exposure. At cidal concentration excessive membrane production was apparent after one hour and holes were present in the nuclear membrane; after 4 h exposure the nuclear membrane was so distorted as to be unidentifiable, and the internal structure of mitochondria disappeared; further exposure to cidal levels resulted in complete loss of the nuclear membrane. At lower fungistatic levels of clotrimazole the main effect noted on *C. albicans* was gradually increasing damage to mitochondria. In addition to its direct action on sensitive fungal cell, clotrimazole may also be capable of stimulating at least one factor in host resistance, that due to leucocyte myeloperoxidase (MPO). This enzyme in the polymorphonuclear leucocyte is involved in the intracellular killing of micro-organisms after their phagocytosis, and myeloperoxidase deficiency results in

decreased intracellular destruction of *C.albicans*, which has been noted in systemic candidiasis. And have been reported that MPO activity was increased in healthy adult males on moderate clotrimazole dosage, and observed a marked and sometimes progressive increase in MPO levels in 15 out of 17 infants, almost all less than 1 month old, who received clotrimazole for oral thrush. In contrast, a control series given nystatin showed no such increase, the mean MPO levels in the leucocytes of these babies, in fact showing a reduction to about one-third of that before treatment. In the same study it was found that cord blood MPO levels were generally elevated, probably because of contamination from the maternal circulation, in which leucocyte MPO activity is known to be raised.

#### **4. Resistance**

Wild *in vitro* resistance to clotrimazole among fungi of clinical interest is exceedingly rare and laboratory studies continue to reveal broad and almost universal antimycotic activity at low drug concentrations. Very little has been reported on interactions between clotrimazole and other antimycotic drugs.

#### **5. Pharmacokinetics**

For external use, Tettenborn, 1972 applied 1% clotrimazole cream and solution to intact and scarified skin of rabbits daily for long periods, (1) sometimes up to 90 days, and found no adverse local or systemic reactions with either preparation, nor was he able to detect clotrimazole in the serum or any biochemical change. Beagles and Rhesus monkeys were treated daily by the same worker for 2-3 weeks with 100 mg vaginal tablets, and again no absorption was detected. Additionally by radioactively labelled drug, clotrimazole cream and solution 1% were applied to intact human skin under occlusive dressing by Duhm et al., 1972 who found that the highest concentration remained in epidermis, particularly the stratum corneum; they estimated that drug concentrations attained or exceeded the MIC for most dermatophytes 6 h after application of the solution. They found very low subcutaneous levels, and 48 h after application serum were below detection level of 0.001 mg/l; urine excretion of drug was invariably below 0.5% of the activity applied to the skin, and similar levels followed application of the solution to acutely inflamed areas. Autoradiographic studies by those workers suggest that the drug is concentrated mainly along the hair follicles. The same workers found negligible systemic absorption of the drug after

human intravaginal insertion of 100 mg tablets and the average serum level 24 h after insertion was approximately 0.03 mg/l, estimated by a physical method.

### **C. Buccal Route Delivery**

The oral cavity is an attractive site for drug delivery due to ease of administration, that accepted by patient than any of the other mentioned alternative routes and avoidance of possible drug degradation in the gastrointestinal tract. Moreover this route is not first pass metabolism. There are four potential regions for drug delivery in the oral cavity, namely buccal, sublingual, palatal, and gingival. For buccal drug delivery specifically refers to the delivery of drugs within/through the buccal mucosa to affect local/systemic pharmacological actions. Buccal-delivered drugs may be used for treatment of diseases in the oral cavity or for systemic use (26). However, inherent limitations, including short residence time, small absorption area, and barrier property of the buccal mucosa, are challenges to buccal drug delivery.

#### **1. Anatomy and biochemistry of oral mucosa**

Oral mucosa is lined with an epithelium supported by a connective tissue termed lamina propria and separated from the epithelium by a basal membrane. The epithelium of oral mucosa is stratified with regional variation in terms of structure and function (26). Three types of oral mucosa are referred to as masticatory, lining, and specialized mucosa. The epithelium of masticatory mucosa in gingival and hard palate regions is keratinized and further subdivided into four layers, namely, keratinized, granular, prickle-cell, and basal layers. The nonkeratinized epithelium of lining mucosa covers the remaining regions, except the dorsal surface of the tongue and is made up of superficial, intermediate, prickle-cell, and basal layers. Specialized mucosa in the dorsum of the tongue consists of both keratinized and nonkeratinized mucosa. The physiological structure of buccal mucosa is illustrated in Figure 2. Small vessels and capillaries that open to the internal jugular vein distribute within the lamina propria, thus avoiding the hepatic first-pass clearance of buccal-delivered drugs. Blood flow in the oral mucosa is generally faster and richer than that in the skin (26, 27). The nonkeratinized buccal mucosa was reported to have approximately a thickness of 500–600  $\mu\text{m}$  and surface area of 50.2  $\text{cm}^2$  (26). Membrane-coating granules are small lipid organelles in the prickle-cell layer (26). The intercellular

lipids discharged from membrane-coating granules are responsible for the epithelial cohesion and formation of the superficial permeability barrier in the epithelium (27). This main penetration barrier exists in the outermost quarter to one-third of the epithelium.

The keratinized epithelium contain more neutral lipids that are associated with the barrier function, while nonkeratinized epithelia contain more polar lipids (28). The loosely packed intercellular lipids and the presence of large amounts of phospholipids in nonkeratinized, even in keratinized mucosa, account for the overall higher permeability of the oral mucosa than that of the skin stratum corneum (29). The nonkeratinized mucosa is more permeable than the keratinized mucosa, forming the major administration site in the oral cavity. The oral mucosal membranes do not have tight junctions as seen in intestinal membranes (26). The secretion of saliva from salivary glands features regional, individual, and time variations (26). The buccal region contains minor salivary glands. The mucus layer covers the oral mucosal surface and serves to lubricate and protect as well as to act as a wetting agent. Mucin is a group of glycoproteins composed of oligosaccharide side chains attached to a protein core. Three-quarters of the protein core are heavily glycosylated and impart a gel-like characteristic to mucus. The remaining nonglycosylated groups are involved in cross-linking via disulfide bonds among mucin molecules (28). Mucus is negatively charged at physiological saliva pH of 5.8–7.4 because of the presence of sialic acids ( $pK_a=2.6$ ) and ester sulfates at the terminals of some pendant oligosaccharide side chains (28).

## 2. Physiological aspects

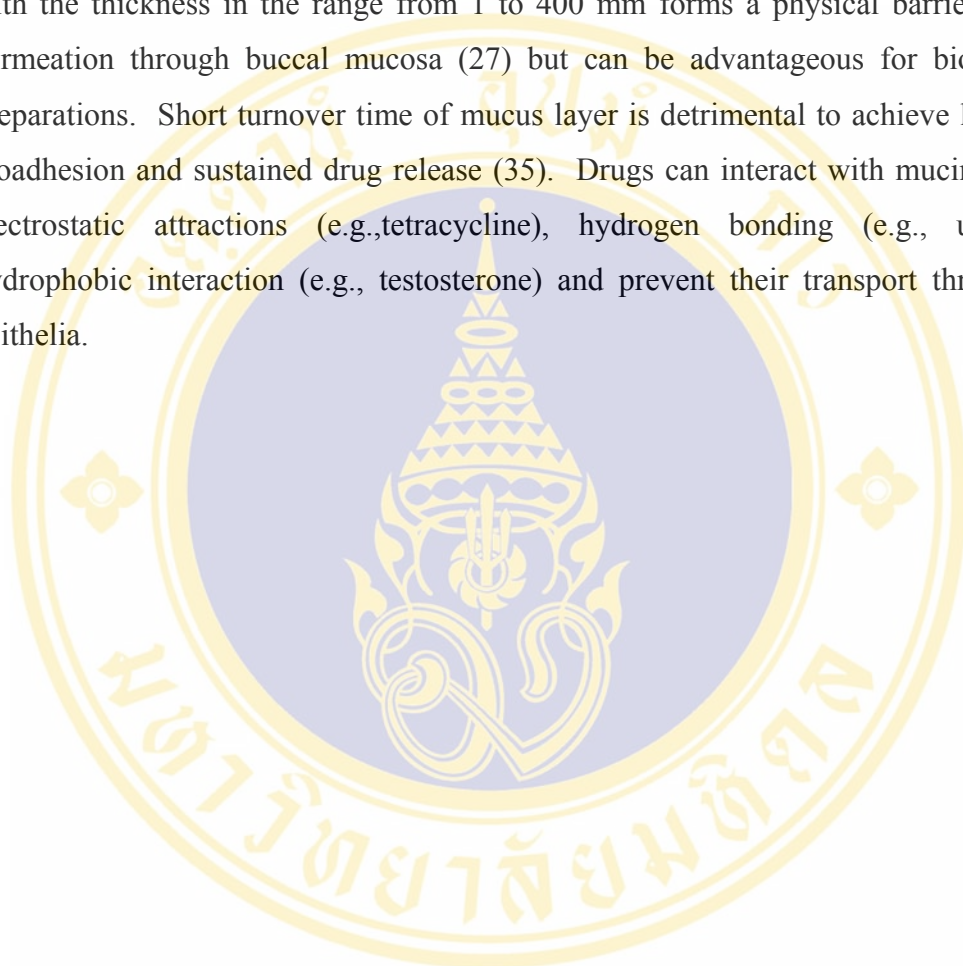
The buccal mucosa has a very limited area for application of the buccal delivery system, thus limiting device size and drug load. The actual area for drug absorption depends on the size of the dosage form. Generally, a device with the size of 1–3 cm<sup>2</sup> and a daily dose of 25 mg or less would be preferred for buccal delivery (28, 30). The maximal duration of buccal drug delivery is approximately 4–6 h, as meal intake and/or drinking may require the removal of the delivery device (30). Faster turnover of buccal mucosal epithelium (3–8 days) relative to the skin (about 30 days) may affect drug absorption by continually changing permeability characteristics(27). The epithelial layer is not uniformly hydrophobic and has two

possible drug penetration routes, the transcellular route and the paracellular route (Figure 2).

The lipophilic drugs penetrate mainly through the more lipophilic transcellular route, while the less lipophilic paracellular route, characterized by loosely packed polar intercellular lipids, is the principle route for hydrophilic drugs (26). Both routes coexist for all drugs, but the route with the least penetration resistance is usually preferred over the other, depending on the physicochemical properties of the drugs. However, smaller paracellular route area limits the penetration of hydrophilic drugs, whereas lipophilic drugs usually have high penetration rates through transcellular routes. This indicates that chemical modification of drug lipophilicity may increase drug penetration through buccal mucosa via the transcellular route. The permeability of ionizable drugs across buccal mucosa follows the pH-partitioning theory characteristic of passive diffusion (27).

Increasing nonionized fraction of ionizable drugs could favor drug penetration through the transcellular route. Control of pH is critical for successful buccal delivery of ionizable drugs. Lidocaine is a weak, basic drug with a pKa value of 7.9. The decrease in dissolution pH increased the ionic fraction of the drug and thus its apparent solubility, but decreased its permeability through buccal mucosa (31). This accounted for the insignificant relationship between the penetration rate through buccal mucosa and release rate of the drug from film into artificial saliva but significant relationship between the penetration rate and the release rate of nonionized drug. Nicotine is a diacidic base with pKa values of approximate 3 and 8. Nonionized nicotine permeated mainly via the transcellular pathway while the mono- and di-protonized molecules permeated via the paracellular pathway (32). Variation in saliva pH influenced the serum levels of nicotine after administration of nicotine chewing gum (33). The secretion of saliva is affected by disease and various stimuli (26). An acidic excipient can stimulate the secretion of saliva, which is an important consideration in selecting formulation excipients. Saliva has a weak buffering capacity to maintain pH value within local regions. Saliva contains no proteases but moderate levels of esterases, carbohydrases, and phosphatases, (29) which may degrade certain drugs. Although saliva secretion facilitates the dissolution of drug, involuntary swallowing of saliva can result in drug loss from the site of absorption.

Also, the non-uniform distribution of drugs within saliva on release from delivery systems implies that some areas of the oral cavity might not receive therapeutic levels of drugs (34), which is thus an important concern in the development of a locally administered buccal drug delivery system. The mucus layer with the thickness in the range from 1 to 400  $\mu\text{m}$  forms a physical barrier to drug permeation through buccal mucosa (27) but can be advantageous for bioadhesive preparations. Short turnover time of mucus layer is detrimental to achieve long-term bioadhesion and sustained drug release (35). Drugs can interact with mucin through electrostatic attractions (e.g., tetracycline), hydrogen bonding (e.g., urea), or hydrophobic interaction (e.g., testosterone) and prevent their transport through the epithelia.



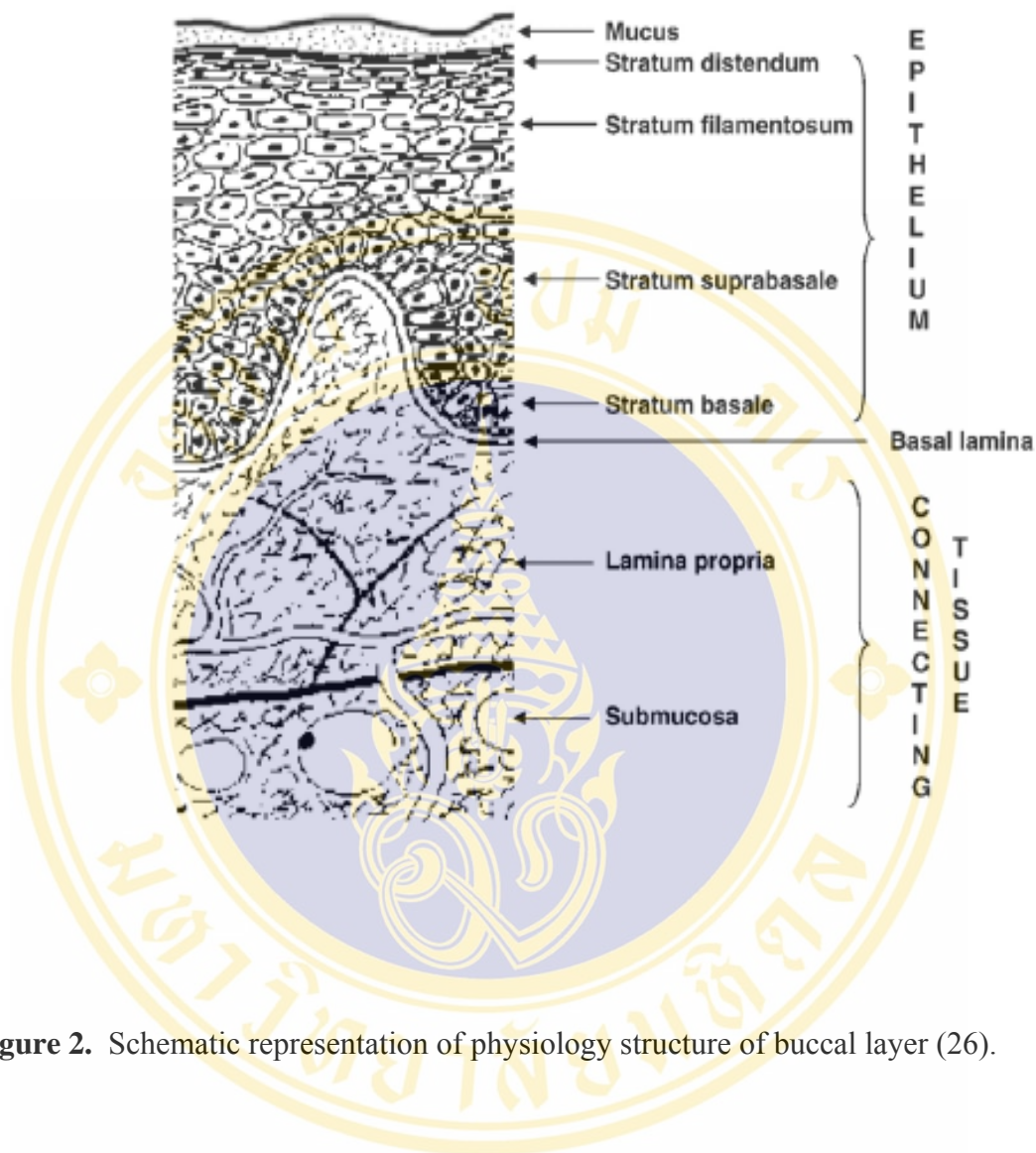


**Figure 2.** Schematic representation of physiology structure of buccal layer (26).

## **D. Polymeric Nanoparticles**

### **Method to preparation of nanoparticles**

#### **1. Emulsion – Evaporation procedure (36, 37)**

This techniques require the formation of an emulsion as first step of the procedure. To produce nanometer-scale-sized particles, the size of emulsion droplet must be small enough. This can be achieved by the use of special equipments such as high pressure homogenizers and microfluidizers. The energy input produced by these apparatus is important and is mainly due to high turbulence and cavitation forces. It allows an efficient dispersion of the polymer solution in the continuous phase. Once the desired emulsion is prepared, the formation of the nanoparticles can be induced according to two routes including the gelation of the polymer and the precipitation of the polymer either by solvent displacement or by solvent evaporation. Nanocapsules can also be prepared with the solvent evaporation technique from double water-in-oil-in-water emulsion.

#### **2. Salting-Out procedure**

The salting-out technique was introduced and patented by Bindschaedler et al. and Ibrahim et al. in 1988 (38). They have proposed replacing water-immiscible solvents, such as chloroform (all trace of which must be eliminated for an injectable dosage-form) by a miscible one such as acetone, which can easily be removed by evaporation. The method consists of adding under continuous to an acetone solution of polymer an electrolyte or non-electrolyte saturated aqueous solution containing poly vinyl alcohol (PVA) as viscosity and stabilizer. The saturated aqueous solution prevents acetone from mixing with water by a salting-out process and a W/O emulsion is obtained. Addition of water to this emulsion allows complete diffusion of acetone into the aqueous phase inducing the formation of nanospheres. Subsequent washings by ultracentrifugation or dialysis allow the eliminating of the salt or of the nonelectrolyte used to trigger the salting-out process. One of the investigator's claim is that surfactants are not necessary to obtain nanosphere.

#### **3. Chemical cross-linking of the polymer.**

Based on the gelation properties, chitosan can form nanosphere when cross-linking with tripolyphosphate (TTP) with the appropriated concentration. Bodmerier et al. (39) first reported to the ionotropic gelation of chitosan with TPP for

drug encapsulation. Cross-linking chitosan with glutaraldehyde can immobilized 5-fluorouracil rather than encapsulated (19). And other polymer such as alginate can be prepared nanosphere by adding calcium. The formation of nanosphere is resulting from inter and intramolecular aggregation of alginate molecule with interacted to calcium (40).

#### **4. Precipitation procedure**

This method was first described and patented by Fessi et al (41). They were first to propose a new and simple method yielding polymeric nanospheres without the use of preliminary solution emulsification or the use of auto-emulsifying polymeric material. Briefly, an organic solution of the polymer is prepared and added to a nonsolvent. Both solvent and nonsolvent must have low viscosity and high mixing capacity in all proportions. As an example, acetone and water meet these condition. The only complementary operating following the mixing of two phases is thus the remove of volatile solvent by vaporization under reduced pressure. Further concentration of the aqueous suspension can be carried out under the same conditions or by freeze drying. The mean diameter of the particles obtained was about 200 nm with a low dispersity. It was observed that the size of the particles was mainly related to polymer used and less to experimental condition. This method has been successfully applied to various polymeric materials.

#### **5. Freeze-Drying**

Recently, an innovative one-step procedure was described, based on the dissolution of both the polymer and the drug in a water/tert-butanol (TBA) mixture with subsequent lyophilization of the solvents. Drug-loaded micelles are formed spontaneously upon reconstitution of the freeze-dried polymer–drugcake in an injectable vehicle. TBA, a Class 3 category water-miscible solvent, was chosen as the co-solvent because of its high vapor pressure which accelerates its sublimation and, hence, the lyophilization process (42). Moreover, TBA induces the formation of fine, needle-like ice crystals that sublime rapidly, leaving behind freeze-dried cakes with a high degree of porosity. With this procedure, two hydrophobic anticancer agents, paclitaxel and docetaxel, were loaded successfully into a PVP-b-PDLLA copolymer, yielding stable spherical micelles with a monodisperse size distribution and a mean diameter of 30–60 nm. But increasing proportion between water/TBA raised from

80/20 to 50/50 influenced to mean diameter of micelles after lyophilization larger from 52 to 86 nm (43).

## 6. Dialysis method

Drug-loading procedures applies to amphiphilic copolymers which are not readily soluble in water and for which an organic solvent common to both the copolymer and the drug (such as dimethylsulfoxide (DMSO), N,N-dimethylformamide (DMF), acetonitrile, THF, acetone or dimethylacetamide) is needed. The mechanism by which micelle formation is induced depends on the solvent-removal procedure. For water-miscible organic solvents, the copolymer mixture can be dialyzed against water, whereby slow removal of the organic phase triggers micellization. Physical entrapment of a hydrophobic drug may be further achieved by this method.

By investigated the study concerning the influence of dialysis method to prepare nanoparticles, it was found that many preparation parameter such as selective solvent, initial drug loading, temperature and pH affected to the characteristics of polymeric nanoparticles. For example, by preparing indomethacin-loaded di-block copolymer compose of methoxy polyethylene glycol (mPEG) and  $\epsilon$ -caprolactone, the using DMF proved to be more stable solvent for micelles preparation than THF and having smallest mean particle size (44, 45). In case of paclitaxel-loaded Poly(*N*-isopropylacrylamide-co-*N,N*-dimethylacrylamide)-*b*-poly(D,L-lactide-co-glycolide) [P(NIPAAm-co-DMAAm)-*b*-PLG, encapsulation efficiency and loading level of paclitaxel into this polymeric was affected by the initial drug loading, fabrication temperature, polymer composition. The results were found that the increasing of initial paclitaxel loading to the polymeric from 9.1% to 20.0%, the encapsulation efficiency decrease from 50% to 27%. When increasing the temperature the encapsulation efficiency and loading level of paclitaxel increased and the longer hydrophobic segment of PLGA could be yielded higher the encapsulation efficiency and loading level of paclitaxel than the shorten one (46).

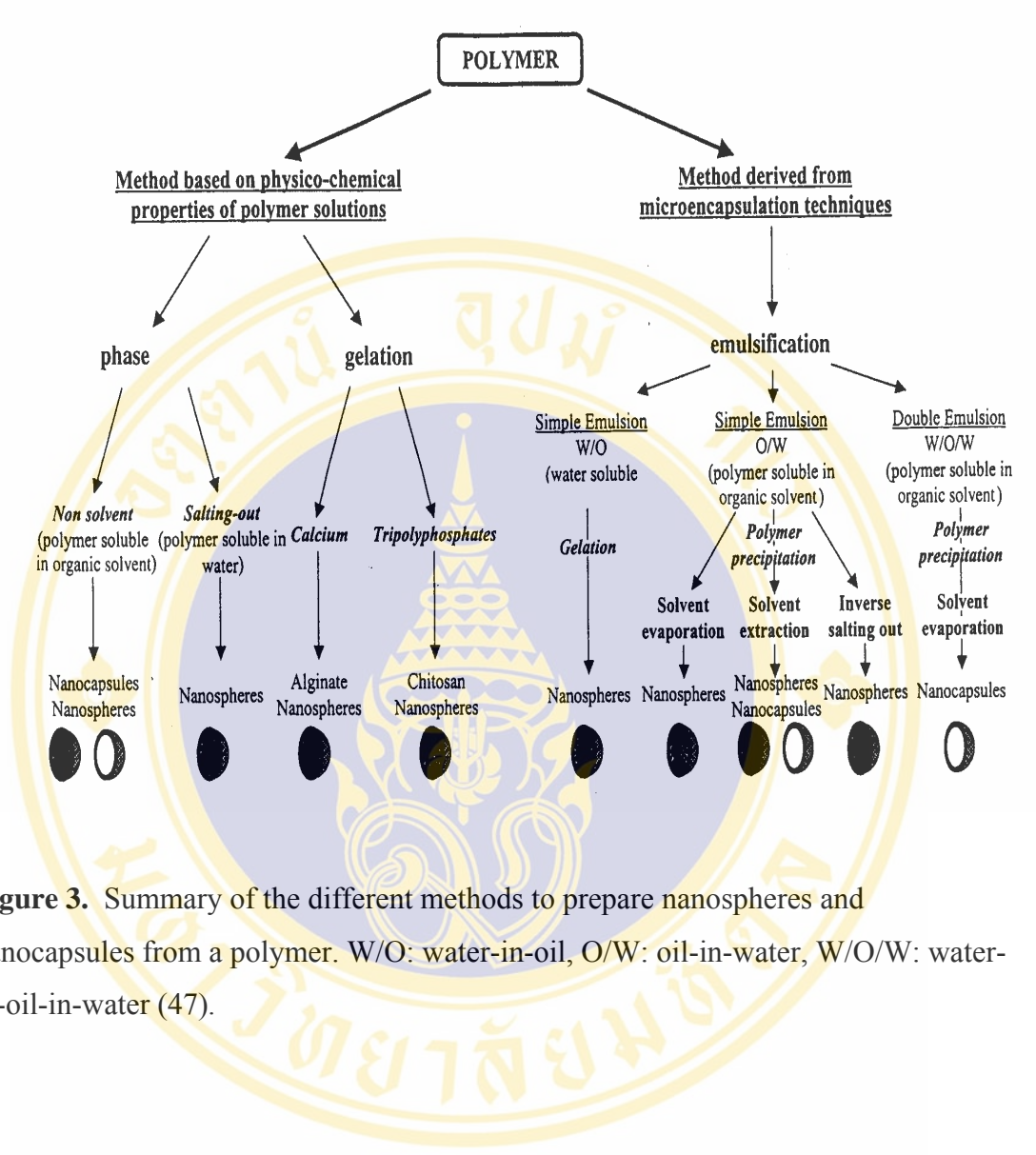


**Figure 3.** Summary of the different methods to prepare nanospheres and nanocapsules from a polymer. W/O: water-in-oil, O/W: oil-in-water, W/O/W: water-in-oil-in-water (47).

## E. Chitosan Nanoparticles

The properties of chitosan and its potentials application are described in the following.

### 1. Properties of chitosan

Chitosan (poly[ $\beta$ -(1-4)-2-amino-2-deoxy-D-glucopyranose]) is a biodegradable cationic polysaccharide produced by partial deacetylation of chitin derived from naturally occurring crustacean shells. The molecular formula is  $C_6H_{11}O_4N$  and its structure is shown in Figure 4. The polymer is comprised of copolymers of *N*-acetyl-*D*-glucosamine and *D*-glucosamine residues linked together by  $\beta(1 \rightarrow 4)$  glycosidic bonds (48, 49). Usually, chitosan has less than 40% *N*-acetyl-*D*-glucosamine (50). The degree of acetylation does not tend to increase by extending the reaction time. To achieve complete deacetylation, it is necessary to isolate chitosan and repeat the alkaline treatment in the same manner. However, the main chains can be depolymerized to some extent during the deacetylation, as shown by a considerable reduction in the molecular weight (51). The degree of deacetylation and molecular weight are the most important characteristic to determine the properties of chitosan (52).

Commercially available chitosan has an average molecular weight ranging from 3,800 to 2,000,000 and degree of deacetylation from 66 to 95% (48). The nitrogen content of chitosan is generally 5 to 8% depending on the degree of deacetylation. Chitosan has nitrogen mostly in the form of primary aliphatic amino groups which predominate the chemistry of chitosan. The presence of amino groups in the chitosan molecules make them suitable for further chemical modification, which in turn allow extensive adjustment of the chemical and biological properties of the chitosan. Chitosan is insoluble in either water or organic solvents, but is soluble in most aqueous dilute acids at a pH below 6.5. Aqueous solutions such as phosphoric, sulfuric, citric, and sebacic acids are not good solvents (51). Acetic acid has been mostly used as a standard solvent for chitosan. The extent of solubility depends on the degree of deacetylation, concentration, and type of acid and pH. Chitosans with a relatively low degree of deacetylation (40%) have been found to be soluble only up to pH 9, whereas chitosans with a degree of deacetylation of about 85% have been found to be soluble only up to a pH of 6.5 (pKa 6.5) (49, 53).

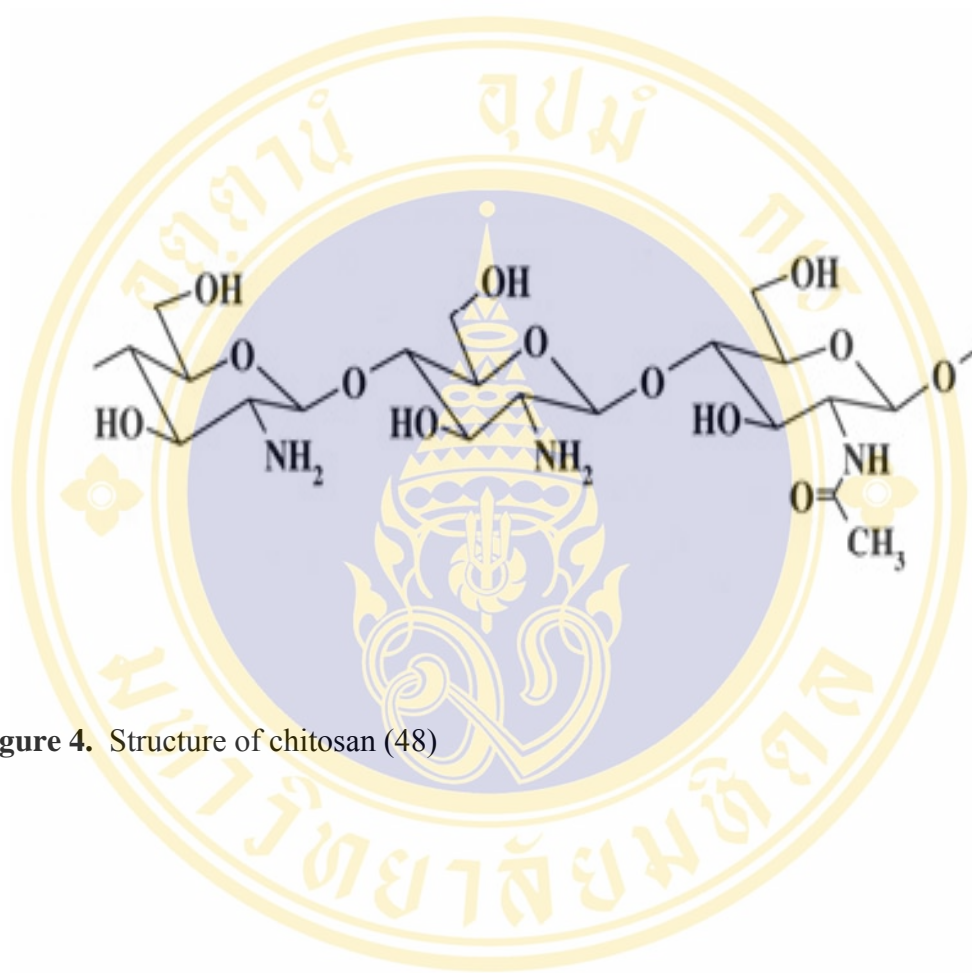


**Figure 4.** Structure of chitosan (48)

Solubility diminishes with increasing concentration of acid (51). Upon dissolution, the amine groups of the polymers are protonated and the resultant soluble polysaccharide is positively charged. One of the interesting properties of chitosan is the ability to bind to negatively charged surfaces like mucosal membranes, to act as a bioadhesive molecule. The polycationic character and ability to interact with negatively charged molecules.

The degradation of implanted intramuscularly chitin is reported to degrade completely in about 2 months (54). Chitosan can be degraded by lysozyme in the human serums to a common amino sugar that is incorporated into the synthetic pathway of glycoproteins, and is then excreted as carbon dioxide (55-57).

## **2. Mechanism of the formation of chitosan nanoparticles**

### **2.1. Ionotropic gelation**

Many authors have reported the formation of chitosan nanoparticles or microspheres by ionotropic gelation, for medical or pharmaceutical application. To address the potential toxicity of reagents and undesirable effects many researchers have used another approach based on ionotropic gelation (ionic crosslinking) (58). When polyelectrolytes of opposite charges are mixed, they may gel (physical hydrogel) or precipitate (particles), depending on their concentration, the ionic strength, and pH of the solution. The products of such ionic crosslinked systems are considered as desolvated particles. Briefly, chitosan is soluble in the acidic condition and becomes protonated, forming a polycation. From the physicochemical point of view, positively charged chitosan has the special quality of gelling upon contact with anions, thus allowing the formation of particles under very mild conditions. Anions electrostatically attract to the protonated amine groups of chitosan molecules, leading to the ionic crosslinking. Ionic crosslinking diminishes the solubility of chitosan, and chitosan molecules precipitate in the particle formation. Inter and intramolecular linkages created between chitosan and anions are responsible for the success of the gelation process. It is known that incorporating increasing amounts of anions with respect to chitosan leads to formation of a greater number of particles, and the positive chitosan amine groups are neutralized by their interaction with anions.

Calvo et al. 1997 (59) reported the formation of hydrophilic chitosan-polyethylene oxide nanoparticles and studied their potential application for administrating therapeutic molecules. Incorporation of PEO-PPO was achieved by dissolving these block polymers in the chitosan solution. These block polymers formed an intramolecular hydrogen bond with chitosan, leading to increased particle size and decreased zeta potential. It was shown that the nanoparticles have a great protein loading capacity and provide continuous release of the entrapped protein (up to 1 week) (59, 60).

A stable freeze-dried formulation of insulin-loaded chitosan nanoparticles was prepared for nasal administration by ionotropic gelation followed by freeze-drying in the presence of cryoprotective agents (61). Fresh chitosan nanoparticles showed that insulin was loaded with high efficiency, and released totally in less than 1 hour. Freeze-drying did not significantly influence the size, zeta potential, insulin loading, or release rate. It was proposed that freeze-dried chitosan nanoparticles are useful vehicles for increasing the nasal absorption of insulin.

Ionic bridging with a co-incorporated polyanion enabled positively charged chitosan nanoparticles to entrap the cationic anthracycline drug, doxorubicin (DOX) (62). Polyanion, dextran sulfate, was incorporated to mask the positive charge of DOX before particle formation, overcoming the charge repulsion. This method showed high DOX encapsulation efficiency and minimal burst release. Chitosan particles prepared by ionotropic gelation can be considered as a small physical hydrogel in the aqueous phase, because they are held together by molecular entanglement and/or ionic forces (63). They are not homogenous because clusters of molecular entanglements, (hydrophobically or ionically associated domains) can create inhomogeneities. Free chain ends or chain loops are considered to represent defects in physical networks and make some pores which may exist within the network (64).

The character and amount of water in the chitosan particles can determine the diffusion and adsorption (or partitioning) of nutrient and molecules into and cellular products out of gel through the physical network. Water molecules enter into the particle and hydrate the polar and hydrophilic groups. They are called bound water. The network will imbibe additional water due to the osmotic driving forces of

the network chains. The additional swelling is opposed by the physical crosslinking, leading to an elastic network-retraction force. Thus, the chitosan particles in the aqueous phase will reach an equilibrium swelling level. The additional swelling water (that is imbibed after the bound water) is called free water and is assumed to fill the space between the network chains and voids, and then come out of the particle readily, to reach the equilibrium state. This ionotropic gelation has the following interesting features. Chitosan particles are obtained spontaneously under mild conditions without involving high temperature and organic solvents (58, 65). It is possible to manipulate the size and surface charge by varying the ratio between positively charged chitosan and polyanion. Chitosan particles have a great drug loading capacity (61).

## 2.2. Complex coacervate

When two oppositely charged polyelectrolytes are mixed in an aqueous solution, microspheres are formed by electrostatic interactions between two species of the macromolecules, resulting in the separation of a coacervate (polymer-rich phase) from the supernatant (polymer-poor phase) (66). This phenomenon is a process of spontaneous phase separation (called complex coacervation). The coacervation process has been used to form microspheres and encapsulate living cells and labile molecules in drug delivery systems, because it can occur under mild conditions. Electrostatic interactions of chitosan with various negatively charged polyions have been well characterized in the literature. The properties of complexes were found influenced by the characteristics of polyelectrolytes including charge density and variation in chain conformation, in response to changes in pH, ionic strength and temperature (67).

Complex coacervation was also found to be dependant on molecular weight of polymers and ionic strength. Chitosan has been used to directly condense drugs or genes to be delivered. plasmid/chitosan complexes were prepared as a gene carrier (68). The plasmid/chitosan complexes most likely condensed to form large aggregates (5 to 8  $\mu\text{m}$ ) that can adsorb to the cell surface. Transfection ability and cell uptake were shown to be affected by the molecular weight of chitosan and stoichiometry of complexes. High molecular weight chitosan binds toward plasmid with high affinity, and produces condensed plasmid particles that are more stable. Depolymerized chitosan oligomers were also used for *in vivo* plasmid delivery (49). It

was reported that chitosan oligomers condensed plasmid into toroids and rod-shaped particles with a diameter of 66 nm. There have been some reports on the complex coacervates of chitosan with other polyelectrolytes for drug delivery. Chitosan was reported to form complex coacervates with gelatin with an optimum ratio 1:10 to 1:20 at a very diluted concentration over a narrow pH (69). Drugs or genes are incorporated in the chitosan complexes before the complexation, or coated after complexation. For topical genetic immunization, chitosan and chitosan oligomer were complexed with carboxymethylcellulose (CMC) to form stable cationic nanoparticles for subsequent plasmid DNA coating (70). For controlled release, interleukin-2 was incorporated into the alginate/chitosan porous microspheres. The proteins remained active and completely recovered from the release medium (65). The sustained release from alginate/chitosan was found to be longer than release from alginate/polylysine or alginate/CaCl<sub>2</sub>.

### 2.3 Aromatic-Aromatic interaction

$\pi$ - $\pi$  interaction can be defined as a noncovalent interaction between aromatic rings and delocalized  $\pi$  systems (71). It is observed in the molecular recognition responsible for the formation of the double helix of DNA, tertiary structure of proteins, packing of aromatic molecules in crystals, complexation in many host-guest systems, and self-assembled supramolecular architectures (72, 73). This  $\pi$ - $\pi$  interaction also controls the intercalation of certain drugs into DNA. Although the magnitude of this attractive interaction is relatively small, 1-5 kcal/mol, the interaction is believed to play an essential role in many natural self-assemblies and molecular recognition processes (74). The importance of  $\pi$ - $\pi$  interactions is widely recognized, however, their origins, strength and geometry have not been understood completely.

Some authors have suggested that the aromatic-aromatic interaction is driven mainly by electrostatic (Coulombic) interaction, dispersion interaction (van der Waals force), and hydrophobic interaction (desolvation) if water solutions are concerned (72, 75-77). Electrostatic interaction is the interaction between the static molecular charge distributions and depends on the relative charge distribution (71, 76). The  $\pi$  electrons of the aromatic rings are localized on both sides of ring surfaces, so that there is a partial negative charge on the ring center and a positive charge on the

hydrogen on the edges. This partial polarization gives possibility for electrostatic interaction. van der Waals interaction is the sum of the dispersion and repulsion energies and is roughly proportional to the area of  $\pi$  systems. Dispersion force between nonpolar molecules arises from the transient dipoles as a result of fluctuations in the favorable instantaneous positions of their electrons and is attractive between two aromatic ring molecules (73, 74, 78).

Dispersion force between two nonpolar aromatic ring systems is normally so weak that it is easily compensated by the entropy (76). Thus, it can be important only when the interacting groups are brought together by some other interactions such as electrostatic or hydrophobic interaction. The third contribution to the aromatic-aromatic interaction is desolvation known as hydrophobic interaction, in which the hydrophobic surface area of aromatic units exposed to the polar solvent is minimized upon aromatic stacking (79). Hydrophobic interaction is essentially entropy driven (74, 78). When hydrophobic molecules are surrounded by water, water molecules form a clathrate cage, leading to the decrease in water entropy. However, once hydrophobic molecules have herded into the cage, water molecules will be more free to move. The increase in energy (when hydrophobic groups cluster together and reduce their structural demands on the solvent) is the origin of the hydrophobic interaction.

Hydrophobic interaction is an example of an ordering process that is stabilized by a tendency toward greater disorder of the solvents (78). In order for two solute molecules to form complexes they must be desolvated in a solution. The solvent may compete for recognition sites and, hence, destabilize the complex. In polar solvents, hydrophobic interaction can stabilize the complexes. A number of studies have been conducted to understand the structural, geometrical and energetic parameters of this noncovalent interaction (72, 75, 76, 80). Aromatic rings interact in several different configurations contributed from complicated factors. These configurations include the edge-to-face (T-shaped), face-to-face (sandwich) and offset stacking (81), as shown in Figure 5. Hunter and Sanders (82) presented a simple charge distribution model to explain the nature (Figure 6) and the preferred geometry of  $\pi$ - $\pi$  interaction based on their observation on porphyrin  $\pi$ - $\pi$  interaction in solution and crystalline state. This model explicitly represents the out-of-plane  $\pi$  electron

density characteristic of  $\pi$  systems in which a positively charged  $\sigma$ -framework is sandwiched between two negatively charged  $\pi$  electron clouds (71, 82).

Using an idealized  $\pi$  systems, they derived some general rules to predict the geometry of favorable  $\pi$ - $\pi$  interactions. Electrostatic interaction between two idealized  $\pi$  systems is summarized in Figure 7 as a function of orientation (82). In the Figure 7, the face-to-face configuration is inhibited, because  $\pi$ - $\pi$  repulsion dominates. However, there is an attractive region where one  $\pi$ -atom is rotated by up to  $90^\circ$  relative to the other and where one  $\pi$ -atom is offset laterally relative to the other. Attractive interactions between the positively charged  $\sigma$ -framework and negatively charged  $\pi$  electrons dominate in the edge-to-face and offset stacking configuration. The aforementioned rules hold for nonpolar  $\pi$  systems.

Other rules were derived to predict the electrostatic interaction between polarized  $\pi$  systems, because introduction of polarizing substituents on the  $\pi$  systems perturbs the molecular charge distributions and causes large partial atomic charges. First, charge-charge interactions dominate for interaction between highly charged atoms. Second, a favorable interaction with a neutral or weakly polarized site requires the following  $\pi$ -polarization;  $\pi$  deficient atom for a face-to-face configuration, a  $\pi$  deficient atom in the vertical groups for the edge-to-face configuration, and a  $\pi$  rich atom in the horizontal groups in the edge-to-face configuration. Third, with respect to the  $\sigma$  polarization a favorable interaction with a neutral or weakly polarized site requires; a positively charged atom in a face-to-face configuration, a positively charged atom in the vertical groups in an edge-to-face configuration, and a negatively charged atom in the horizontal groups in the edge-to-face configuration.

The key feature of this model is that net favorable  $\pi$ - $\pi$  interactions are driven by the positively charged  $\sigma$  framework and negatively charged  $\pi$  electrons that outweigh the  $\pi$ - $\pi$  repulsion. Brief survey of some relevant experimental and theoretical studies contributing to the description of the aromatic-aromatic interactions follows. Two unsubstituted benzenes were believed to have an offset stacking configuration preferentially, followed by edge-to-face stacking due to the repulsion in  $\pi$  electron clouds (83). It was later suggested based on the energy barriers that the edge-to-face and offset stacking configurations were in dynamic equilibrium.

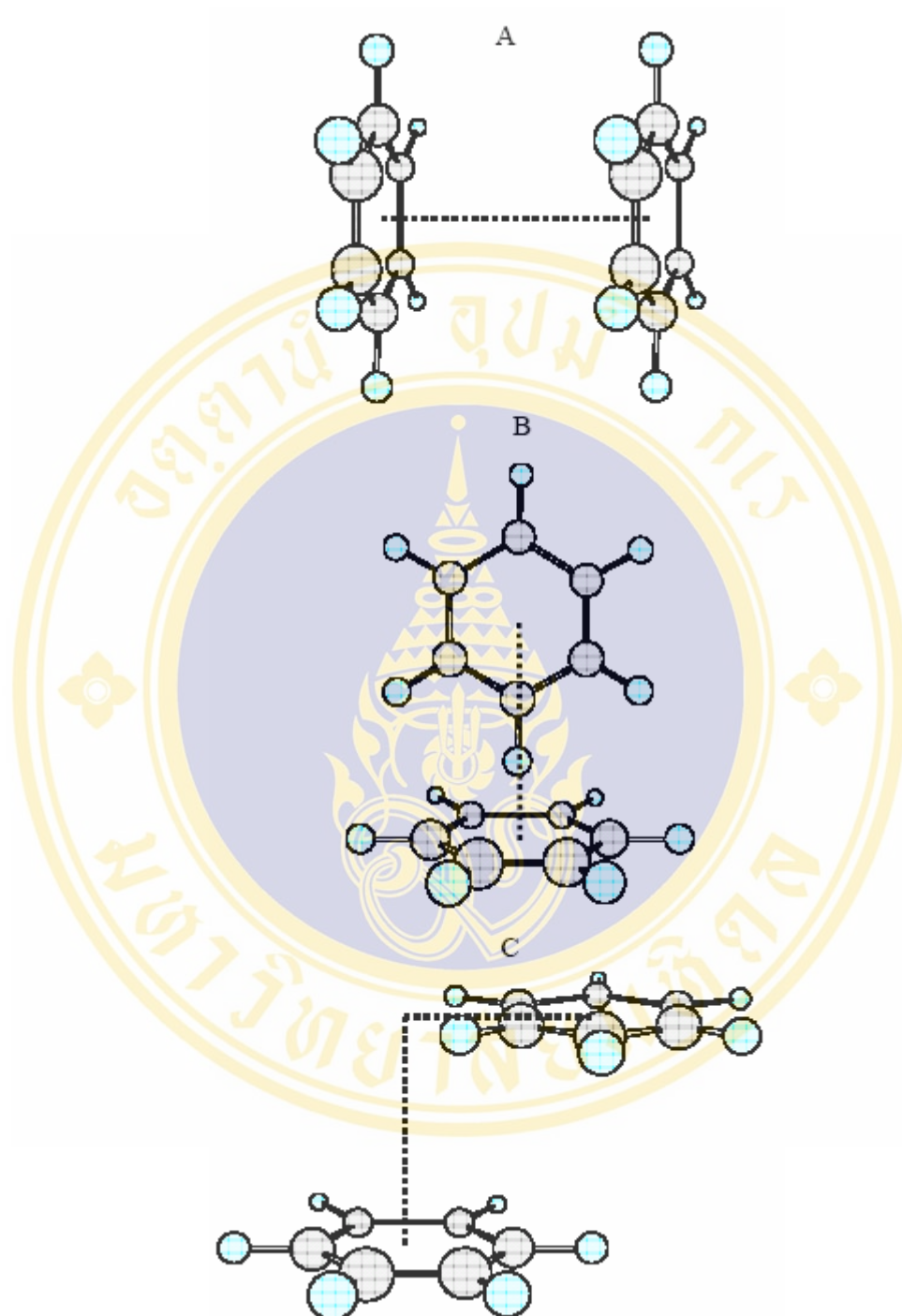


**Figure 5.** Geometries of  $\pi$ - $\pi$  complexes. A) Face-to-face stacking. B) Edge-to-face stacking. C) Offset stacking (81).

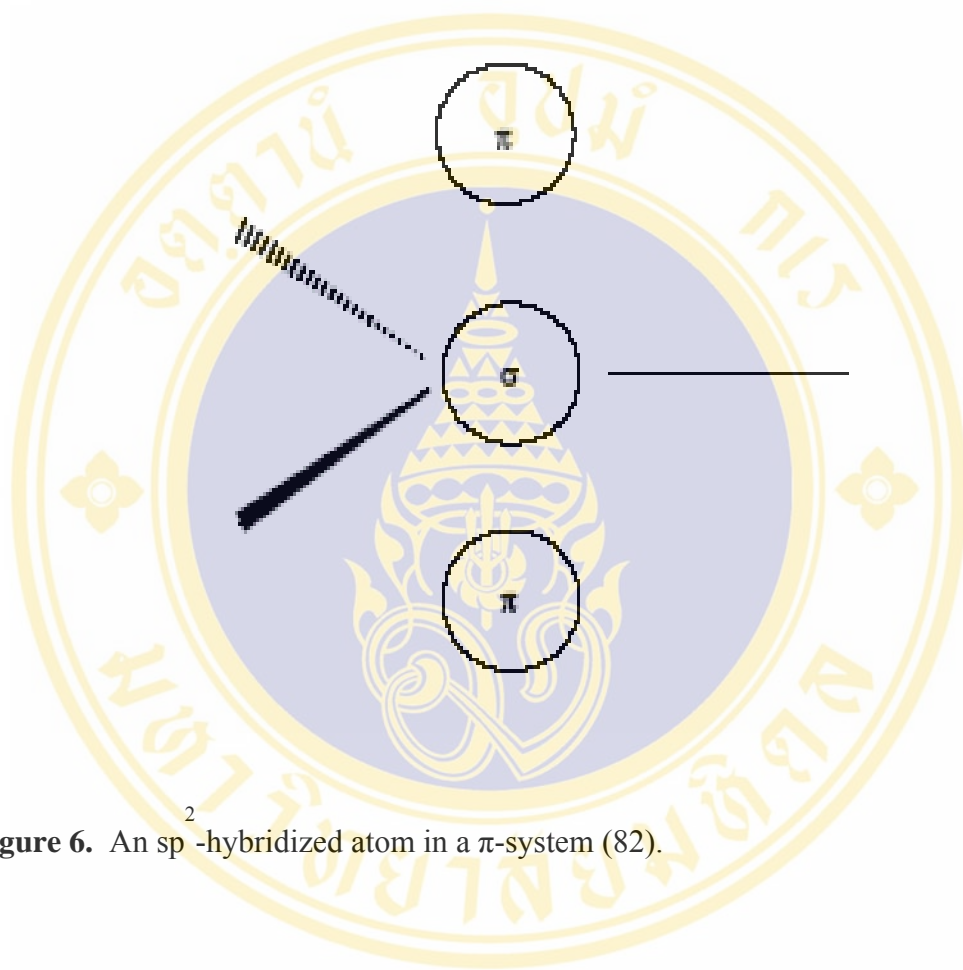


**Figure 6.** An  $sp^2$ -hybridized atom in a  $\pi$ -system (82).

The combined experimental and theoretical work to date suggested that the most favorable and preferred configurations are edge-to-face and offset stacking (73). The experimental and theoretical binding energy of benzene dimers in edge-to-face and offset stacking configuration was determined to be small, 2~3 kcal/mol. Rashkin and Waters (81) presented the unexpected substituent effects in an offset stacked configuration which is believed to be the most common geometry but studied least well. The observation in meta- and para-substituted *N*-benzyl-2-(fluorophenyl)-pyridinium bromide indicated that the orientation of the rings has a significant effect on the magnitude of the offset stacked interactions.

It was proposed that direct interaction between the ring hydrogen and the substituents might influence the magnitude of the interaction, based on the different rotational barrier around the biaryl bond observed for meta- and para-substituents. A face-to-face configuration is always favored by van der Waals forces and hydrophobic effects, but generally disfavored by  $\pi$ - $\pi$  repulsion. A significant driving force for face-to-face stacked geometry could be provided by the complementary electrostatic interaction between electron sufficient and electron deficient aromatic surfaces in solution (84). The face-to-face stacked geometry was observed in the interaction between benzene with perfluorobenzene, in particular hexafluorobenzene (72, 81). Quadrupole moment arising from the aromatic  $\pi$  clouds is changed by introducing substituents on the aromatic motif. Benzene and hexafluorobenzene have quadrupole moments similar in magnitude, but opposite in sign. Face-to-face stacking of the alternative molecules of benzene and hexafluorobenzene can be explained by the minimization of quadrupole-quadrupole interaction energy (85). The quantitative investigation of the intermolecular pentafluorophenyl-aryl interaction showed that electron-donating substituents increase the negative charge on the face of the aryl ring and lead to a strong driving force for the aryl ring to stack with the pentafluorophenyl ring. In this geometry, the high electron density is sitting over the center of the positive charges on the pentafluorophenyl group (72).

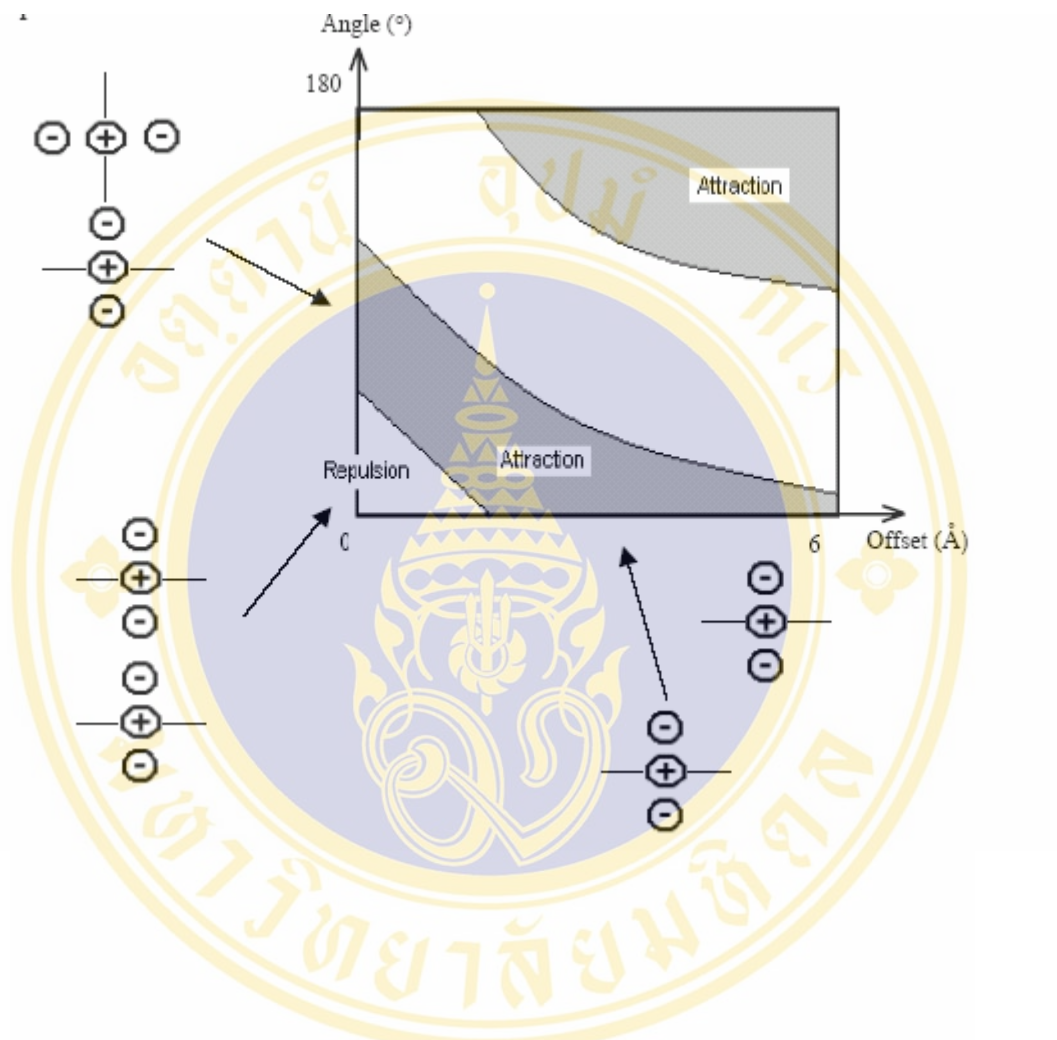


**Figure 7.** Electrostatic interactions between nonpolar  $\pi$  systems as a function of orientation (82).

Aedamers in aqueous solutions were also reported to adopt a compact pleated structure in which aromatic rings stack in a face-to-face geometry (86). Solvent effects in aromatic stacking interaction were reported by some authors (76, 84). From the investigation of the  $^1\text{H-NMR}$  binding constant studies of aedamer in a variety of solvents varying a polarity, Cubberley et al. (84) presented that complexation between electron rich and electron deficient aromatic derivatives is driven mainly by the hydrophobic interaction. An association constant increased with increasing the solvent polarity, suggesting the complexation results from a hydrophobic interaction. However, the magnitude of the hydrophobic interaction, desolvation is modulated by stacking geometry, which is dictated by aromatic electron donor-acceptor interactions in solvents of different polarity.

### 3. Application of chitosan derivatives nanoparticles

Despite its biocompatibility, the using of chitosan in biomedical fields is limited by its poor solubility in physiological media. Chitosan has an apparent pKa value between 5.5 and 6.5 and upon dissolution in acid media the amino groups of the polymer are protonated rendering the molecule positively charged. At neutral and alkaline pH, most chitosan molecules lose their charge and precipitate from solution. To improve the poor water-solubility of chitosan at physiological pH and dissolve those problem, several derivatives have been studied; for example, the modification of chitosan by quaternization of the amino groups (87, 88), N-carboxymethylation (89) and PEGylation (90, 91), *N*-octyl-*O*-sulfate chitosan (8), Trimethyl-chitosan poly-(epsilon-caprolactone) (14) additionally it was successful to be drug delivery. The example of chitosan derivative based delivery of drug as following Table 2. In our previous study, we have modified chitosan by conjugate with both phthanoyl group and PEG based on balancing of polarity on the chitosan chain in order to obtain novel derivatives. *N*-phthaloyl chitosan grafted poly (ethylene glycol) methyl ether (mPEG) (PLC -g-m PEG) which showed self-assembly nanolevel sphere-like particles (80-170 nm) (20). For this study, *N*-phthaloyl chitosan-g-mPEG use chitosan with 90% deacetylation  $M_v = 1.7 \times 10^5$  and mPEG with 5,000 Da. The structure of synthetic copolymer have been reproduced and characterized by NMR. The structure was reveal as the Figure 8.

**Table 2.** Studies using chitosan based delivery systems for drug.

Polymer	Delivery system/purpose	Reference
Chitosan	Nanoparticles	[3]
Trimethyl-chitosan poly-(epsilon-caprolactone)	DNA complex	[14]
N-Alkylated chitosan	DNA complex	[14]
N-Acetyllated chitosan	DNA complex	[16]
Galactosylated chitosan-graft-PEG	DNA complex	[17]
Deoxycholic acid-modified chitosan	DNA complex	[6]
Glycol-chitosan	Doxorubicin	[18]
	Paclitaxel	[4]
<i>N</i> -octyl- <i>O</i> -sulfate chitosan	Paclitaxel	[8]
Chitosan-glutaraldehyde	5-fluorouracil	[19]

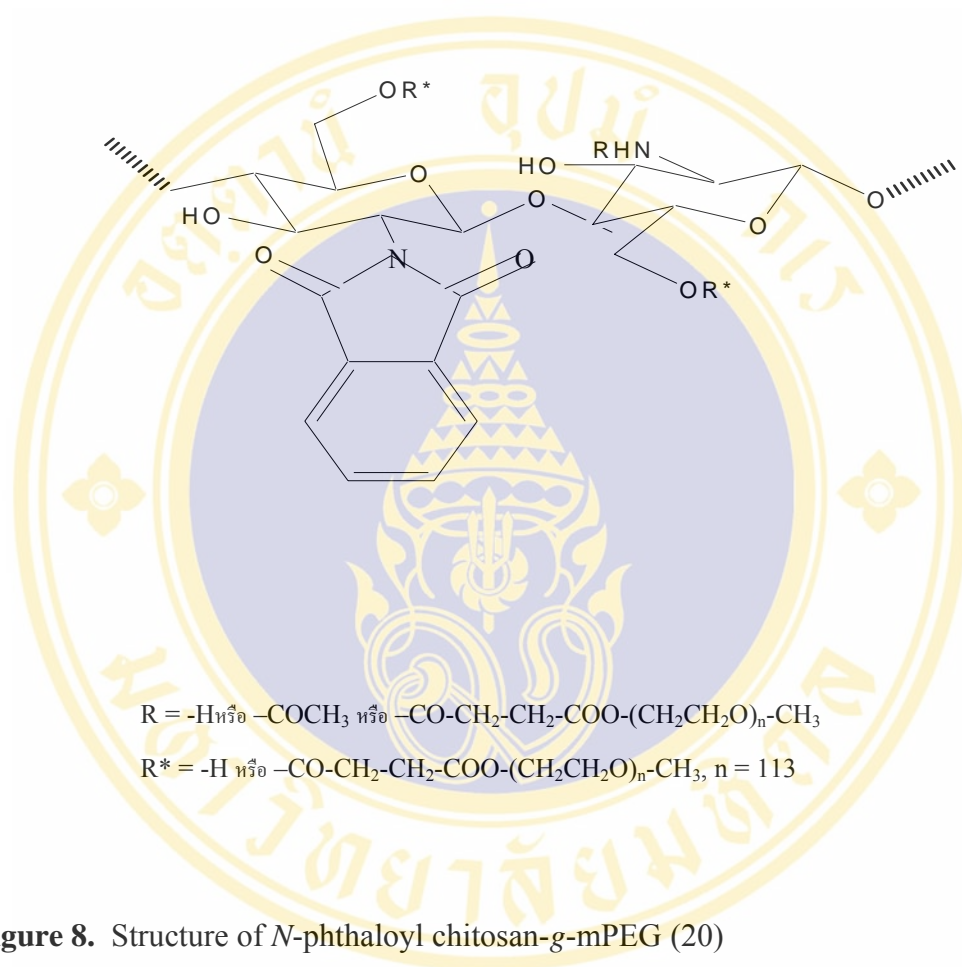


**Figure 8.** Structure of *N*-phthaloyl chitosan-*g*-mPEG (20)

## CHATER III

### MATERIALS AND METHODS

#### MATERIALS

##### Chemicals

1. DMF (Fluka Chemika, Switzerland).
2. Acetonitrile (Fisher Scientific,UK)
3. Methanol (Fisher Scientific,UK)
4. Potassium dihydrogen phosphate (Univar,New zealand)
5. Sterile water for injection (General Hospital Products, Thailand)
6. Distilled water (Mahidol University,Thailand)
7. Sodium hydroxide pellets (Merck K GaA, Darmstadt, Germany)

##### Commercially available clotrimazole products

1. Commercially available clotrimazole products from Thailand (TO chemical ,Ltd., Thailand)

##### Supported available copolymer products

1. *N*-phthaloyl chitosan-*g*-mPEG (90% of deacetylation of chitosan, The Petroleum and Petrochemical College Chulalongkorn University, Bangkok)

##### Equipments

1. Beaker (50, 100, 250, 600, 1000 ml)
2. Volumetric flask (10, 25, 50, 100, 500, 1000 ml)
3. Cylinder (10, 50, 100, 1000 ml)
4. Micropipette (20-200  $\mu$ l)
5. Micropipette (100-1000  $\mu$ l)
6. Measuring pipette (2 ml,5 ml, 10 ml)
7. Cellulose acetate membrane filter, 0.45  $\mu$ m
8. Nylon Membrane filter, 0.45 $\mu$ m

9. Stainless steel forceps
10. Thermometer
11. Water bath
12. Thermostat (B. Braun, Melsungen, Germany)
13. Magnetic stirrer
14. Photon Correlation Spectroscopy (Coulter<sup>®</sup> N<sup>4</sup>D, Germany)
15. Centrifuge (Kubota model 6930, Japan)
16. Franz cell apparatus (Kubota model 6930, Japan)
17. Lyophilizer (Chirst Alpha 1-4, Germany)
18. Transmission Electron Microscopy (TEM, JEM 2100, Chulalong  
University, Thailand)
19. High performance liquid chromatography (HPLC)  
Pressure pump (LC-10AD, Shimadzu, Japan)  
UV absorbance detector (SPD-10AV, Shimadzu, Japan)  
Autosampler (SIL-10A autoinjector, Shimadzu, Japan)  
 $\mu$  Bondapak Hypersil C18 column 5  $\mu$ m, 150 x 4.6 mm (Thermo electron  
corporation, UK)
20. Zeta Malvern Nanosizer (Malvern Instruments, UK)
21. Thermogravimetry analyzer (Germany)

## Methods

### 1. Validation of HPLC method

#### 1.1. Separation and specificity

The separation of the analytical methods was assessed in relation to interference peaks from blank medium (phosphate buffer saline of pH 7.4 with 50% methanol) and blank solution (extracted solution of non-drug-loaded nanoparticles). The specificity was assessed from drug-free constituents by comparing their relation times with clotrimazole standard solution.

#### 1.2. Linearity

Linearity of standard curve was assessed from the square of correlation coefficient ( $R^2$ ) which determined by least-square linear regression analysis of variation (%CV)

### 3.3. The limit of quantitation

The limit of quantitation (LOQ) is defined as the lowest concentration on the standard curve which can be measured with acceptable precision (%CV < 10) and the limit of quantitation was determined by add various known amount of clotrimazole in methanol solution. The lowest concentration of clotrimazole on the standard curve which still be linearly correlated and measured with acceptable precision (%CV < 10) was the limit of quantitation of the assay.

### 3.4. Precision and accuracy

Precision of the assay procedure was assessed from the percentage of coefficient variation (%CV).

The percentage of coefficient of variation (%CV) was calculated by the following equation:

$$\%CV = \frac{SD \times 100}{\bar{X}}$$

Where: SD = standard deviation

$\bar{X}$  = mean value of clotrimazole concentration

## 2. Validation of the extracting method.

The performance of the extracting method, which used methanol to extract clotrimazole from nano-suspension and freeze dried nanoparticles were assessed from the percentage of clotrimazole recovery by following this method. Five hundred  $\mu$ l of the blank nano-suspension were added by known amount of clotrimazole and adjusted by methanol to 1 ml in the same 1.5 ml volumetric tip. Subsequent, clotrimazole was extracted by centrifuge at 10,000 rpm for 10 minutes 25 ° C. Also, the freeze dried nanoparticles were added by known amount of clotrimazole and treated by the same above method. All of experiment were triplicate.

The percentage of recovery was calculated by the following equation:

$$\% \text{ recovery} = \frac{\text{content of extracted clotrimazole} \times 100}{\text{Initial adding content of clotrimazole}}$$

### 3. Preformulation.

#### 3.1. Screening suitable solvent to dissolve the copolymer.

The *N*-phthaloyl chitosan-*g*-mPEG was accurately weighing 5 mg. After that, 10 ml of the solvent was dropped to the copolymer until the clear solution. The characteristics of the copolymer in the aqueous solution such as water, methanol, chloroform and DMF were observed by visual method.

#### 3.2. Screening suitable concentration of the copolymer.

The suitable concentration of the copolymer to prepare drug-loaded nanoparticles was assessed from the particle size by direct observing by TEM. The preparation drug-loaded nanoparticles were conducted by following:

##### **Preparation of colloidal suspension by dialysis method (97).**

First, to make mixed solution compose of the polymer and clotrimazole by following, accurately weighing *N*-phthaloyl chitosan-*g*-mPEG and transfer to 5 ml volumetric flask. Then aliquot stock solution or accurately weighing powder of clotrimazole transfer to same 5 ml volumetric flask qs. DMF until 5 ml. The mixed solution was stirrer for overnight in dark room (incubation). After finishing, the mixed solution was transfer to membrane cellulose acetate to dialysis against 2 L of distilled water. The water was changed 8 times with in 48 hours. After finishing the preparation, the milky solution was stored at 4 °C.

To investigate the effect of dialyzed medium, the same experiment was established but varying condition such as distilled water, 0.02 M phosphate buffer pH 7.4 and pH 5.5.

To investigate the effect of stirring time, the experiment was established by using distilled water but varying the stirring time to non-use stirring and use stirring for the first three hours of dialysis time.

### 4. Characterization of colloidal solution

#### 4.1. Particle size and morphology by transmission electron microscopy (TEM)

Size and the internal morphology of the nanoparticles can investigate by TEM by following; the milky solution was diluted by distilled water about 10 times. Then sonicate diluted solution for 30 minutes to disperse particles. After that, one drop of it

was dropped into tungsten grid and dried it in open air for one day. The prepared grid was kept in desiccator before examination.

#### **4.2 Mean particle size and polydispersity index by photon correlation spectroscopy (PCS)**

It is a light scattering experiment in which the statistical intensity fluctuations in light scattered from the particle are measured. These fluctuations are due to the random Brownian motion of the particles. Particles size approximately 5 nm -3  $\mu\text{m}$  is suitable to use this device. And the polydispersity index in range 0.01 to 0.1 mean narrow distribution size, 0.1 to 1.0 mean broad distribution size, if  $PI=0$  it mean monodisperse. In the present work, For PCS measurements all samples have been diluted with double distilled water to suitable concentration and measured by PCS apparatus in six times.

#### **4.3. Zeta potential ( $\zeta$ , ZP)**

Zeta potential is useful for the assessment of the physical stability of colloid dispersion in various mediums and characterizes the surface chemistry of the particles. Surface of particles in suspension develop a charge due to adsorption of ions or ionization of surface groups and the charge is correspondingly dependent on both the surface chemistry and the environment of the particles.

For this experiment the colloid suspension had been diluted with sterile water for in injection, PBS pH 5.5 and PBS pH 7.4 adjusted to conductivity 50  $\mu\text{S}/\text{cm}$  before measured. All of the measurements are triplicate.

#### **4.4. Residue solvent by thermal gravimetry analysis (TGA)**

The freeze dry sample, such as clotrimazole, blank nanoparticles or clotrimazole nanoparticles (approx. 2-5 mg) were placed in alumina crucibles for TGA. The weight loss was measured during heating from 25 $^{\circ}\text{C}$  to 600  $^{\circ}\text{C}$  at a heating rate of 10  $^{\circ}\text{C}/\text{min}$  followed by holding at 60 min. The percentage of weight loss of residue solvent was the difference between the initial weight at 0  $^{\circ}\text{C}$  and the final weight at 158  $^{\circ}\text{C}$ .

#### 4.5 Determination of encapsulation efficiency

The percentage drug loading was calculated from the actual drug loading with respect to weight of drug-loaded nanoparticles. The drug loading was calculated as:

$$\% \text{ Drug loading} = \frac{\text{Amount of drug (wt)} \times 100}{\text{Amount of nanoparticles (wt)}}$$

The percentage of encapsulation efficiency was calculated from the theoretical loading of drug in the nanoparticles respect to the initial drug loading.

$$\% \text{ Drug encapsulation efficiency} = \frac{\text{Amount of drug (wt)} \times 100}{\text{Initial drug loading (wt)}}$$

The drug content of clotrimazole was obtained from HPLC condition. The drug was extracted by methanol with centrifuge at 10,000 rpm for 10minutes.

#### 4.6. The in vitro release profile

The in vitro release studies of clotrimazole colloidal suspension were performed by placing accurately 500  $\mu\text{l}$  of sample into the donor part of Franz cell and subsequently adding of 10 ml pre-warmed release medium (phosphate buffer pH 7.4 containing methanol 1:1). Then, they were horizontally shaken at 37  $^{\circ}\text{C}$  using a temperature controlled shaker (200 rpm). At predetermined time intervals 500  $\mu\text{L}$  were withdrawn through the filtered needle and the same volume of fresh medium was replaced. The drug concentration was measured by HPLC condition. Each experiment was conducted in duplicate.

#### 4.7. Stability study

The physical stability of colloid suspension was investigated by the observing the turbidity of colloidal suspension.

The chemical stability of the drug was assessed from the percentage of the existing clotrimazole concentration after storing at 4  $^{\circ}\text{C}$  for 1 month. All of the experiment were triplicate.

#### 4.8. HPLC condition

Column	Hypersil ODS $\mu$ Bondapak C18, 5 $\mu$ m, 150 x 4.6 mm
Mobile phase	Methanol:Acetonitrile:0.02 M Phosphate buffer pH 6.8 (40:35:30)
Flow rate	1.2 ml/min
Detector	UV detector 254
Injection volume	20 $\mu$ l
Temperature	25 $^{\circ}$ C

#### 5. Data analysis

Statistic analysis for comparison of percentage of drug encapsulation efficiency (%DE), percentage of drug loading (%DL), mean particle size, polydispersity index and stirring time was performed employing one-way analysis of variance (ANOVA).

## CHAPTER IV

### RESULTS AND DISCUSSIONS

#### 1. High Performance Liquid Chromatography Analysis and Validation Method

##### 1.1 Separation and specificity

Figure 9 and Figure 10 show the typical chromatograms obtained from HPLC analysis of blank medium (phosphate buffer pH 7.4 with 50% methanol, medium for the experiment of drug release study,) and blank solution (the extracted solution of blank nanoparticles) respectively. Both of chromatogram were base line and did not have any interfere peaks. Chromatograms of the extracted solution from drug-loaded *N*-phthanoylchitosan-g-mPEG and drug release showed peak at 7.5 min as Figure 11. Those have the same retention time with the standard solution (Figure 12).

##### 1.2. Linearity

The linearity was demonstrated by multiple analyses of standard solution, with a series of concentration ranging from 750 ng/ml to 300 µg/ml. The average peak areas (n=5) at corresponding concentrations are presented in Table 3. The linear regression equation of the standard curve between absorbance at 254 nm (Y) versus clotrimazole concentration (X) was

$$Y = 1570X + 1559.2$$

It showed a good linear relationship with square of correlation coefficient ( $R^2$ ) of 0.9997 (Figure 13).

##### 1.3. The limit of quantitation (LOQ)

The limit of quantitation was established at 750 ng/ml (0.75 µg/ml) with coefficient of variation of 7.49%. It was represented in Table 3.

#### 1.4 Precision and accuracy

The within-run (intraday) precision expressed from the percentage of coefficient of variation (%CV). The %CV of each concentrations between 0.75 µg/ml to 300 µg/ml were presented in Table 3.

The between-run (interday) precision was assessed from the percentage of coefficient of variation (%CV) in three day.

### 2. Validation of the Extraction Method

Clotrimazole was extracted by methanol from the blank nano-suspension. The recovery of clotrimazole was  $93.12 \pm 6.46\%$ . When using methanol to extract clotrimazole from freeze dried blank nanoparticles. The recovery was  $107.20 \pm 0.34\%$ .

### 3. Preformulation Studies

#### 3.1. Screening suitable solvent to dissolve *N*-phathanoyl chitosan– g-mPEG

The copolymer was dissolved in 10 ml of water, methanol, chloroform or DMF. The characteristics of copolymer solution are presented in Table 5.

The results showed that only DMF could completely dissolve the copolymer. Compare with other solvents, 10 ml of chloroforms could not completely dissolve (cloudy solution). Either 10 ml of water or methanol precipitated the copolymer.

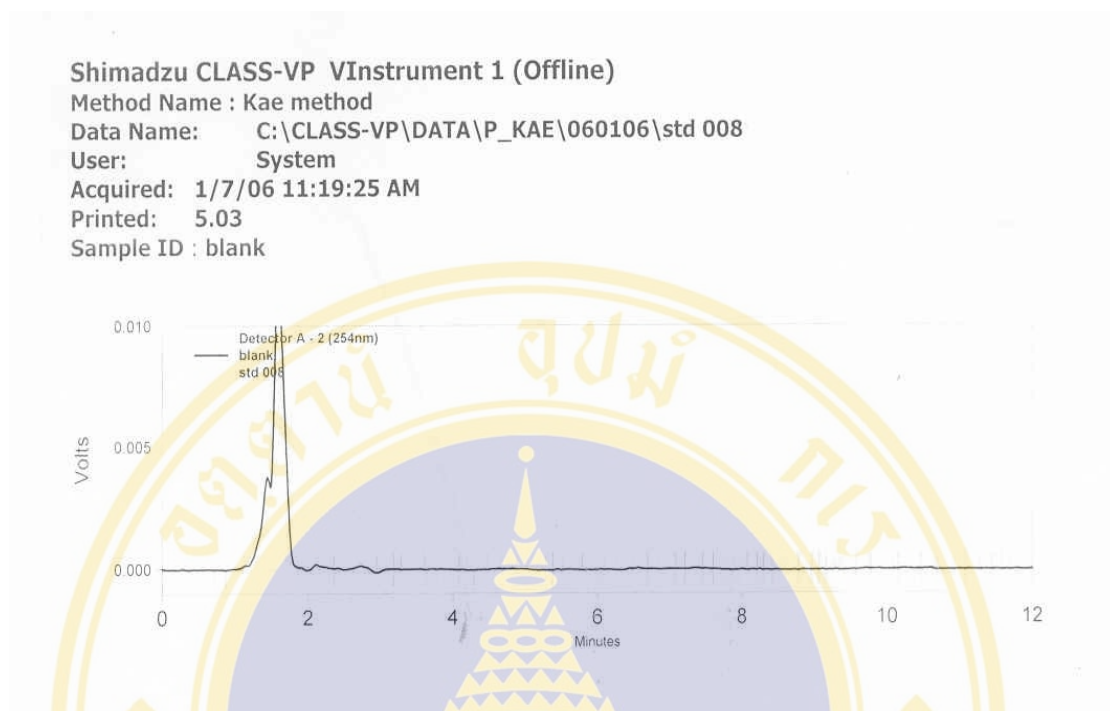


**Figure 9.** Chromatogram of buffer pH 7.4 with 50% methanol, medium for the experiment of drug release study

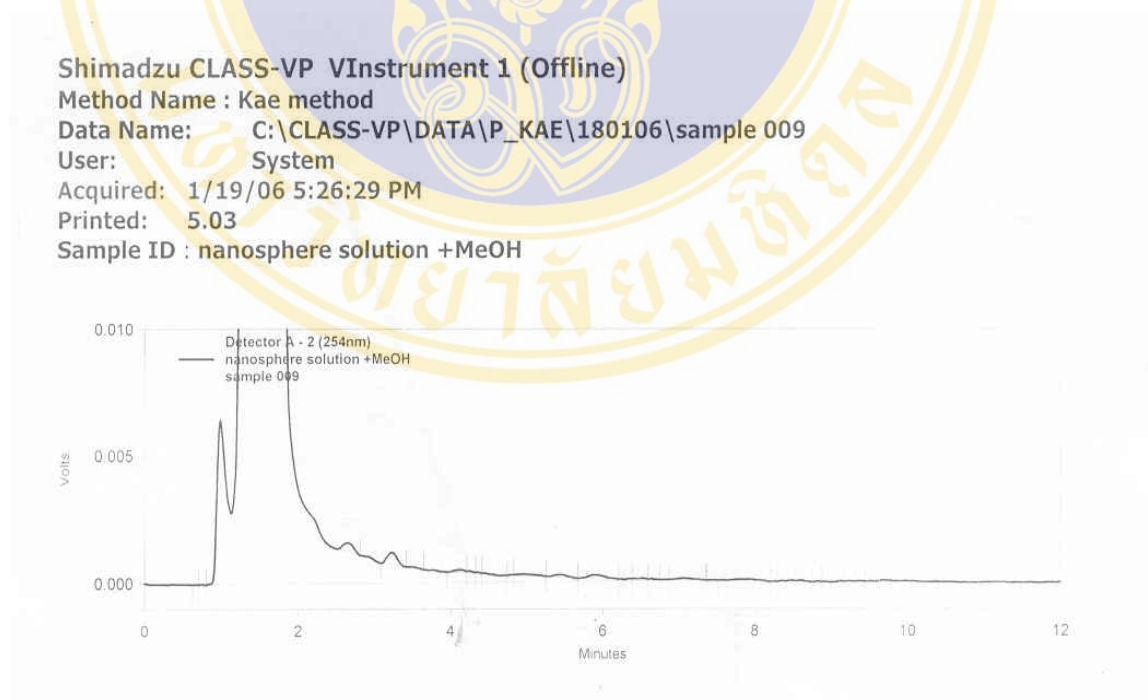


**Figure 10.** Chromatogram of the extracted solution of the non-drug loaded nanoparticles.

Method Name: C:\CLASS-VP\Methods\kaemethod\kaeclotrimazole 2.met  
 Data Name: C:\CLASS-VP\Sequence\kae\A2 09 24 001  
 User: System  
 Printed: 6.10  
 Sample : A 09 batch5 no.2drug release 24 hr

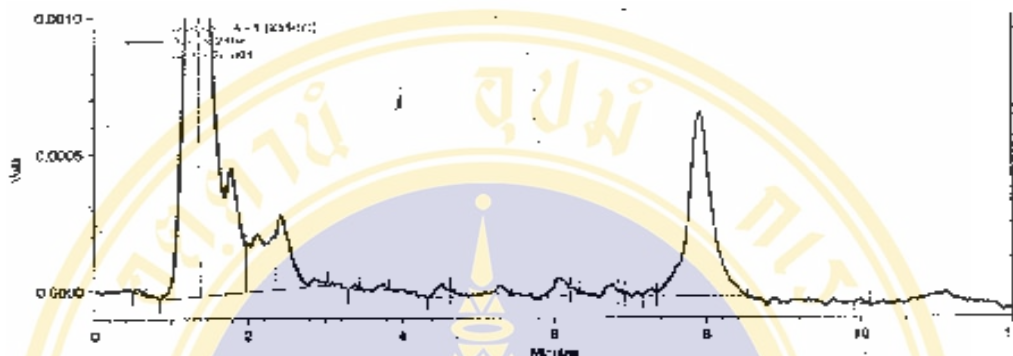


**Figure 11.** Chromatogram of clotrimazole from drug release study.

Method Name: C:\CLASS-VP\Methods\kaemethod\kaeclotrimazole 2.met  
 Data Name: C:\CLASS-VP\Data\kae\130307\sample 033  
 User: System  
 Printed: 6.10  
 Sample : CLT 6 mcg/ml

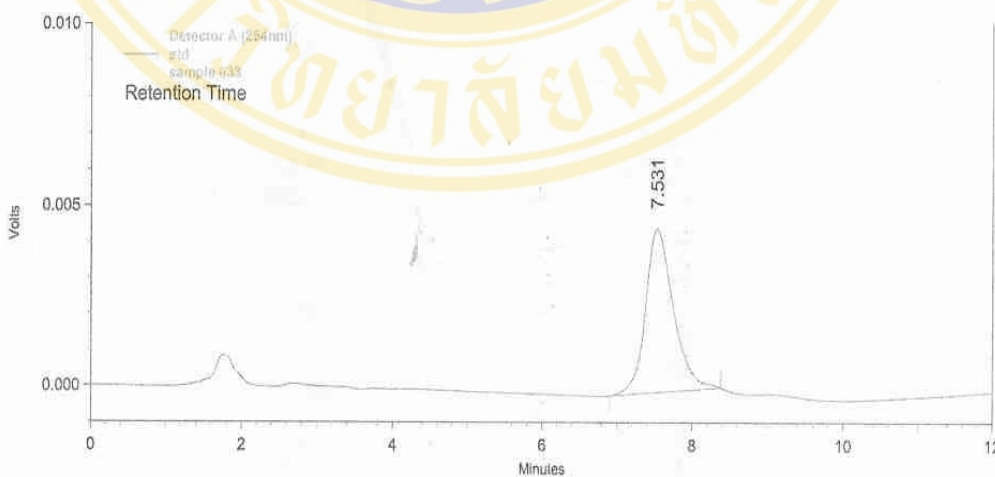


**Figure 12.** Chromatogram of clotrimazole standard solution.

**Table 3.** Average peak area versus concentrations of clotrimazole standard solution and percentage of coefficient of variation (%CV).

Concentration	Average peak area	% CV
0.75 µg/ml	1733	7.49
1.5 µg/ml	2920	6.67
3 µg/ml	5116	5.50
6 µg/ml	9373	3.76
15 µg/ml	24785	1.04
75 µg/ml	122930	0.79
150 µg/ml	241642	1.74
300 µg/ml	469412	0.93

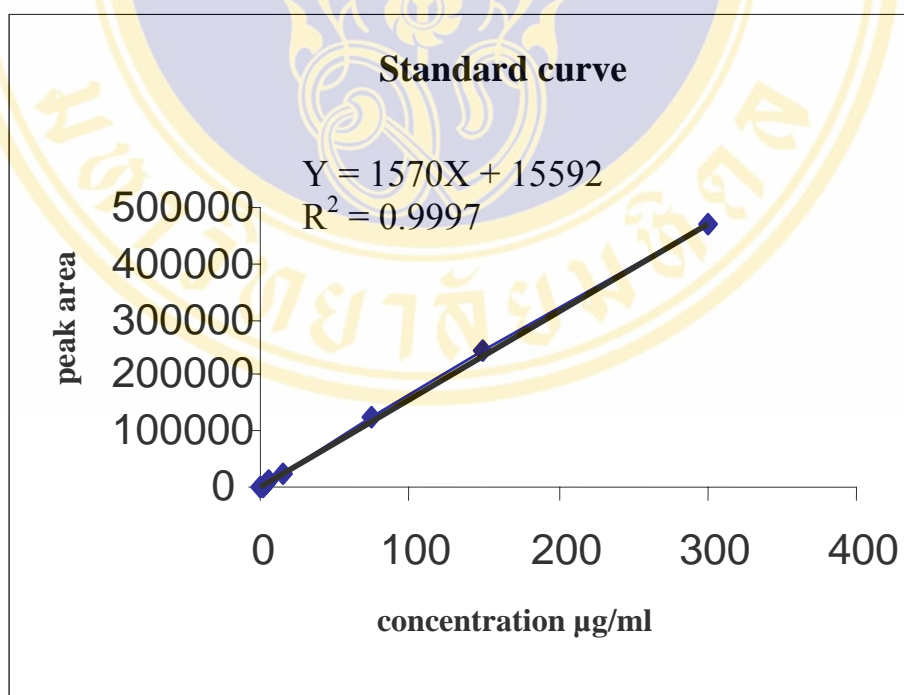


**Figure 13.** Standard curve and linear equation.

**Table 4.** Average of peak area (n=5) with percentage of coefficient of variation for three days corresponding to 150 µg/ml of clotrimazole standard solution.

Concentration	Average peak area (n=5)			
	Day 1	Day 2	Day 3	%CV
150 µg/ml	24785.40	22011.40	21500.40	6.68

**Table 5.** Represent characteristics of copolymer in various solvent.

Solvent	Results
Water	Precipitate
Methanol	Precipitate
Chloroform	Cloudy solution
DMF	Clear solution

### **3.2. Screening suitable concentration of the copolymer based on particle size.**

The percentage of initial drug loading was 50% weight by weight to the copolymer. To investigate the appropriate concentration of copolymer solution to obtain desired nanosize of drug-loaded nanoparticles, two concentrations of the copolymer solution, 3.0 mg/ml and 11.56 mg/ml, were chosen to prepare nanosuspension. Firstly, the mixture solution of each known concentration of the copolymer with the ratio of clotrimazole loading 50% weight by weight to the copolymer were incubated for 24 hours. Subsequently, the mixture of solution was transferred to dialysis bag and dialyzed against distilled water with constant stirrer for 48 hours. The distilled water was changed every 8 hours. After finishing the preparation, the nanoparticles were directly observed by TEM. The morphology of clotrimazole-loaded nanoparticles prepared from 11.56 mg/ml and 3.0 mg/ml of the copolymer solution are showed in Figure 14 and Figure 15, respectively.

The particle of clotrimazole-loaded nanoparticles using 3.0 mg/ml of the copolymer showed a spherical shape in the acceptable range size of 160-600 nm, less than 1  $\mu\text{m}$ , with the percentage of drug encapsulation efficiency (%DE) of 23.64%. In case of using 11.56 mg/ml of the copolymer, the particle of clotrimazole-loaded nanoparticles was a rod shape with the size of about 1100 nm; however, the percentage of drug encapsulation efficiency (%DE) was not evaluated. The results showed that in comparison of the particle size of clotrimazole-loaded nanoparticles, the lower concentration of the copolymer possessed smaller size than the higher concentration. Therefore, it could be concluded that the concentration of the copolymer solution affected on the particle sizes of clotrimazole-loaded nanoparticles. This result is in agreement with Vangeyte et al. (92) that the concentration of the copolymer significantly impact on the particle size and polydispersity index of nanoparticles.

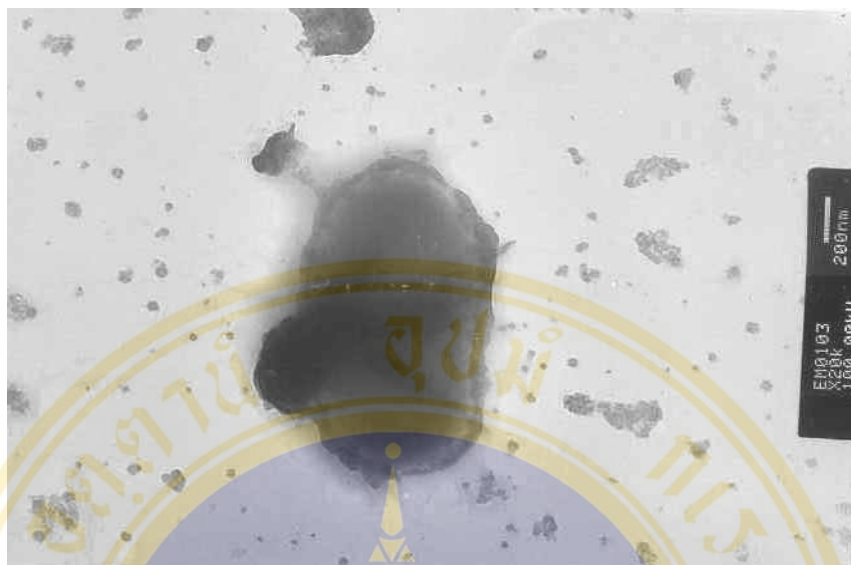


**Figure 14.** Morphology of CLT-loaded nanoparticles with using 11.56 mg/ml of the copolymer and initial drug loaded 50% w/w.

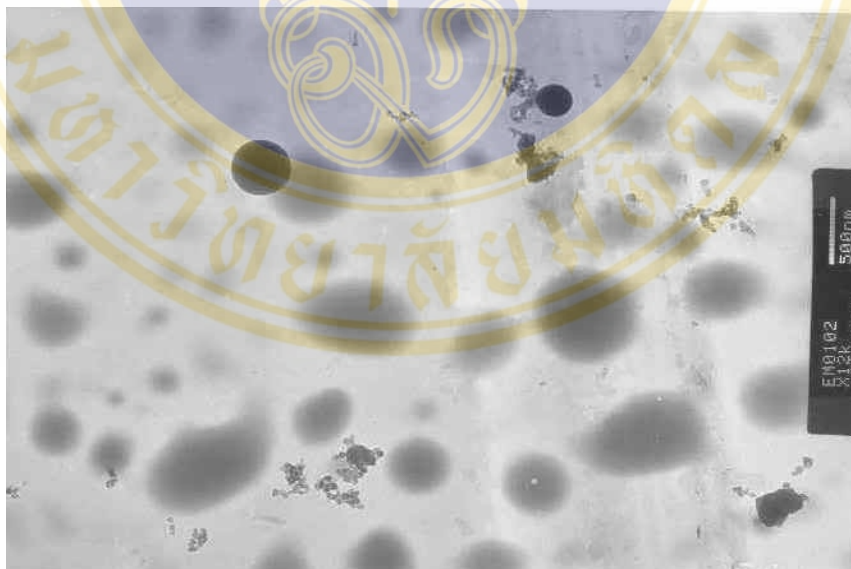


**Figure 15.** Morphology of CLT-loaded nanoparticles with using 3.0 mg/ml of the copolymer and initial drug loaded 50% w/w.

## 4. Characterization of CLT-Loaded Nanoparticles

### 4.1. Method I

This method was modified from above method by increasing the concentration from 3.0 mg/ml to 3.33 mg/ml and decreased the changing of distilled water from every 8 hours to 1 hour in the first three hours of dialysis and following by changing distilled every 6 hr and 12 hours until 48 hours. After finishing the preparation, the nanoparticles were observed by TEM.

#### 4.1.1. Morphology by TEM

During the preparation by this method, the mixture of copolymer and drug changed to milky suspension thoroughly within 30 minutes and the white precipitates were found in the bag. The similar observation was found in the control suspension. When observed by TEM, the uniform particle size of bare nanoparticles was 133 nm with the aggregation of particles. After loading clotrimazole, the particle size of drug-loaded nanoparticles increased approximately 80–250 nm as compared with that of drug-free nanoparticles. Concerning the shape of drug-free and drug-loaded nanoparticles, it almost was spherical with the low degree of aggregation. According to above results, it could be deduced that the increasing in the particle size of drug-loaded nanoparticles compared with bare nanoparticles might be due to the incorporation of clotrimazole in the core nanoparticles. The morphology of clotrimazole-loaded nanoparticles and bare nanoparticles are showed in Figure 16 A-C and Figure 16 D respectively.

#### 4.1.2. Mean particle size and polydispersity index

Mean particle size calculated from particle size of the population nanoparticles, and polydispersity index referring to size distribution and degree of aggregation of the particles (the latter was noticed from experiment that the PI of aggregation particles was more than 0.50) were obtained from PCS.

The mean particles size and the PI of bare nanoparticles (control) were  $81.75 \pm 1.56$  nm and  $0.34 \pm 0.04$ , respectively. After loading clotrimazole, the mean particle size and the PI were significantly increased to  $215.09 \pm 19.15$  nm and  $0.435 \pm 0.03$ , respectively ( $P < 0.05$ ). The PI of bare nanoparticles was lower than that of drug-loaded nanoparticles which was due to the uniform size of the former one whereas the latter one showed broad range size. However, the mean particles size of

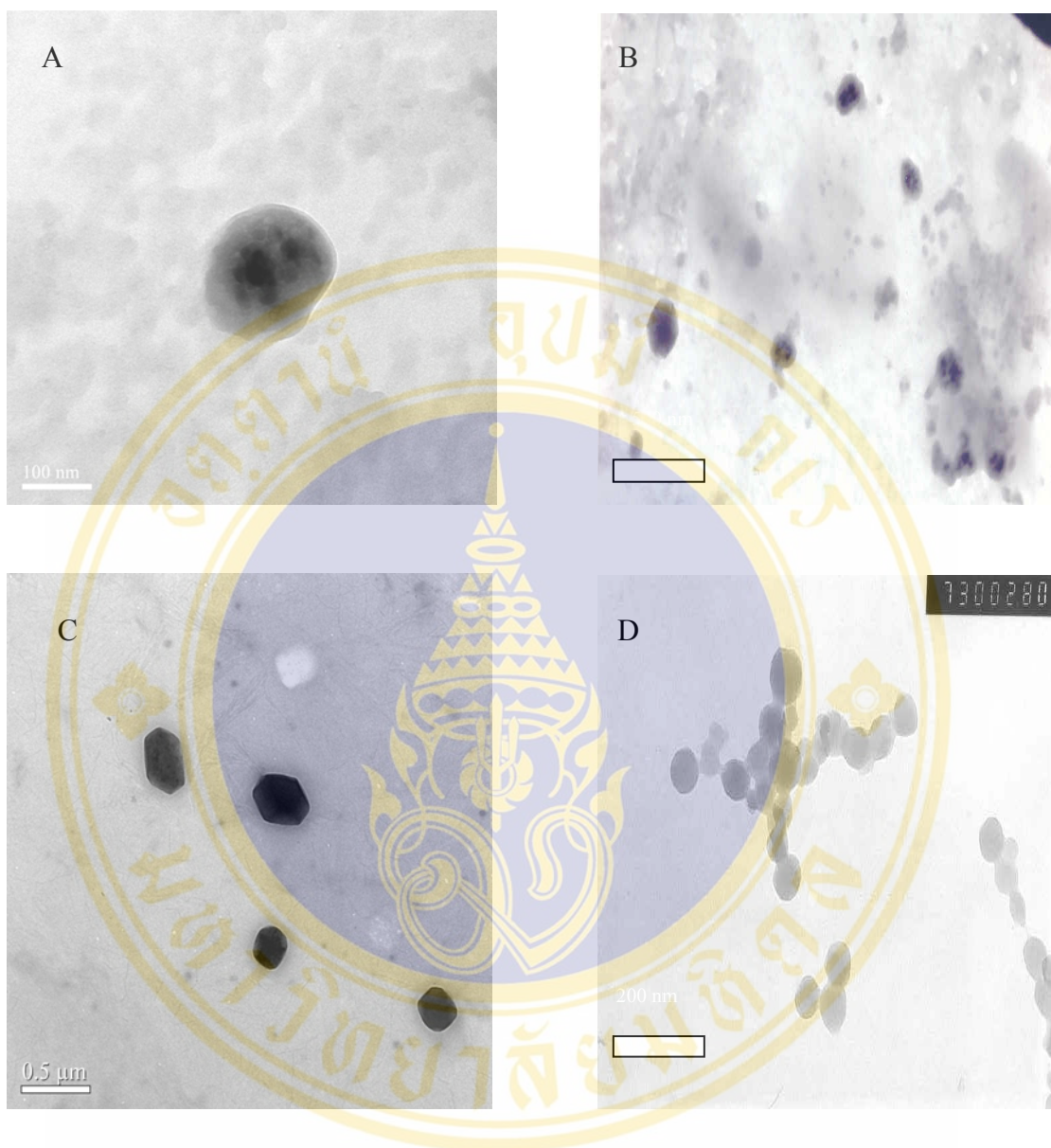


**Figure 16.** A-C show morphology of CLT-loaded nanoparticles and D show bare nanoparticles were prepared by dialysis against distilled water with constant stirring.

drug-loaded nanoparticles obtained from PCS showed consistent with the particle size from TEM. On the other hand, the mean particles size of bare nanoparticles was not consistent. The results are presented in Table 6 and 7.

#### **4.1.3. Percentage of drug loading (%DL).**

The average %DL obtained from two batches of drug-loaded nanoparticles was  $5.06 \pm 0.2$  %.

#### **4.1.4. Percentage of drug encapsulation efficiency (%DE).**

The average %DE obtained from two batches of drug-loaded nanoparticle was  $8.08 \pm 0.21$ %.

#### **4.1.5. Differential scanning calorimetry.**

The physical status of clotrimazole inside the nanoparticles and residue solvent were further studied by thermal analysis. According to Table 10, clotrimazole powder exhibited a melting point of  $144.4^{\circ}\text{C}$ . Interestingly, the melting point of clotrimazole was not observed in the clotrimazole-loaded nanoparticles, indicating that clotrimazole molecules were completely included or dissolved within the nanoparticles. The similar finding was also reported by Memisoğlu et al (9). In addition, bare nanoparticles showed a glass transition temperature, which was approximately at  $360.2^{\circ}\text{C}$  (Table 10). After loading of clotrimazole,  $T_g$  of drug-loaded micelles slightly decreased to  $348.5^{\circ}\text{C}$  (Table 10).

Since the boiling point of DMF is  $158^{\circ}\text{C}$ . Therefore, the weight loss of clotrimazole-loaded and bare nanoparticles from  $0^{\circ}\text{C}$  to  $158^{\circ}\text{C}$  associated with the loss of DMF owing to evaporation (data not shown). The method is useful tool for evaluating the residue solvent in the nanoparticles. Regarding the TGA data, the weigh loss of bare nanoparticles and clotrimazole-loaded nanoparticles in the range of temperatures from  $0^{\circ}\text{C}$  to  $158^{\circ}\text{C}$  was 3.94% and 8.95%, respectively (Table 11).

#### **4.1.6. Physical stability.**

The stability of the dispersion can be clarified by the separation of the suspension into two phases, i.e. precipitate and clear supernatant. This was used to determine instability of the colloidal dispersion. Nanoparticles containing clotrimazole showed stability for 10 days indicated by absence of the separation of dispersion. During stored 1 month at  $4^{\circ}\text{C}$ , the separation of suspension was found; however, it could be easily redispersed by hand shaking.

**Table 6.** Mean particle size of control and CLT-loaded nanoparticles were prepared by dialysis against distilled water with constant stirring (n=6).

Mean particle size			
Sample	Control	batch 1	batch 2
No.1	79.50	211	222
No.2	83.70	167	214
No.3	81.10	214	221
No.4	80.30	215	254
No.5	82.60	214	215
No.6	83.30	224	210
Average	81.75	207.50	222.67
SD	1.56	18.55	14.60

**Table 7.** Polydispersity index of control and CLT-loaded nanoparticles were prepared by dialysis against distilled water with constant stirring (n=6).

Polydispersity index			
Sample	Control	batch 1	batch 2
No.1	0.39	0.51	0.42
No.2	0.39	0.41	0.43
No.3	0.31	0.44	0.42
No.4	0.32	0.49	0.41
No.5	0.32	0.45	0.44
No.6	0.31	0.36	0.43
Average	0.34	0.44	0.43
SD	0.04	0.05	0.01

**Table 8.** Percentage of drug loading of CLT-loaded nanoparticles were prepared by dialysis against distilled water with constant stirring

% Drug loading		
Sample	batch 1	batch 2
no.1	4.39	5.99
no.2	4.21	5.65
Average	4.30	5.82
SD	0.15	0.24

**Table 9.** Percentage of drug encapsulation efficiency of CLT-loaded nanoparticles were prepared by dialysis against distilled water with constant stirring

% Drug encapsulation efficiency		
Sample	batch 1	batch 2
no.1	8.07	8.11
no.2	7.74	8.35
Average	7.90	8.23
SD	0.24	0.17

**Table 10.** Glass transition temperatures ( $T_g$ ) and melting points ( $T_m$ ) of CLT, bare nanoparticles, CLT-loaded nanoparticles, which were prepared by dialysis against distilled water with constant stirring.

	$T_g$ 1 <sup>st</sup> /°C	$T_g$ 2 <sup>nd</sup> /°C	$T_m$ /°C
Clotrimazole	-	-	144.4
Bare nanoparticles	360.2	-	-
Clotrimazole-loaded nanoparticles	348.5	-	-

**Table 11.** Percent residue solvent of bare nanoparticles and CLT-loaded nanoparticles, which were prepared by dialysis against distilled water with constant stirring

Formulation	Residue solvent
Bare nanoparticles	3.94%
Clotrimazole-loaded nanoparticles	8.95%

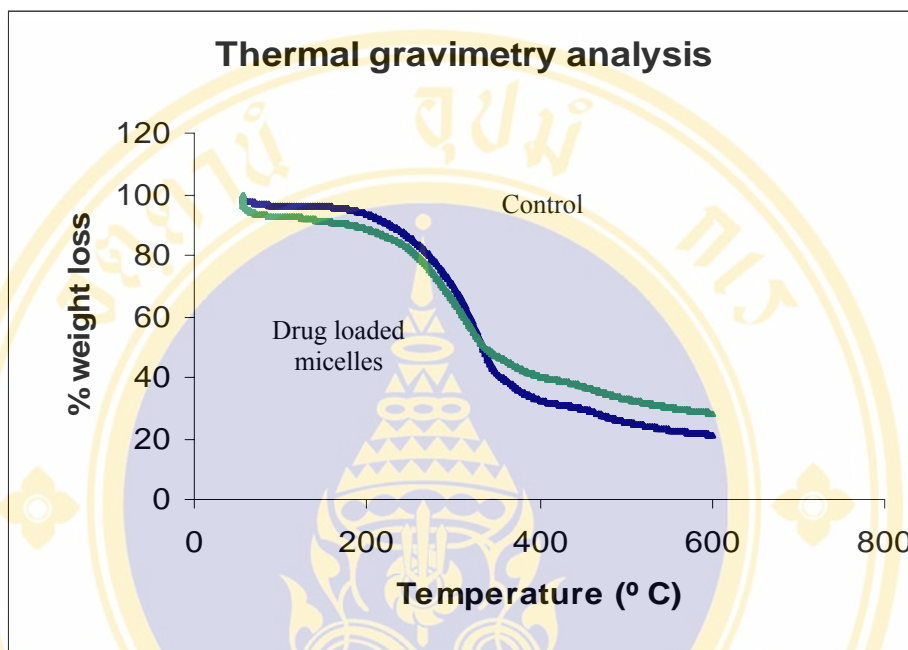


**Figure 17.** Curves represent percentage weight loss of bare nanoparticles and CLT-loaded nanoparticles, which were prepared by dialysis against distilled water with constant stirring, corresponding to temperature with rate of heating was 10° C/min

## 4.2 Method II

This method was modified from method I by using the 0.02 M PBS pH 5.5 as dialysis medium instead of distilled water.

### 4.2.1. Morphology by TEM

During the preparing, the mixture solution of the copolymer and the drug turned to white precipitate and agglomeration was found in the bottom of the bag within one hour. The agglomerating particles could disperse to be the milky suspension when it was dialysis against distilled water toward until 48 hours. After finishing, the milky suspension with floating large particles and a lot of the precipitate of particles were observed. The control had the same observation.

By TEM, the non-filtrated sample had a lot of the aggregation particles, they were irregular shape with large size more than 1  $\mu\text{m}$  (Figure 19). Because of the interfering from aggregation particles for observing by TEM, the nanosuspension was passed through 0.45  $\mu\text{m}$  pore size cellulose membrane filter for removing the aggregation particles. After removing aggregation particles, the morphology of the sample was changed dramatically to only discrete spherical particles. They were wide range size with 70 - 800 nm (Figure 18 A-C). Additional the percentage drug encapsulation efficiency (%DE) of the filtrated solution (batch 1) was 2.18% whereas the %DE of the non-filtrated sample was  $22.87 \pm 3.87\%$ . The results were found that the content of encapsulated clotrimazole of the filtrated sample were dramatically less than non-filtrated sample about 11 folds. It was deduced that the most of the drug located in the aggregated particles. When observing in the control nanosuspension, the most of the bare nanoparticles were the aggregation particles. It had a few nanospheres which having the size about 130 nm (Figure 18 D). The results cloud suggested that the presence of alkaline salts at pH 5.5 affected to the formation of nanosphere in the way to increased aggregation. But the addition of clotrimazole could be improved the formation of nanosphere.

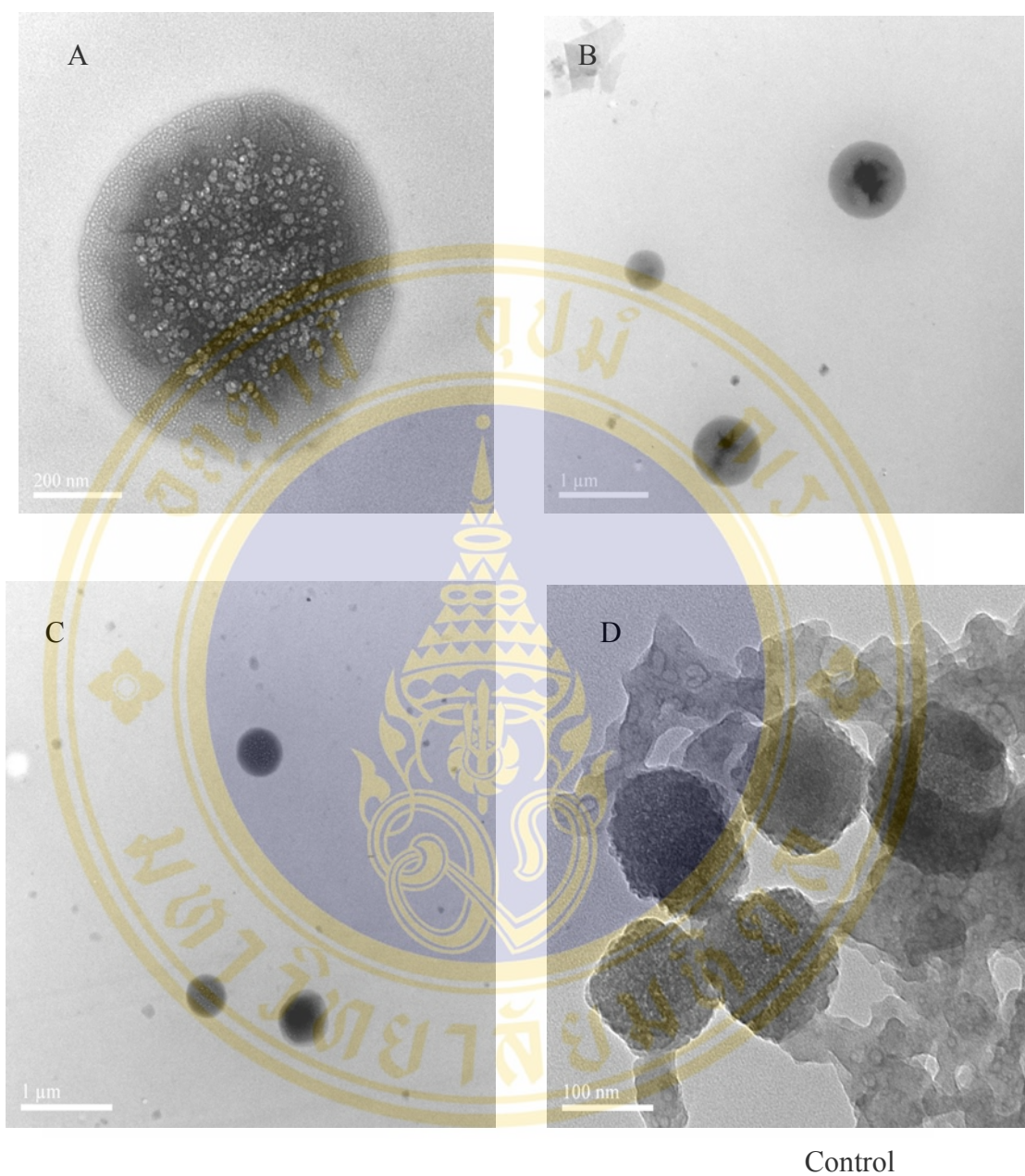


**Figure 18.** A-C show morphology of CLT-loaded nanoparticles and D show bare nanoparticles were prepared by dialysis against 0.02 M PBS pH 5.5 with constant stirring.

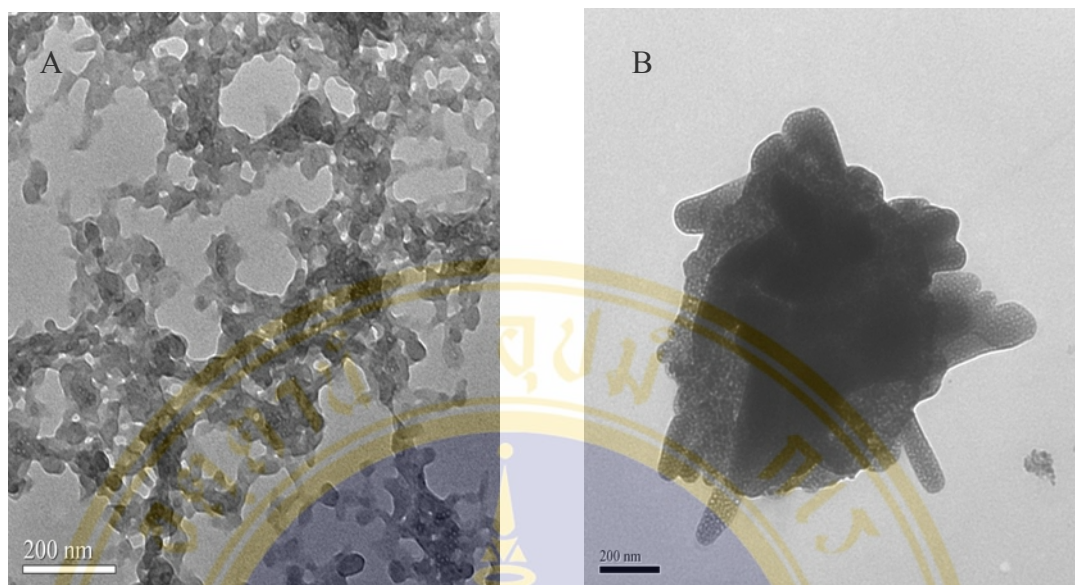


**Figure 19.** Aggregation particles were founded in CLT-loaded nano-suspension which was prepared by dialysis against 0.02 M PBS pH 5.5 with constant stirring.

#### 4.2.2. Mean particle size and polydispersity index

The mean particle size and PI of bare nanoparticles were  $1754.17 \pm 673.02$  nm and  $1.05 \pm 0.14$ , respectively. After loading clotrimazole, the mean particle size and PI were significantly decreased to  $964.50 \pm 104.54$  nm and  $0.55 \pm 0.035$ , respectively ( $P < 0.05$ ). The mean particle size of drug-loaded nanoparticles and bare nanoparticles observed by PCS was not consistent with that by TEM. The PCS measurement provided the larger size than the TEM which could be seen the presence of many aggregated particles in both drug-loaded and bare nano-suspension possibly leading to the detected larger mean particle size and higher PI. The results are presented in Table 12-13

#### 4.2.3. Percentage of drug loading (%DL)

The average %DL obtained from two batches of drug-loaded nanoparticles was  $8.85 \pm 0.12\%$ .

#### 4.2.4. Percentage of drug encapsulation efficiency (%DE)

The average %DE obtained from two batches of drug-loaded nanoparticles was  $22.55 \pm 3.74\%$ .

#### 4.2.5. Differential scanning calorimetry.

The physical status of clotrimazole inside the nanoparticles and residue solvent were further studied by thermal analysis. According to Table 16, clotrimazole powder exhibited a melting point of  $144.4^\circ\text{C}$ . Interestingly, the melting point of clotrimazole was not observed in the clotrimazole-loaded nanoparticles, indicating that clotrimazole molecules were completely included or dissolved within the nanoparticles. The similar finding was also reported by Memisoğlu et al (9). In addition, After loading of clotrimazole,  $T_g$  of drug-loaded micelles was  $215.15^\circ\text{C}$  but  $T_g$  of bare nanoparticles was not evaluated (Table 16).

Since the boiling point of DMF is  $158^\circ\text{C}$ . Therefore, the weight loss of clotrimazole-loaded and bare nanoparticles from  $0^\circ\text{C}$  to  $158^\circ\text{C}$  associated with the loss of DMF owing to evaporation (data not shown). The method is useful tool for evaluating the residue solvent in the nanoparticles. Regarding the TGA data, the weigh loss of clotrimazole-loaded nanoparticles in the range of temperatures from  $0^\circ\text{C}$  to  $158^\circ\text{C}$  was  $3.59\%$  (Table 17).

**Table 12.** Mean particle size of control and CLT-loaded nanoparticles were prepared by dialysis against 0.02 M PBS pH 5.5 with constant stirring.

Mean Particle Size			
Sample	Control	batch 1	batch 2
no.1	1080.00	974	1020
no.2	1280.00	1070	1000
no.3	3140.00	859	931
no.4	1450.00	765	893
no.5	1680.00	889	1150
no.6	1895.00	1050	973
Average	1754.17	934.50	994.50
SD	737.25	118.12	89.60

**Table 13.** Polydispersity index of control and CLT-loaded nanoparticles were prepared by dialysis against 0.02 M PBS pH 5.5 with constant stirring.

Polydispersity Index			
Sample	Control	batch 1	batch 2
no.1	0.92	0.52	0.58
no.2	1.10	0.60	0.54
no.3	1.00	0.62	0.52
no.4	0.93	0.54	0.51
no.5	0.96	0.52	0.57
no.6	0.75	0.51	0.59
Average	1.05	0.55	0.55
SD	0.14	0.04	0.03

**Table 14.** Percentage of drug loading of CLT-loaded nanoparticles were prepared by dialysis against 0.02 M PBS pH 5.5 with constant stirring.

Drug loading (%)		
Sample	batch 1	batch 2
no.1	9.51	8.15
no.2	9.71	8.01
Average	9.61	8.08
SD	0.14	0.10

**Table 15.** Percentage of drug encapsulation efficiency of CLT-loaded nanoparticles were prepared by dialysis against 0.02 M PBS pH 5.5 with constant stirring.

Drug encapsulation efficiency (%)		
Sample	batch 1	batch 2
no.1	20.19	26.84
no.2	20.57	nd
Average	20.38	-
SD	0.27	-

**Table 16.** Glass transition temperatures ( $T_g$ ) and melting point ( $T_m$ ) of CLT, bare nanoparticles, CLT-loaded nanoparticles, which were prepared by dialysis against 0.02 M PBS pH 5.5 with constant stirring.

	$T_g$ 1 <sup>st</sup> /°C	$T_g$ 2 <sup>nd</sup> /°C	$T_m$ /°C
Clotrimazole			250
Bare nanoparticles	nd	nd	-
Clotrimazole-loaded nanoparticles	215.15	-	-

**Table 17.** Percent residue solvent of bare nanoparticles and CLT-loaded nanoparticles, which were prepared by dialysis against 0.02 M PBS pH 5.5 with constant stirring.

Formulation	Residue solvent
Bare nanoparticles	nd
Clotrimazole-loaded micelles	3.59 %

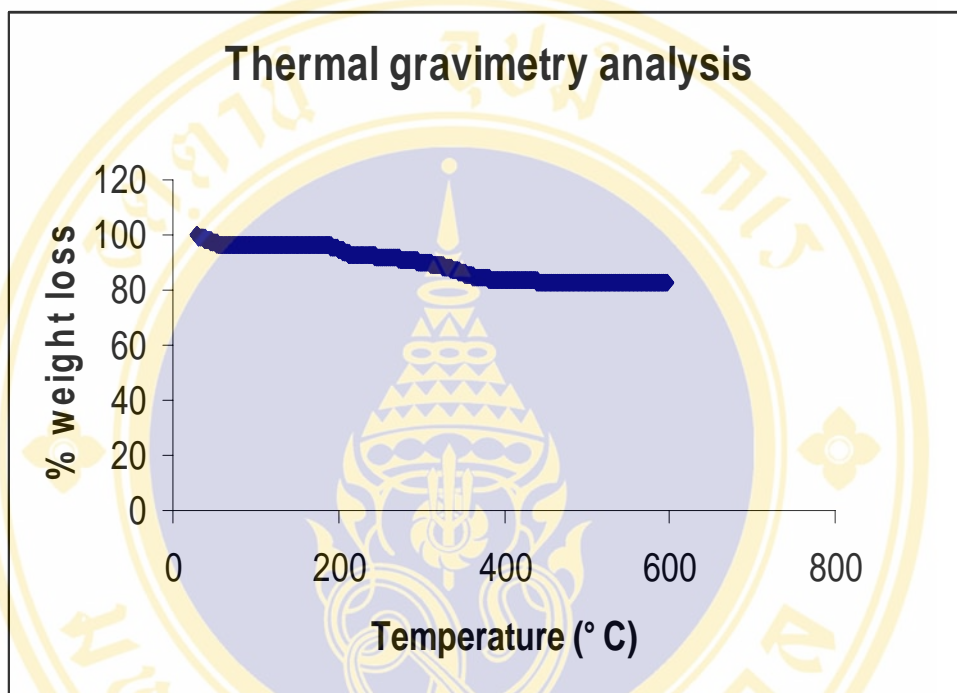


**Figure 20.** Curves represent percentage weight loss of CLT-loaded nanoparticles, which were prepared by dialysis against 0.02 M PBS pH 5.5 with constant stirring, corresponding to temperature with rate of heating was 10°C/min

#### **4.2.6. Physical stability.**

The stability of the dispersion can be clarified by the separation of the suspension into two phases, i.e. precipitate and clear supernatant. This was used to determine instability of the colloidal dispersion. Nanoparticles containing clotrimazole showed stability for 4 days indicated by absence of the separation of dispersion. During stored 1 month at 4°C, the separation of suspension was found; however, it could be easily redispersed by hand shaking.

#### **4.3. Method III**

This preparation of nanosuspensions was modified from method I by using 0.02 M PBS pH 7.4 as dialysis medium instead of distilled water.

##### **4.3.1. Morphology by TEM**

During the preparation by this method, the mixture of the copolymer and the drug changed to milky suspension thoroughly within 30 minutes. After finishing of dialysis, the white precipitate particles were found in the bag. The similar observations were found in the control nanosuspension. When observed by TEM, the most of bare nanoparticles were aggregate, they were large size more than 500 nm whereas the morphology of drug-loaded nanoparticles were uniformity with the range size 50–70 nm.

##### **4.3.2. Mean particle size and polydispersity index**

The mean particle size and PI of bare nanoparticles were  $736.83 \pm 74.14$  nm and  $0.60 \pm 0.06$  respectively. After loading clotrimazole, the mean particle size and PI were significantly decreased with  $216.17 \pm 108.32$  nm and  $0.54 \pm 0.03$  respectively ( $P < 0.05$ ). The mean particle size of drug-loaded nanoparticles and bare nanoparticles obtained from PCS was not consistent with the particle size from TEM, the results from PCS were larger. The results are presented in the Table 18 and Table 19.

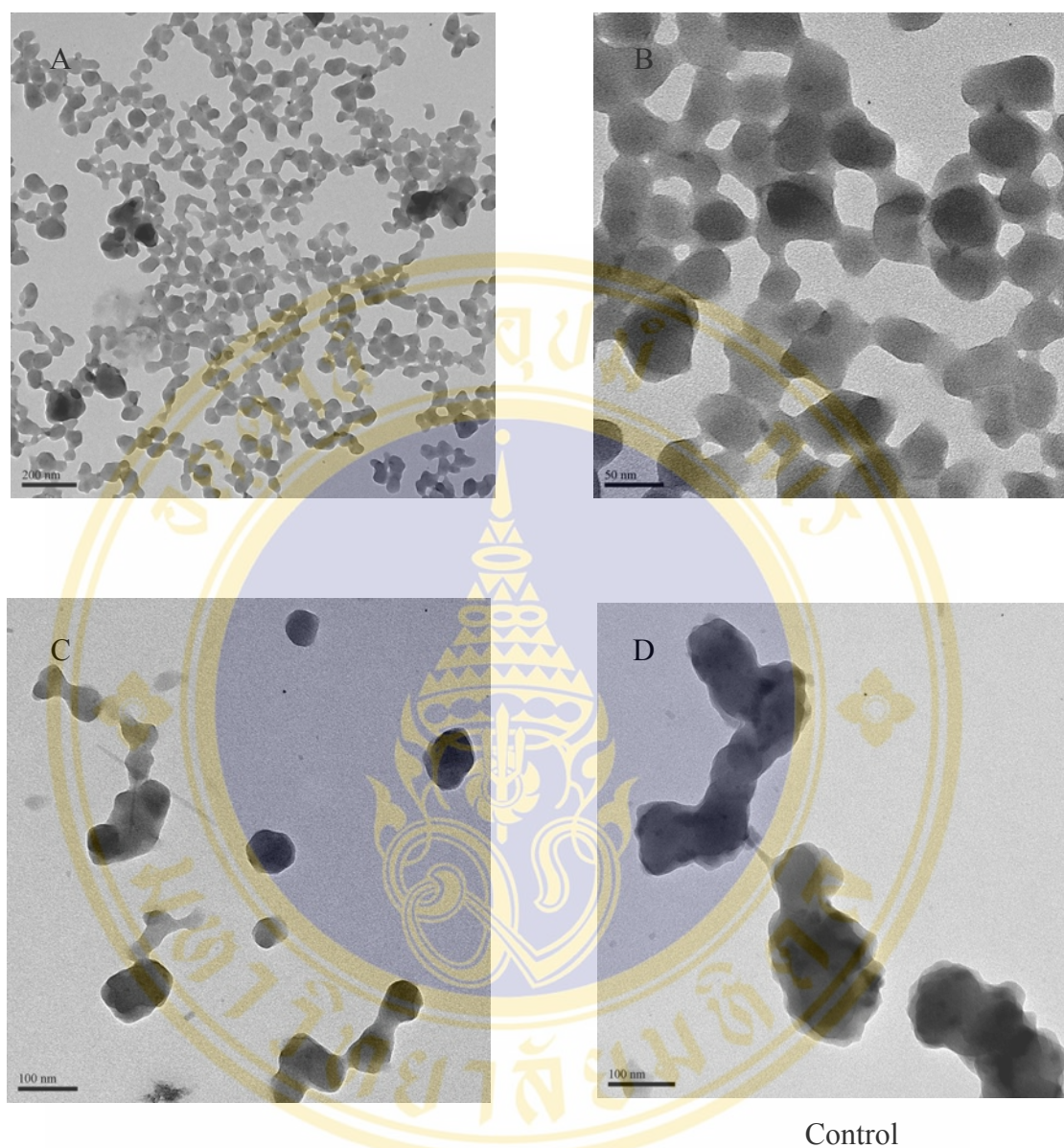


**Figure 21.** A-C show morphology of CLT-loaded nanoparticles and D show bare nanoparticles were prepared by dialysis against 0.02 M PBS pH 7.4 with constant stirring.

**Table 18.** Mean particles size of control and CLT-loaded nanoparticles were prepared by dialysis against 0.02 M PBS pH 7.4 with constant stirring.

Mean particle size			
Sample	Control	batch 1	batch 2
No.1	635.00	195	211
No.2	659.00	212	217
No.3	736.00	220	217
No.4	800.00	219	227
No.5	786.00	212	220
No.6	805.00	213	221
Average	736.83	211.83	218.83
SD	74.14	8.19	4.84

**Table 19.** Polydispersity index of control and CLT-loaded nanoparticles were prepared by dialysis against 0.02 M PBS pH 7.4 with constant stirring.

Polydispersity index			
Sample	Control	batch 1	batch 2
No.1	0.57	0.54	0.51
No.2	0.58	0.51	0.55
No.3	0.51	0.56	0.54
No.4	0.66	0.57	0.52
No.5	0.67	0.59	0.52
No.6	0.67	0.56	0.49
Average	0.61	0.56	0.52
SD	0.06	0.03	0.02

#### 4.3.3. Percentage of drug loading (%DL).

The average %DL obtained from two batches of drug-loaded nanoparticles were  $11.57 \pm 0.76\%$ .

#### 4.3.4. Percentage of drug encapsulated efficiency (%DE).

The average %DE of two batches of drug-loaded nanoparticles were  $25.52 \pm 1.06\%$ .

#### 4.3.5. Differential scanning calorimetry.

The physical status of clotrimazole inside the nanoparticles and residue solvent were further studied by thermal analysis. According to Table 22, clotrimazole powder exhibited a melting point of  $144.4^\circ\text{C}$ . Interestingly, the melting point of clotrimazole was not observed in the clotrimazole-loaded nanoparticles, indicating that clotrimazole molecules were completely included or dissolved within the nanoparticles. The similar finding was also reported by Memisoğlu et al (9). In addition, bare nanoparticles showed a glass transition temperature, which was approximately at  $352.94^\circ\text{C}$  (Table 10). After loading of clotrimazole,  $T_g$  of drug-loaded micelles slightly decreased to  $322.35^\circ\text{C}$  (Table 22).

Since the boiling point of DMF is  $158^\circ\text{C}$ . Therefore, the weight loss of clotrimazole-loaded and bare nanoparticles from  $0^\circ\text{C}$  to  $158^\circ\text{C}$  associated with the loss of DMF owing to evaporation (data not shown). The method is useful tool for evaluating the residue solvent in the nanoparticles. Regarding the TGA data, the weigh loss of bare nanoparticles and clotrimazole-loaded nanoparticles in the range of temperatures from  $0^\circ\text{C}$  to  $158^\circ\text{C}$  was  $2.80\%$  and  $6.46\%$ , respectively (Table 23).

#### 4.3.6. Physical stability.

The stability of the dispersion can be clarified by the separation of the suspension into two phases, i.e. precipitate and clear supernatant. This was used to determine instability of the colloidal dispersion. Nanoparticles containing clotrimazole showed stability for 10 days indicated by absence of the separation of dispersion. During stored 1 month at  $4^\circ\text{C}$ , the separation of suspension was found; however, it could be easily redispersed by hand shaking.

**Table 20.** Percentage of drug loading of CLT-loaded nanoparticles were prepared by dialysis against 0.02 M PBS pH 7.4 with constant stirring.

% Drug loading		
Sample	batch 1	batch 2
no.1	10.69	13.27
no.2	10.93	11.38
Average	10.81	12.32
SD	0.17	1.34

**Table 21.** Percentage of drug encapsulation efficiency were prepared by dialysis against 0.02 M PBS pH 7.4 with constant stirring.

% Drug encapsulation efficiency		
Sample	batch 1	batch 2
no.1	24.65	26.63
no.2	25.89	24.88
Average	25.27	25.76
SD	0.88	1.23

**Table 22.** Glass transition temperatures ( $T_g$ ) and melting points ( $T_m$ ) of CLT, bare nanoparticles, CLT-loaded nanoparticles which were prepared by dialysis against 0.02 M PBS pH 7.4 with constant stirring.

	$T_g$ 1 <sup>st</sup> /°C	$T_g$ 2 <sup>nd</sup> /°C	$T_m$ /°C
Clotrimazole	-	-	250
Bare nanoparticles	352.94	-	-
Clotrimazole-loaded nanoparticles	352.94	-	-

**Table 23.** Percent residue solvent of bare nanoparticles and CLT-loaded nanoparticles were prepared by dialysis against 0.02 M PBS pH 7.4 with constant stirring.

	Residue solvent
Bare nanoparticles	2.80 %
Clotrimazole-loaded nanoparticles	6.46 %

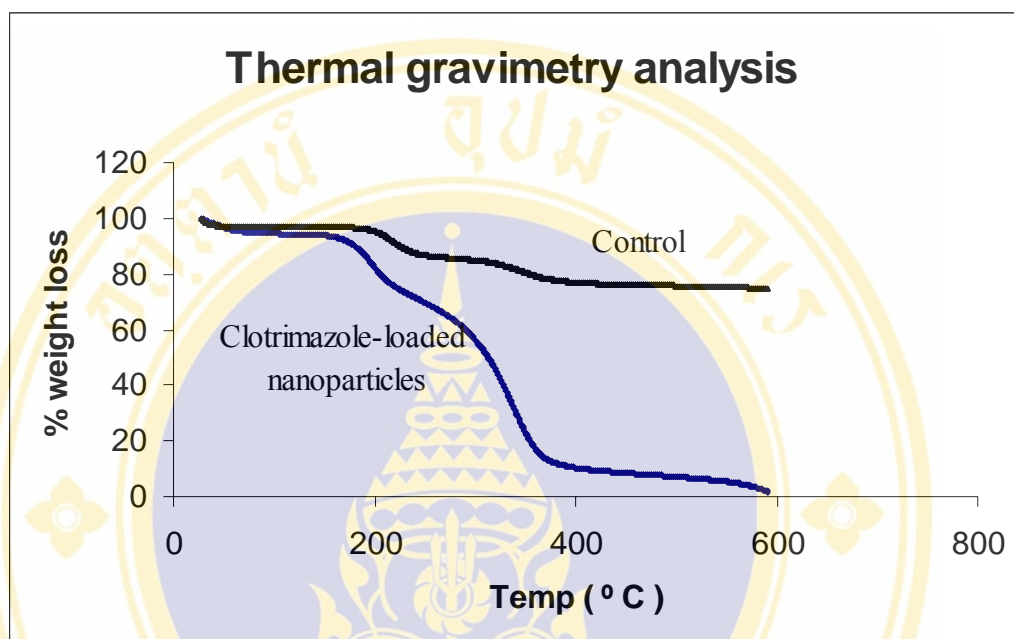


**Figure 22.** Curves represent percentage weight loss of clotrimazole-loaded nanoparticles and control, which were prepared by dialysis against 0.02 M PBS pH 7.4 with constant stirring, corresponding to temperature with rate heating 10°C/min.

#### 4.4. Method IV.

The preparation of nano-suspension was modified from method III by using distilled water as dialyzed medium without stirring for the first three hours.

##### 4.4.1. Morphology by TEM

During the preparation, the mixture of the copolymer and the drug became milky suspension thoroughly within 30 minutes. The white precipitates occurred within 2 hours. After finishing the dialysis procedure, the amount of white precipitates was less than that prepared by method III. Likewise, in case of bare nano-suspension, the similar result was also observed. When observed by TEM, the most of bare nanoparticles were aggregate. Moreover, there were a few nanospheres having the size in the range of 80-175 nm. After loading clotrimazole, the particle size of drug-loaded-nanoparticles rose to 130 to 250 nm without aggregation. By this method, the diversity of shape could be detected such as rod and sphere. This finding was similar to other results that the diversity of nanoparticle shape was discovered among the various methods for the preparation of drug-loaded nanoparticle (93). The morphology of nanoparticles is shown in Figure 23.

##### 4.4.2. Mean particle size and polydispersity index

The mean particle size and the PI of bare nanoparticles were  $798.33 \pm 93.79$  nm and  $0.65 \pm 0.07$ , respectively. After loading clotrimazole, the mean particle size and the PI were significantly decreased to  $686.17 \pm 28.26$  nm and  $0.39 \pm 0.05$ , respectively ( $P < 0.05$ ). The mean particle size of drug-loaded nanoparticles measured by PCS was not consistent with that observed from TEM. The measured mean particle size from PCS was larger than the actual size from TEM. Similar to the drug-loaded nanoparticles, the particle size and the PI of bare nanoparticles was also observed.

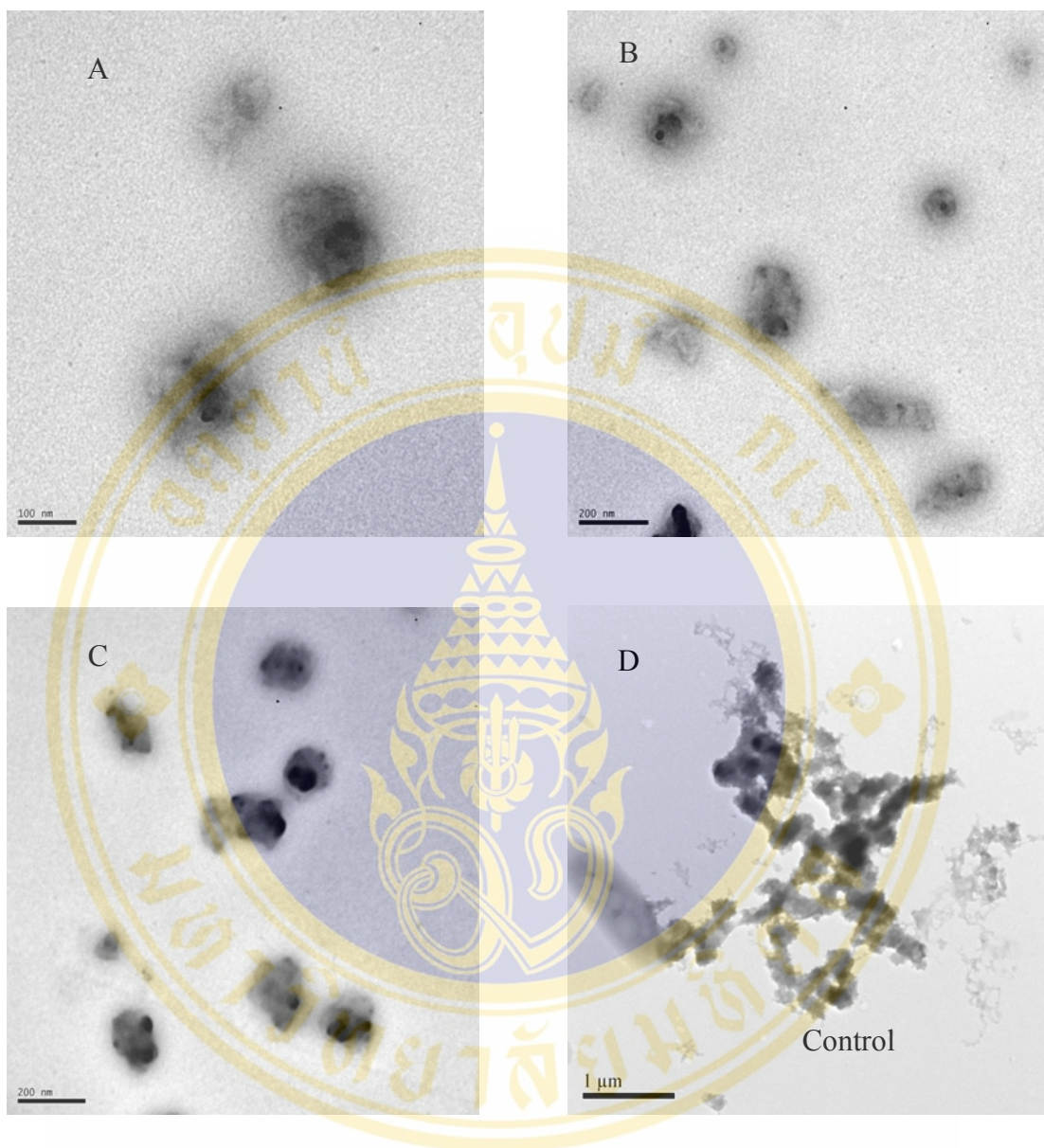


**Figure 23.** A-C show morphology of CLT-loaded nanoparticles and D show bare nanoparticles were prepared by dialysis against distilled water and non-used stirring in the first three hours of the dialysis time.

**Table 24.** Mean particle size of control and CLT-loaded nanoparticles were prepared by dialysis against distilled water and non-used stirring in the first three hours.

Mean particle size (nm)			
Sample	Control	batch 1	batch 2
No.1	791	638	704
No.2	845	668	719
No.3	866	587	697
No.4	883	686	728
No.5	663	659	707
No.6	688	748	693
Average	789.33	664.33	708.00
SD	93.79	53.26	13.30

**Table 25.** Polydispersity index of control and CLT-loaded nanoparticles were prepared by dialysis against distilled water and non-used stirring in the first three hours.

Polydispersity Index			
Sample	Control	batch 1	batch 2
No.1	0.68	0.35	0.31
No.2	0.66	0.45	0.3
No.3	0.59	0.56	0.33
No.4	0.64	0.42	0.36
No.5	0.57	0.44	0.36
No.6	0.75	0.41	0.35
Average	0.65	0.44	0.34
SD	0.07	0.07	0.03

#### 4.4.3. Percentage of drug loading

The average %DL obtained from two batch of drug-loaded nanoparticle was  $8.28 \pm 0.42\%$  (Table 26).

#### 4.4.4. Percentage of drug encapsulation efficiency

The average %DE obtained from two batches of drug-loaded nanoparticle was  $13.56 \pm 0.12\%$  (Table 27).

#### 4.4.5. Differential scanning calorimetry.

The physical status of clotrimazole inside the nanoparticles and residue solvent were further studied by thermal analysis. According to Table 28, clotrimazole powder exhibited a melting point of  $144.4^{\circ}\text{C}$ . Interestingly, the melting point of clotrimazole was not observed in the clotrimazole-loaded nanoparticles, indicating that clotrimazole molecules were completely included or dissolved within the nanoparticles. The similar finding was also reported by Memisoğlu et al (9). In addition, bare nanoparticles showed a glass transition temperature, which was approximately at  $353.13^{\circ}\text{C}$  (Table 28). After loading of clotrimazole,  $T_g$  of drug-loaded micelles slightly decreased to  $246.88^{\circ}\text{C}$  for the first stage of  $T_g$  and  $326.56^{\circ}\text{C}$  for the second stage (Table 28).

Since the boiling point of DMF is  $158^{\circ}\text{C}$ . Therefore, the weight loss of clotrimazole-loaded and bare nanoparticles from  $0^{\circ}\text{C}$  to  $158^{\circ}\text{C}$  associated with the loss of DMF owing to evaporation (data not shown). The method is useful tool for evaluating the residue solvent in the nanoparticles. Regarding the TGA data, the weigh loss of bare nanoparticles and clotrimazole -loaded nanoparticles in the range of temperatures from  $0^{\circ}\text{C}$  to  $158^{\circ}\text{C}$  was  $0.50\%$  and  $3.38\%$ , respectively (Table 29).

#### 4.4.6. Physical stability.

The stability of the dispersion can be clarified by the separation of the suspension into two phases, i.e. precipitate and clear supernatant. This was used to determine instability of the colloidal dispersion. Nanoparticles containing clotrimazole showed stability for 4 days indicated by absence of the separation of dispersion. During stored 1 month at  $4^{\circ}\text{C}$ , the separation of suspension was found; however, it could be easily redispersed by hand shaking.

**Table 26.** Percentage of drug loading of CLT-loaded nanoparticles were prepared by dialysis against distilled water with non-using stirring in the first three hours.

Drug loading (%)		
Sample	batch 1	batch 2
no.1	7.45	8.50
no.2	8.00	9.13
Average	7.73	8.82
SD	0.39	0.45

**Table 27.** Percentage of drug encapsulation efficiency of CLT-loaded nanoparticles were prepared by dialysis against distilled water with non-using stirring in the first three hours.

Drug encapsulated efficiency (%)		
Sample	batch 1	batch 2
no.1	15.82	11.73
no.2	15.11	11.56
Average	15.47	11.65
SD	0.12	0.12

**Table 28.** Glass transition temperatures ( $T_g$ ) and melting points ( $T_m$ ) of CLT, bare nanoparticles, CLT-loaded nanoparticles, which were prepared by dialysis against distilled water and non-used stirring in the first three hours.

	$T_g$ 1 <sup>st</sup> /°C	$T_g$ 2 <sup>nd</sup> /°C	$T_m$ /°C
Clotrimazole	-	-	250
Bare micelles	184.4	-	-
Clotrimazole-loaded micelles	246.88	326.56	-

**Table 29.** Percent residue solvent of bare nanoparticles, CLT-loaded nanoparticles were prepared by dialysis against distilled water and non-used stirring in the first three hours.

Formulation	Residue solvent
Bare micelles	0.50 %
Clotrimazole-loaded micelles	3.38 %

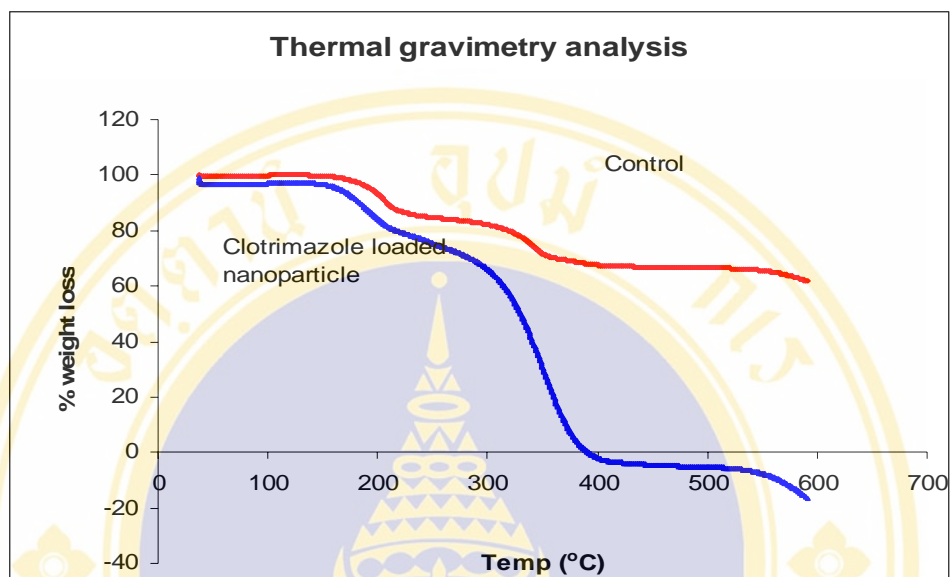


**Figure 24.** Curves represent percentage weight loss of CLT-loaded nanoparticles and bare nanoparticles, which were prepared by dialysis against distilled water and non-used stirring in the first three hours, corresponding to temperature with rate of heating was 10 °C/min..

#### 4.4.7. Chemical stability

Table 30 shows the concentration of clotrimazole in the nano-suspension stored at 4°C before 1 month.

Table 31 shows the concentration of clotrimazole in the nano-suspension stored at 4°C after 1 month.

The chemical stability of the sample can be calculated by equation below :

$$\begin{aligned}
 &= \frac{\text{Concentration of clotrimazole stored at 4}^\circ\text{C after 1 month} \times 100 \%}{\text{Concentration of clotrimazole stored at 4}^\circ\text{C before 1 month}} \\
 &= \frac{38.28}{40.24} \times 100\% \\
 &= 95.12\%
 \end{aligned}$$

The drug-loaded nano-suspension showed chemical stable (95.12%) when storing at 4°C for 1 month.

#### 4.4.8. Zeta potential value

The sample from batch 1 was dispersed in the three types of medium before measurement. The zeta potentials are shown in Table 32.

The zeta potential of both control and drug-loaded nanoparticles in SWI, 0.02 M PBS pH 5.5 and 0.02 M PBS pH 7.4 showed negative charge. The negative charge may be attributed to PEG which has carboxylic group (COO<sup>-</sup>) in the side chain. It was suggested that the conformation of the copolymer to form nanospheres in aqueous solution preferred to allow the hydrophobic segment (*N*-phathanoyl group) with the hydrophobic drug (CLT) into an inner core and to allow the hydrophilic segment (chitosan-PEG) to an outer shell. Additionally, the non-encapsulated clotrimazole can be removed by dialysis against distilled water. The structure of CLT-loaded nanosphere can be illustrated in Figure 25. In the same dispersing medium, the zeta potentials of both control and drug-loaded nanoparticles were not significantly different ( $P > 0.05$ ). However, the zeta potential of dispersed nanoparticles in PBS solution showed lower than that in SWI. The lower zeta potential may be related to the absorbed potassium ion on the shell of the nanoparticles (Table 32).

**Table 30.** The concentration of clotrimazole in nano-suspension was storage before 1 month.

Sample	Concentration ( $\mu\text{g/ml}$ )
No.1	42.36
No.2	36.85
No.3	41.50
Average	40.24
SD	2.96

**Table 31.** The concentration of clotrimazole in nano-suspension was storage after 1 month.

Sample	Concentration ( $\mu\text{g/ml}$ )
No.1	38.15
No.2	39.67
No.3	37.01
Average	38.28
SD	1.34

**Table 32.** Zeta potential value of control and CLT-loaded nano-suspension which were prepared by method I were dispersed and evaluated in SWI, 0.02 M PBS pH 5.5 and 0.02 M PBS pH 7.4, respectively.

Type of medium	Control	Clotrimazole-loaded
Sterile water for injection	$-24.73 \pm 2.03$	$-28.10 \pm 3.52$
0.02 M PBS pH 5.5	$-14.77 \pm 1.95$	$-14.83 \pm 2.06$
0.02 M PBS pH 7.4	$-13.30 \pm 2.43$	$-13.40 \pm 1.22$

Barratt G. et.al. (94) demonstrated the similar result that the surface charge was affected by changing in environment. Also, the zeta potential was affected by the surface composition of the nanoparticles, the presence of absorbed compound and the composition of the dispersing phase, mainly the ionic strength and the pH.



Shell :PEG

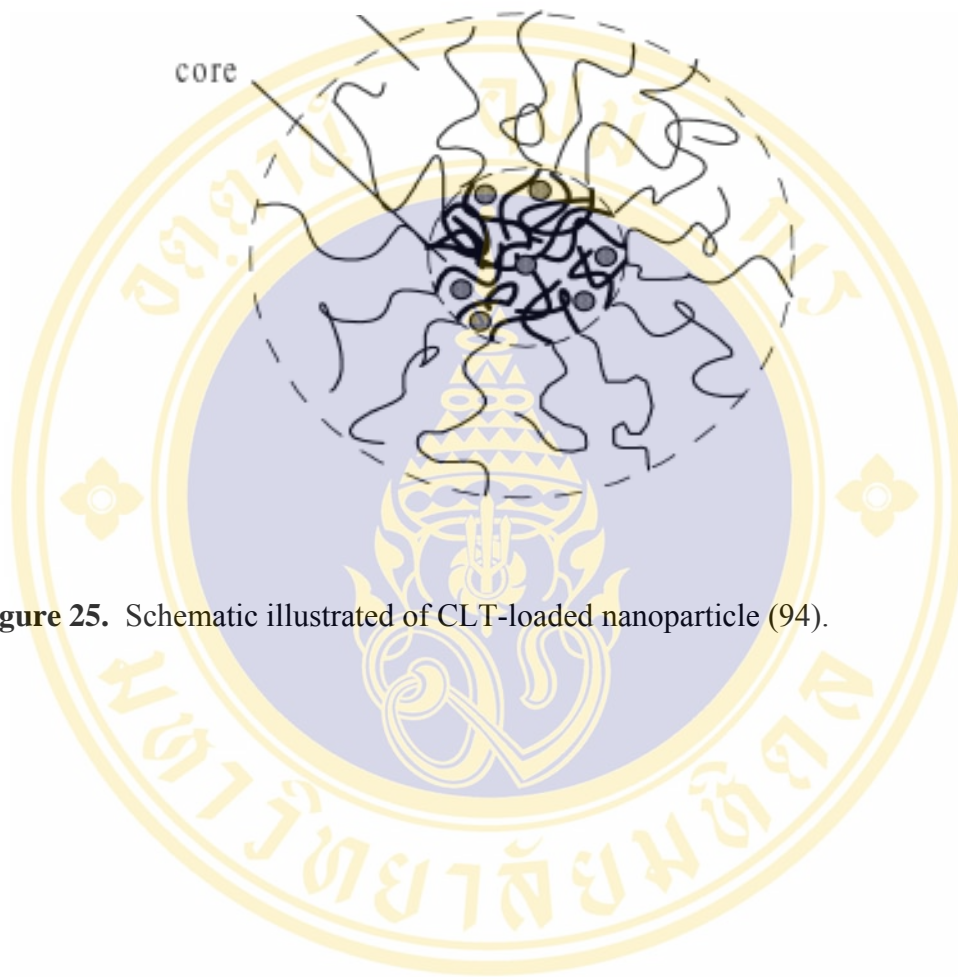


**Figure 25.** Schematic illustrated of CLT-loaded nanoparticle (94).

## **5. Reproducibility of Method IV on Characteristic of CLT-Loaded N-Phthaoylchitosan-g-mPEG.**

Good reproducibility in the preparation of nanoparticles could be achieved by using the same experimental set up and carefully controlling the factors. It was founded that using distilled water and unstirred condition in the first three hours of dialysis procedure. All of the batches showed a good reproducibility. This is exemplified with three batches of CLT-loaded nanoparticles, which used the different batch of the copolymer.

### **5.1. Morphology by TEM**

Observing by TEM, all of batches showed spherical shape with uniform size 250-300 nm. The results was suggested that, this method can prepare good reproducible on the morphology (Figure 26).

### **5.2. Reproducible of percentage of drug loading.**

The average percentage of drug loading with the standard deviation which obtained from three batches of drug-loaded nanoparticle were  $9.84 \pm 2.51\%$  (Table33).

### **5.3. Reproducible drug of encapsulation efficiency.**

The average of percentage of drug encapsulation efficiency with the standard deviation which obtained from three batches of drug-loaded nanoparticle were  $15.87 \pm 3.99\%$  (Table34).

### **5.4. Reproducible of mean particle size (nm) and polydispersity index**

The average mean particle size with the standard deviation which obtained from three batches of drug-loaded nanoparticle were  $601.33 \pm 128.78$  nm (Table35).

Tohe average polydispersity index with the standard deviation which obtained from three batches of drug-loaded nanoparticle were  $0.35 \pm 0.10$  (Table 35).

### **5.5. Drug release profile of CLT-loaded nanoparticles.**

After observing the characteristic of drug released from drug-loaded nanoparticles. Those obtained from concentration of clotrimazole released into 0.02 M PBS pH 7.4 in Franz cell apparatus. From three batches, the average lag time of drug releasing was  $3.8 \pm 2.05$  hours. The average of initial cumulative drug release at 2 hr. was  $7.94 \pm 10.87\%$ . whereas at this time the average of initial cumulative drug release of positive control was  $17.04 \pm 3.73\%$  (Table 36). Until at 6 hr. cumulative drug release of positive control was  $87.84 \pm 2.16\%$  (Table 36) whereas cumulative

drug release of drug-loaded nanoparticles was  $21.53 \pm 11.17\%$  (Figure 29). The clear difference of drug releasing profile from both of the positive control and the drug-loaded nanoparticles could be observed in Figure 30. In any time point, the cumulative drug release of drug-loaded nanoparticles showed lower than positive control. The results showed the sustained release of CLT-loaded nanoparticles and reproducible more than 24 hours (Figure 28). Additional, the morphology of drug-loaded nanoparticles was observed after releasing into PBS pH 7.4 medium. It was founded that the structure were stable for 5 days (120 hours).

The sustained release of drug from nanoparticles may be controlled by existing of interaction between the solubilized drug and core. Subsequently, the lag time may be concerned to the timing for water penetrated into the core and timing for overcoming the interaction between the drug and the inner core. Many studies detailed the sustained release of drug-loaded micelles that it concerning the physically and chemically encapsulation of drug in nanoparticles (95-97). Those were referred to the important role to controlled drug release.

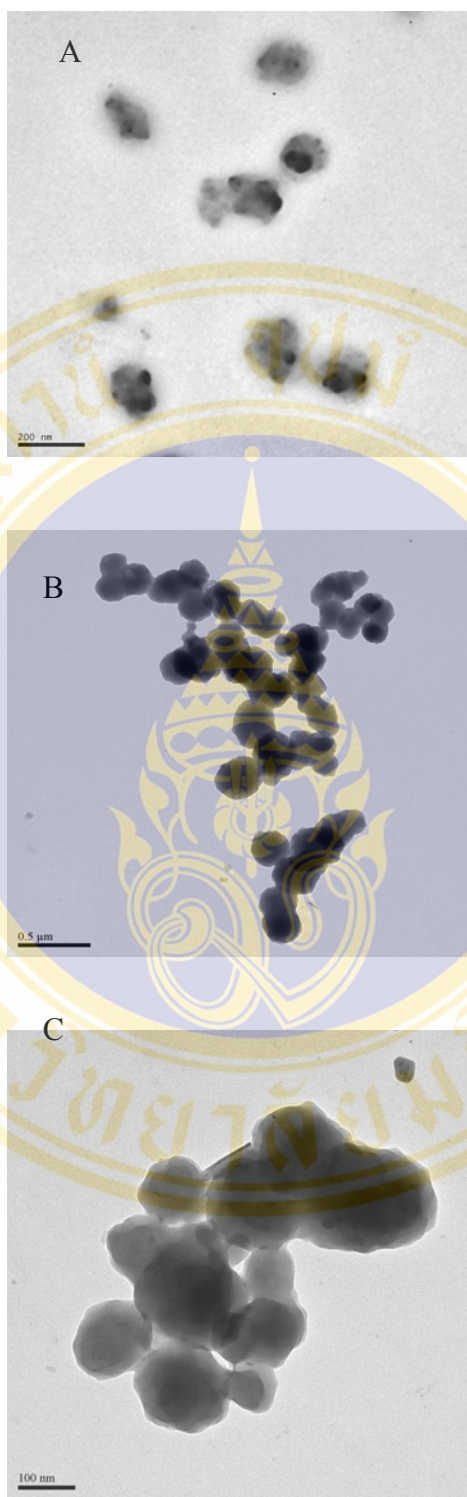


**Figure 26.** A-C represent morphology of clotrimazole-loaded nanoparticles from batch 1-3 which was prepared by against distilled water with non-used stirring constant in the first three hours.

**Table 33.** Percentage of drug loading (%DL) obtained from three batches of CLT-loaded nanoparticles which were prepared by method I.

Sample	DL (%)	SD
Batch 1	7.73	0.39
Batch 2	8.82	0.45
Batch 3	12.99	0.66
Average	9.84	2.51

**Table 34.** Percentage of drug encapsulation efficiency (%DE) obtained from three batches of CLT-loaded nanoparticles which were prepared by method I.

Sample	DE (%)	SD
Batch 1	15.47	0.50
Batch 2	11.65	0.12
Batch 3	20.50	0.60
Average	15.87	3.99

**Table 35.** Mean particle size (nm) and polydispersity index with standard deviation obtained from three batches of CLT- loaded nanoparticles which were prepared by method I.

Sample	Mean particle size (nm)	SD	Polydisperse index	SD
batch 1	664.33	53.26	0.44	0.07
batch 2	708.00	13.30	0.34	0.03
batch 3	431.67	20.39	0.26	0.10
Average	601.33	128.78	0.35	0.10

**Table 36.** Represent percentage cumulative drug release, average percentage of cumulative drug release of positive control (clotrimazole standard solution 110 µg/ml, 2 ml) with standard deviation (n=2).

Positive control				
Time (hr)	%cumulative no.1	%cumulative no.2	Average	SD
0	0	0	0	0
1	14.4	19.67	17.04	3.73
2	27.78	37.96	32.87	7.20
3	36.32	57.04	46.68	14.65
6	82.75	92.92	87.84	7.19
12	70.89	98.17	84.53	19.29
24	79.67	87.13	83.40	5.28
48	78.25	86.45	82.35	5.80
72	79.50	86.75	83.13	5.13
120	79.12	85.87	82.50	4.77

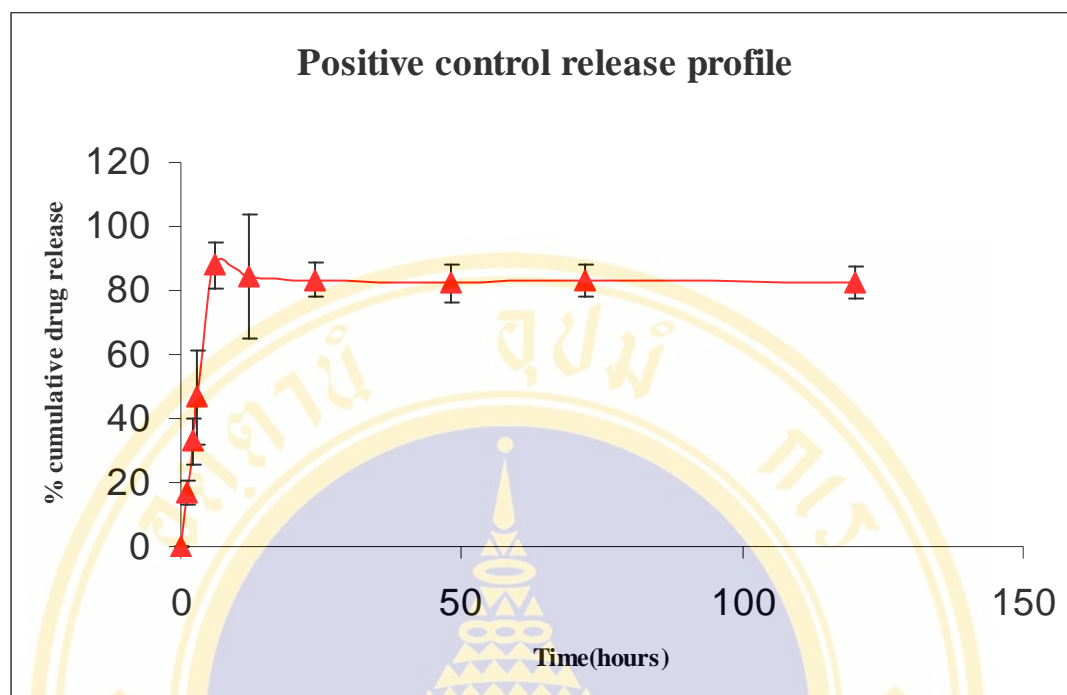


**Figure 27.** Average of cumulative drug release $\pm$ SD of positive control (n=2).

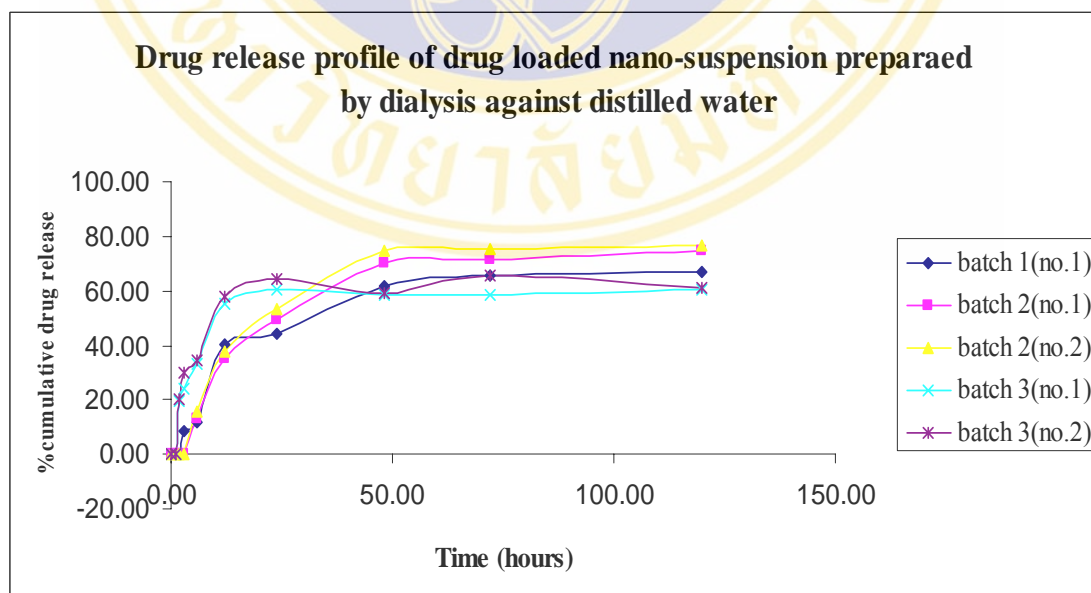


**Figure 28.** Drug release profile of CLT-loaded nanoparticles obtained from three batches (n=5)

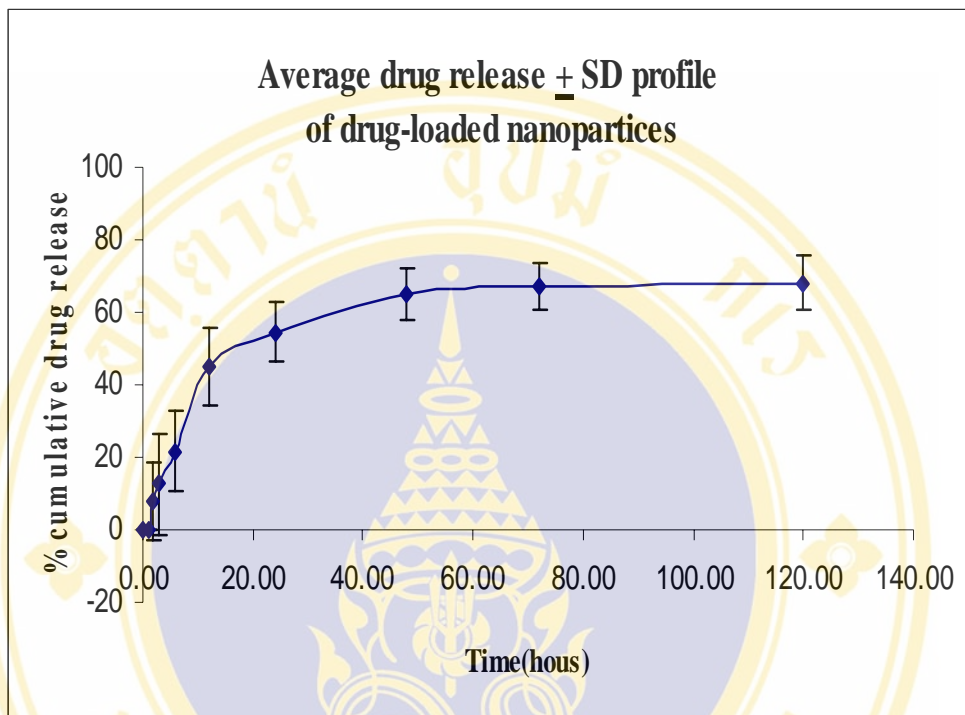


**Figure 29.** Average percentage of cumulative drug release  $\pm$ SD of CLT-loaded nanoparticles (n=5).

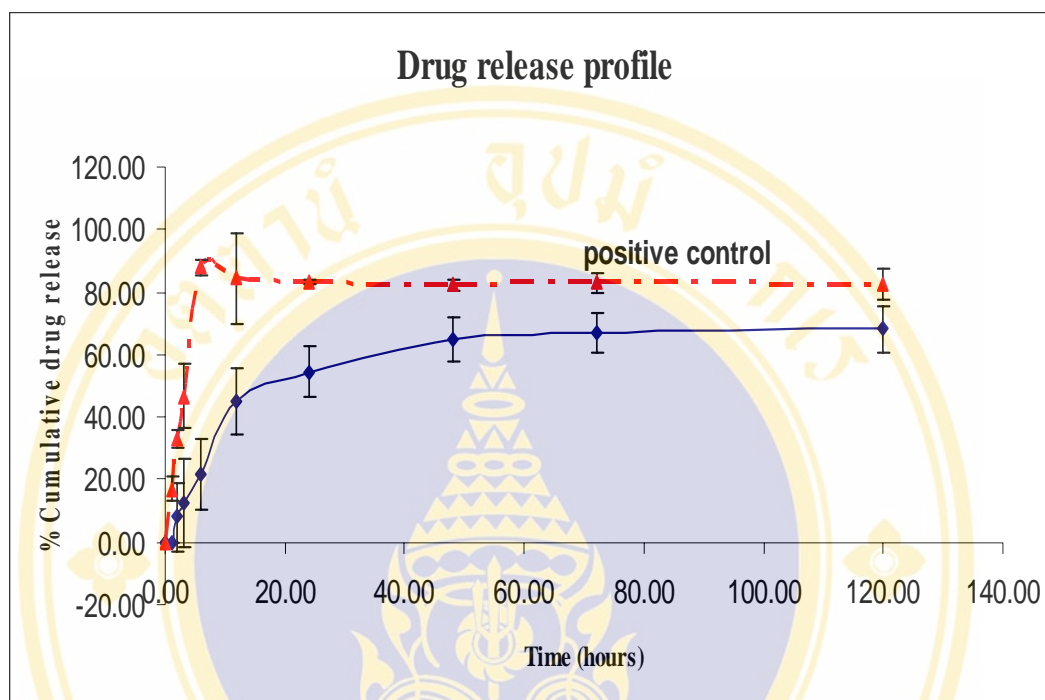


**Figure 30.** The average percentage of cumulative drug release  $\pm$  SD of CLT-loaded nanoparticles (n=5) and the average percentage of cumulative drug release  $\pm$  SD of positive control (n=2).

## **6. The Influence of Dialysis Method on Clotrimazole Encapsulation in to *N*-Phthanoyl-chitosan-g-mPEG.**

### **6.1. Effect of initial drug loading on characteristics of CLT-loaded nanoparticles**

This experiment was established by the same parameter of the preparation. By using distilled water as dialysis medium and non-using stirring in the first three hours of the dialysis procedure.

#### **6.1.1. Effect of initial drug loading to percentage drug encapsulation efficiency (%DE )**

Table 37 showed the significant decreasing of %DE from  $6.89 \pm 0.94$  to  $5.83 \pm 0.01$  ( $P < 0.005$ ) when increasing the initial drug loading from 3% to 15%. But when increasing the initial drug loading from 15% to 50%, the % DE increased from  $5.83 \pm 0.01$  to  $11.64 \pm 0.12$ . Finally, the initial drug loading level to polymer was 100 %, %DE decreased to  $10.57 \pm 1.35$ .

Figure 31 showed the optimum of %DE when initial drug loading was 50 % w/w to the copolymer. Those may be concerning loading capacity of the copolymer. The results was similar to Michelland S. et al. (98), they was founded that the percentage of drug adsorption decreased with the quantity of drug dissolved in the polymerization medium. It resulting from the capacity of adsorption which related to the hydrophobic and the specific area of the copolymer.

#### **6.1.2. Effect of initial drug loading to percentage drug loading (% DL)**

Table 38 showed the increasing of percentage of drug loading from  $0.24 \pm 0.06$  % to  $8.81 \pm 0.44$ % when increasing the percentage of initial drug loading to copolymer rise from 3% to 50%. The maximum capacity of the copolymer for drug loading was about 10% when percentage of initial drug loading was 100%. The maximum loading was obtained when percentage of initial drug loading was 100 %. However, the percentage of drug loading was not significant different between the percentage of initial drug loading from 50% to 100%. Figure 32 showed the clearly discussion.

This result can confirm above mention that the increasing of initial drug generally was decreasing of drug encapsulated efficacy because of capacity loading of the copolymer. The results similar to Liu SQ et al. (46).

#### **6.1.3. Effect of initial drug loading to mean particles size.**

Table 33 showed that, when increased percentage of initial drug loading from 3% to 100%, the mean particle size of nanoparticles were relatively increased with  $617.67 \pm 32.1$  to  $941.33 \pm 60.32$  nm. By Comparing, the observing particle size from TEM was not significant different with increasing percentage of initial drug loading. All of batch showed the same particle size with the range size about 250-300 nm.

#### **6.1.4. Effect of initial drug loading to polydispersity index.**

Table 40 showed the increasing of PI from  $0.16 \pm 0.05$  to  $0.45 \pm 0.03$  when increasing percentage of initial drug loading from 3% to 100%. However, PI was not significant different ( $P > 0.05$ ) when increasing percentage of initial drug loading from 15% to 50%

#### **6.1.5. Effect of initial drug loading to morphology.**

When increasing percentage of initial drug loading from 3% to 100%, the degree of aggregation was relatively increased. It was suggested that the increasing of clotrimazole that induced the aggregation of the nanoparticles (Figure 35, 36, 37, 38).

**Table 37.** Percentage of drug encapsulation efficiency corresponding to percentage of initial drug loading to the copolymer w/w (n=2).

DE (%)		
Sample	%DE	SD
3%	6.89	0.94
15%	5.83	0.01
50%	11.64	0.12
100%	10.57	1.35

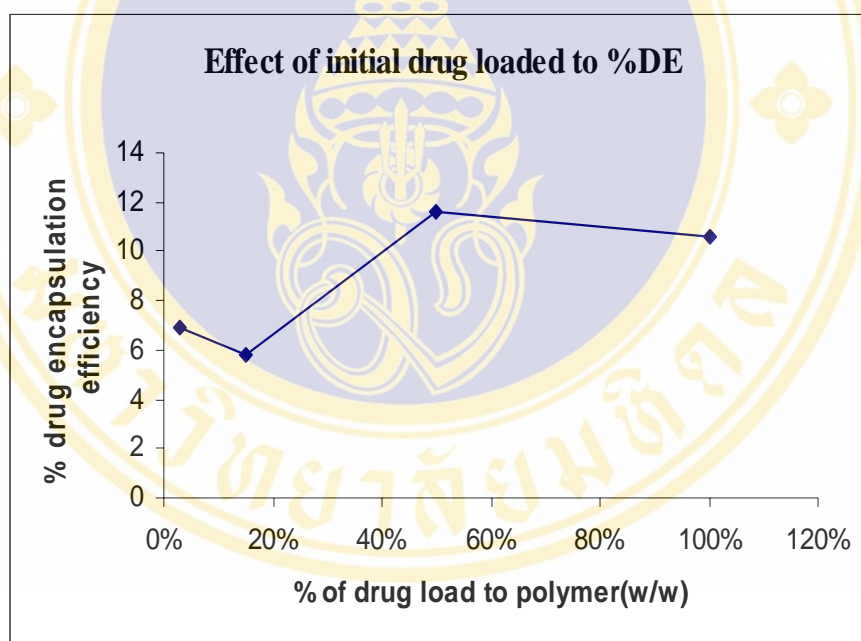


**Figure 31.** Percentage of clotrimazole encapsulation efficiency corresponding to percentage of initial clotrimazole loading to the copolymer w/w (n=2).

**Table 38.** Percentage of drug loading corresponding to percentage of initial drug loading to the copolymer w/w (n=2).

DL (%)		
Sample	%DL	SD
3%	0.24	0.06
15%	1.13	0.05
50%	8.81	0.44
100%	9.66	1.18

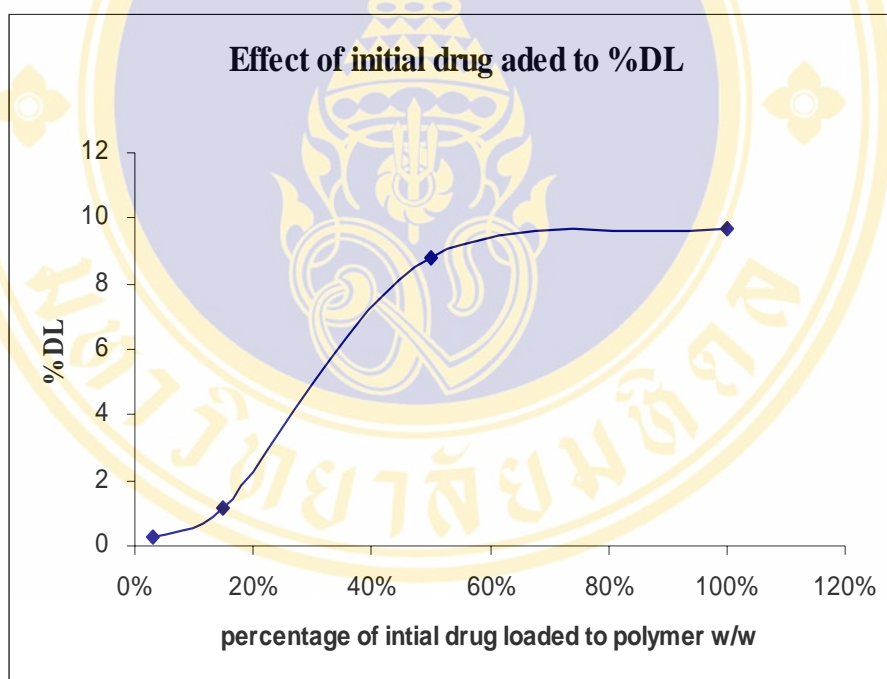


**Figure 32.** Percentage of clotrimazole loaded in nanoparticles corresponding to percentage of initial clotrimazole loading to the copolymer w/w (n=2).

**Table 39.** Mean particle size of CLT loaded nanoparticles corresponding to percentage of initial clotrimazole loading to the copolymer w/w (n=6).

Mean particle size (nm)		
Sample	mean particle size	SD
3%	617.67	32.1
15%	687.67	9.69
50%	708.00	13.3
100%	941.33	60.32

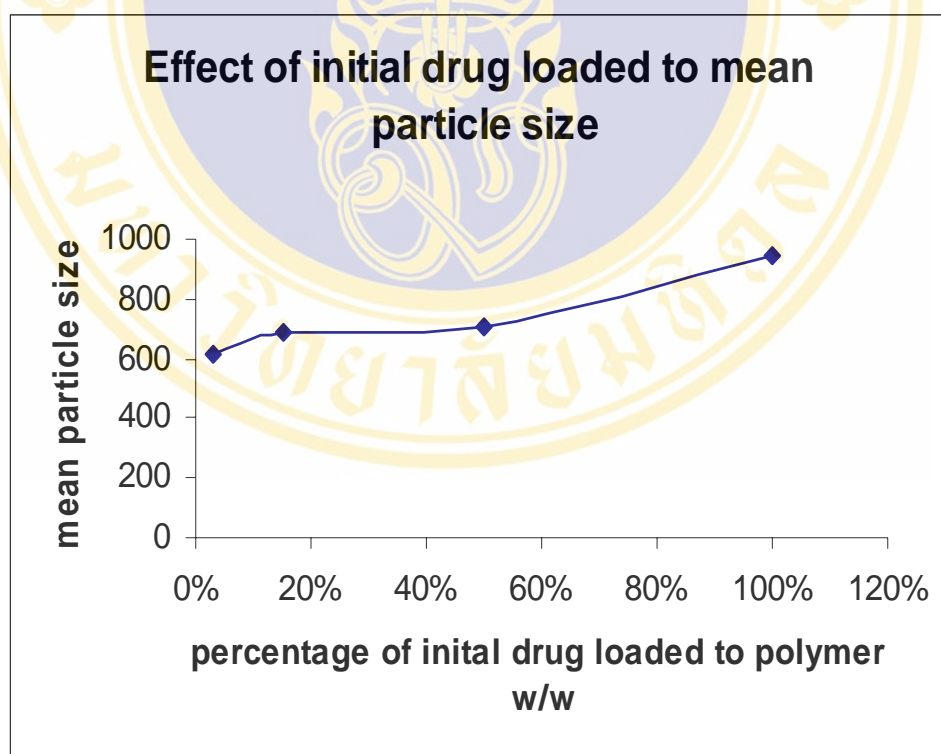


**Figure 33.** Mean particle size corresponding to percentage of initial clotrimazole loading to the copolymer w/w (n=2).

**Table 40.** Polydispersity index of CLT- loaded nanoparticles corresponding to percentage of initial clotrimazole loaded to the copolymer w/w (n=6).

Polydispersity Index (PI)		
Sample	PI	SD
3%	0.16	0.03
15%	0.19	0.05
50%	0.34	0.03
100%	0.45	0.03

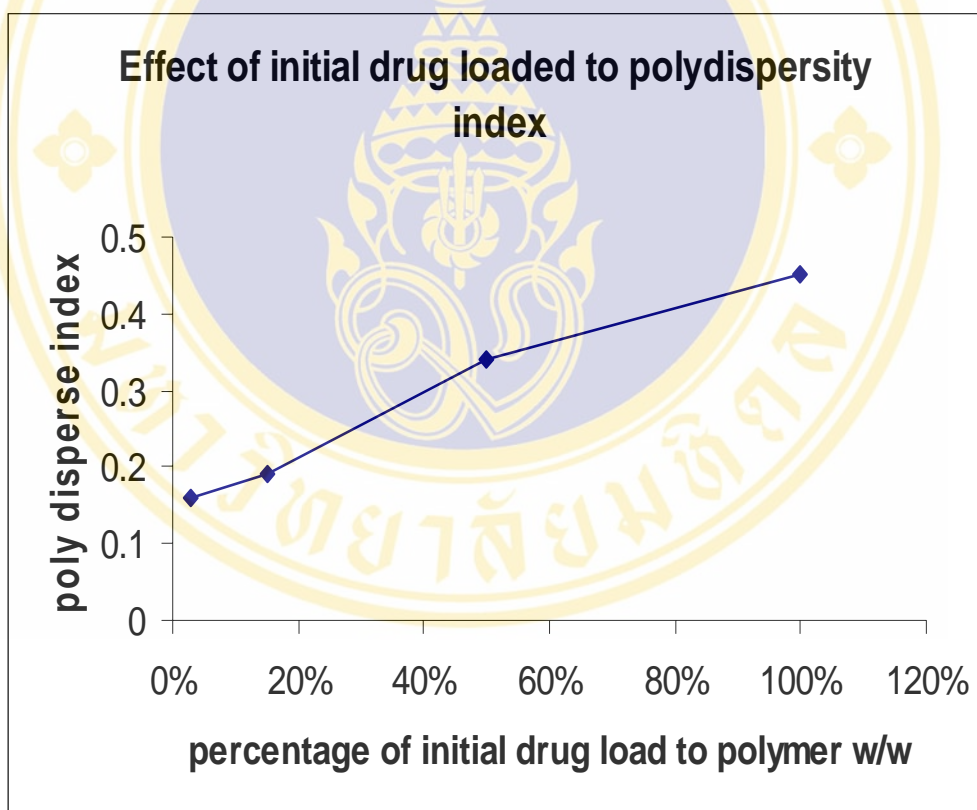


**Figure 34.** Polydispersity index corresponding to percentage of initial clotrimazole loading to the copolymer w/w (n=2).

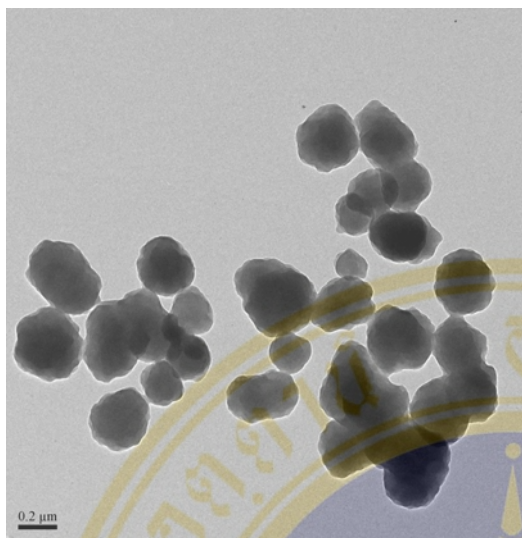


**Figure 35.** 3 % w/w initial drug loaded to polymer

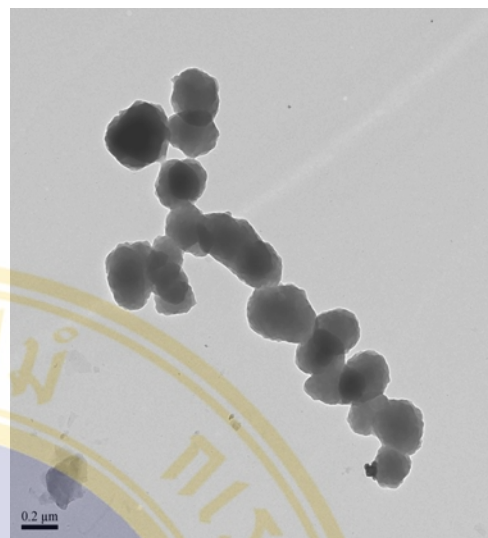


**Figure 36.** 15 % w/w initial drug loaded to polymer

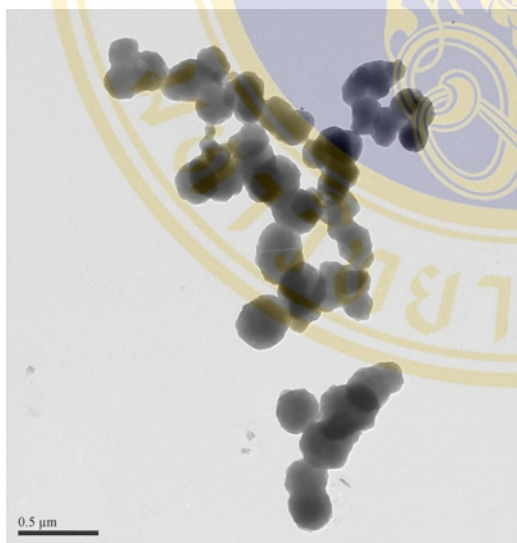


**Figure 37.** 50 % w/w initial drug loaded to polymer

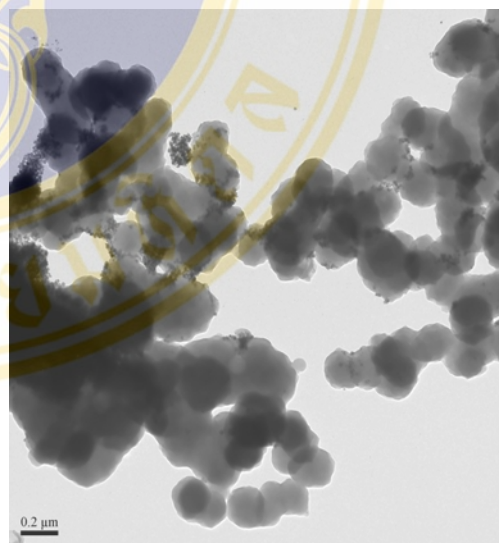


**Figure 38.** 100 % w/w initial drug loaded to polymer

## **6.2. Effect of medium type on characteristics of CLT-loaded nanoparticles.**

To investigate the effect of medium type on characteristics of CLT-loaded nanoparticles, all of the experiments were done by the same parameter of the preparation and using constant stirring thoroughly for dialysis time.

### **6.2.1. Effect of medium type to percentage of drug loading (%DL).**

Figure 39 shows that the using alkaline salts aqueous solution as dialysis medium that can improve the percentage of drug loading than the using distilled water. The highest of percentage of drug loading  $11.57 \pm 1.17\%$  was obtained from the using 0.02 PBS pH 7.4 as dialyzed medium. In case of 0.02 M PBS pH 5.5, the percentage of drug loading was  $8.85 \pm 0.89\%$ . When using distilled water as dialyzed medium the percentage of drug loading was  $5.06 \pm 0.89\%$ . The results are presented in Table 41.

### **6.2.2. Effect of the medium type to percentage drug encapsulation efficiency (%DE).**

Figure 40 shows that, the percentage drug encapsulation efficiency which used 0.02 M PBS pH 7.4, 0.02 M PBS pH 5.5 and distilled water as dialyzed medium were  $25.51\% \pm 0.25$ ,  $22.87\% \pm 3.40$  and  $8.07 \pm 0.25\%$ , respectively. It was suggested that the presence of alkaline salt can improve the encapsulation efficiency especially in pH 7.4. The improvement may be yielded the solubility of drug in the inner core. The results are presented in Table 42.

**Table 41.** The percentage of drug loading corresponding to dialyzed medium (n=4).

DL (%)		
Sample	%DL	SD
Distilled water	5.06	0.89
0.02 M PBS pH 5.5	8.85	0.89
0.02 M PBS pH 7.4	11.57	1.17

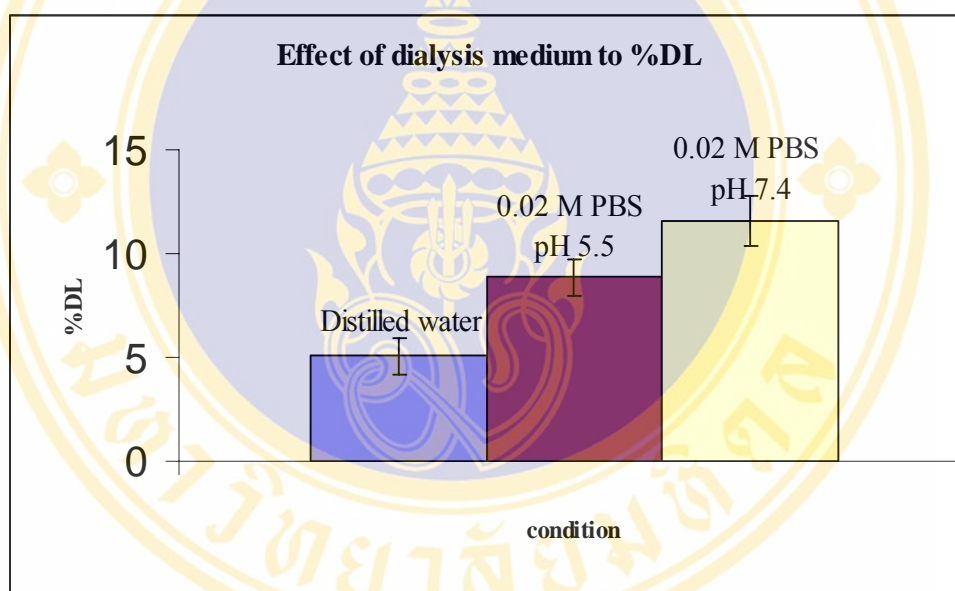


**Figure 39.** The percentage of drug loading corresponding to dialyzed medium, 0.02 M PBS pH 7.4, pH 5.5 and distilled water, respectively (n=4).

**Table 42.** The percentage of drug encapsulation efficiency corresponding to dialyzed medium (n=4).

DE (%)		
Sample	%DE	SD
Distilled water	8.07	0.25
0.02 M PBS pH 5.5	22.87	3.40
0.02 M PBS pH 7.4	25.51	0.92

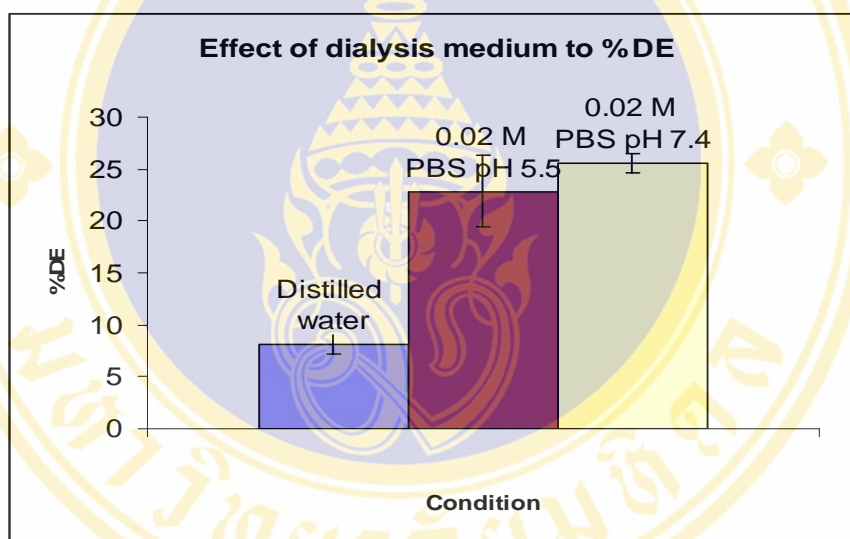


**Figure 40.** The percentage of drug encapsulation efficiency corresponding to dialyzed medium using 0.02 M PBS pH 7.4, pH 5.5 and distilled water, respectively (n=4).

### **6.2.3. Effect of the medium type to mean particle size.**

The largest particle size of developed formulations obtained from condition. This might be due to the aggregation particles or the swelling of the nanoparticles as confirmed by TEM. The composition of the copolymer consisting of chitosan and PEG can swell in the acid aqueous solution. When drug-loaded nanoparticles were prepared in 0.02 M PBS pH 7.4 or distilled water, the obtained particles size of drug-loaded nanoparticles from both conditions was not significantly different. The results are presented in Table 43 and Figure 41

### **6.2.4. Effect of the medium type to polydispersity index (PI).**

Table 44 and Figure 42 show that PI of drug-loaded nanoparticles using 0.02 M PBS pH 7.4 and pH 5.5 as dialyzed medium was  $0.54 \pm 0.03$  and  $0.55 \pm 0.04$ , respectively and was not significantly different ( $P > 0.05$ ). In contrast, the PI of drug-loaded nanoparticles using distilled water was  $0.43 \pm 0.04$ . The high PI of nanoparticles when using PBS at pH 5.5 solution as dialyzed medium may be related to the high degree of aggregation of the particles. In case of 0.02 M PBS pH 7.4, high PI cannot conclude.

### **6.2.5. Effect of the medium type to morphology.**

The morphology of nanoparticles prepared using various dialyzed medium in the preparation was showed in Figure 43 A-C. The degree of aggregation and the particle size of the nanoparticles showed the different depending on the type of dialyzed medium. The nanoparticles prepared from 0.02 M PBS pH 5.5 showed the higher degree of aggregation (Figure 19) as compared to that from distilled water and 0.02 M PBS pH 7.4. The particle size of nanoparticles obtained from 0.02 M PBS pH 7.4 as dialyzed medium showed the smallest with uniform size 50-70 nm. The use of distilled water as a dialyzed medium for preparing nanoparticles possessed the particle size in the range size of 80-250 nm whereas that of 0.02 M PBS pH 5.5 as a dialyzed medium provided broad particle size with 70-800 nm. As a result, it could be deduced that the pH of solution affected the particle size and the formation of nanospheres causing to increase degree of aggregation and size especially in low pH.

**Table 43.** Mean particle size of CLT-loaded nanoparticles corresponding to dialyzed medium. (n=12).

Mean particle size (nm)		
Sample	Mean particle size(nm )	SD
Distilled water	228.08	5.19
0.02 M PBS pH 5.5	964.50	18.76
0.02 M PBS pH 7.4	215.33	2.37

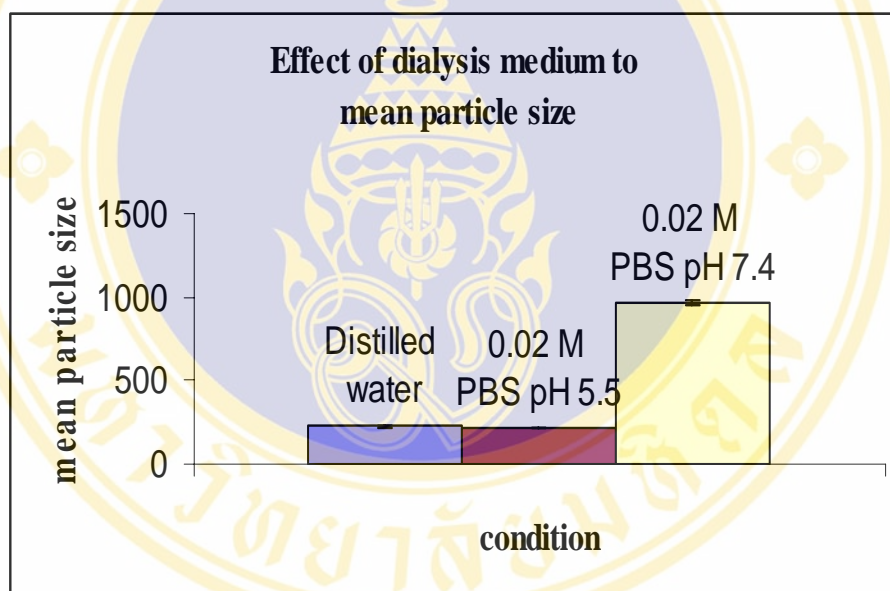


**Figure 41.** Mean particle size corresponding to dialyzed medium, 0.02 M PBS pH 7.4, pH 5.5 and distilled water, respectively (n=12).

**Table 44.** Polydispersity index (PI) of CLT-loaded nanoparticles corresponding to dialyzed medium (n=12).

Polydispersity index (PI)		
Sample	PI	SD
Distilled water	0.43	0.04
0.02 M PBS pH 5.5	0.55	0.04
0.02 M PBS pH 7.4	0.54	0.03

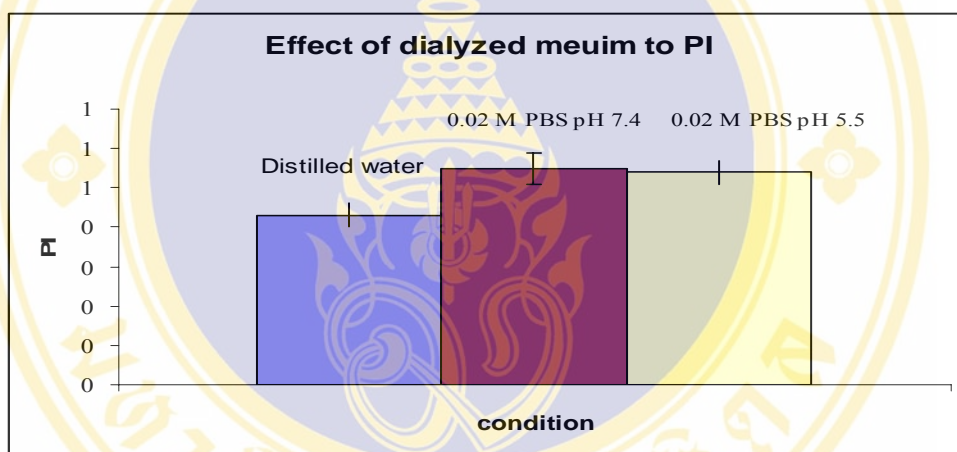


**Figure 42.** Polydispersity index corresponding to dialyzed medium, 0.02 M PBS pH 7.4, pH 5.5 and distilled water, respectively (n=12).

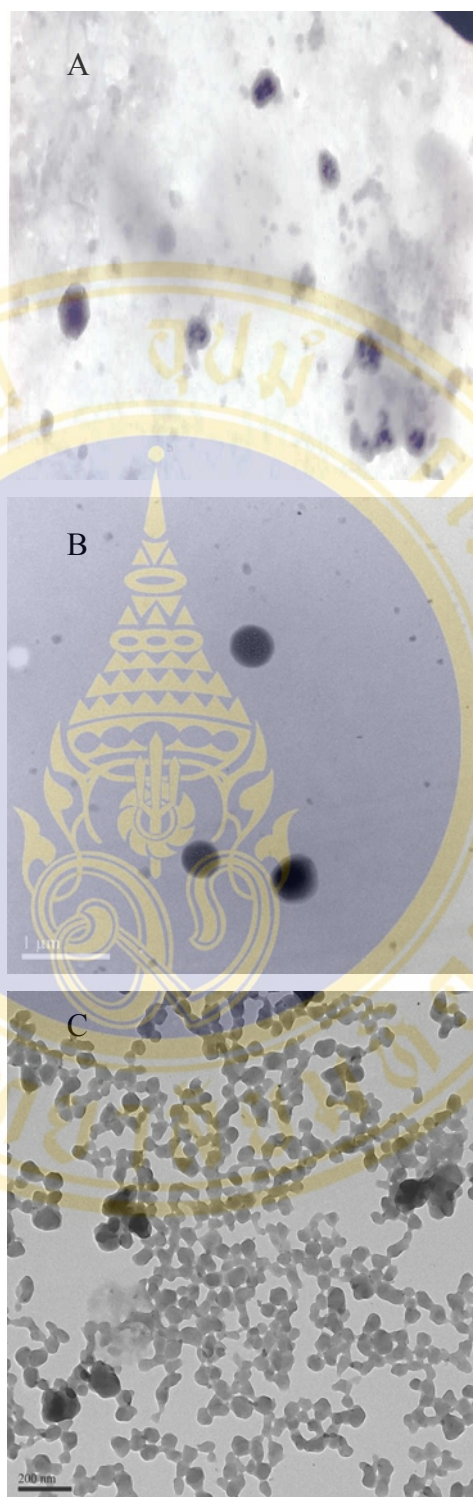


**Figure 43.** A-C show morphology of CLT-loaded nanoparticles which using distilled water, 0.02 M PBS pH 5.5, 0.02 M PBS pH 7.4 as dialyzed medium, respectively with constant stirring.

### **6.3. Effect of stirred and unstirred conditions on the characteristics of CLT-loaded nanoparticles.**

In this experiment, nanoparticles were prepared by using distilled water as a dialyzed medium with and without stirring. The percentage of drug encapsulation efficiency (%DE), the percentage of drug loading (%DL), the mean particle size and the PI of drug-loaded nanoparticles prepared without stirring were  $15.87 \pm 3.99\%$ ,  $9.84 \pm 2.514\%$ ,  $601.33 \pm 21.32$  nm, and  $0.35 \pm 0.04$ , respectively as shown in Table 45 whereas those prepared with stirring were  $8.07 \pm 0.25\%$ ,  $5.06 \pm 0.89\%$ ,  $215.08 \pm 2.79$  nm and  $0.43 \pm 0.33$ , respectively. Therefore, it could be concluded that the use of stirring affected the characteristics of obtained nanoparticles. Without stirring to prepare nanoparticles, DMF, which used to dissolve clotrimazole and polymer, diffused slowly from dialysis bag to dialyzed medium. The slow diffusion of DMF from dialysis bag to dialyzed medium might retard precipitation of clotrimazole; therefore, the higher clotrimazole encapsulation was obtained. The uniform size in the range of 250-300 nm with a lower PI could probably obtain from the appropriate ratio of copolymer and clotrimazole with the suitable condition, e.g. removing the organic solvent without stirring.

**Table 45.** Percentage of drug encapsulation efficiency, percentage drug loading, mean particle size and polydispersity index corresponding to non-using stirring and using stirring with dialysis against distilled water (n=4).

Parameter		
Parameter	non-use stirring	use stirring
%DE	15.87(3.99)	8.07 (0.25)
%DL	9.84 (2.51)	5.06 (0.89)
Mean particle size(nm)	601.33 (21.32)	215.08 (2.79)
PI	0.35 (0.04)	0.43 (0.33)

## CHAPTER V

### CONCLUSION

Colloid delivery system in the nanosize range can be made by using various copolymers. In the previous study, the nanoparticles prepared from *N*-phthanoyl chitosan grafted poly (ethylene glycol) methyl ether (mPEG) (PLC-*g*-mPEG) with sphere shape in aqueous solution were reported. So as to investigate the feasibility of such copolymer as a carrier drug for buccal system, clotrimazole which is hydrophobic drug, was selected as a model drug and was incorporated into nanoparticles made from PLC-*g*-mPEG. The CLT-loaded PLC-*g*-mPEG was prepared by dialysis method and afterwards it was characterized.

Dialysis method is one of nanoparticles preparation. Firstly, the drug was interacted with the polymer in the organic solvent (incubation procedure). Then, the mixed solution of both drug and polymer was contacted with the external phase. The organic solvent diffused into the external phase. Thus, the concentration of organic solvent in the inner phase decreased and the polymer concentration increased with time. At a certain time point, the polymer precipitated and encapsulated the drug and subsequently the nanoparticles were formed. The effect of using various types of external phases as a dialyzed medium on the characteristics of nanoparticles was evaluated.

In this study, *in vitro* drug release was investigated using Franz diffusion cells and concentration of clotrimazole in acceptor medium was analyzed by HPLC method. In the study, several factors affecting the characteristics of CLT-loaded PLC-*g*-mPEG based on dialysis method in terms of the morphology, percentage of encapsulation efficiency (%DE), percentage of drug loading (%DL), mean particle size with polydispersity index were elucidated.

The obtained results showed that the formation of nanoparticles was affected by dialyzed medium, stirring time, and initial drug loading as well as the degree of aggregation of CLT-loaded PLC-*g*-mPEG was observed.

1) The effect of dialyzed medium was following :

In case of using the 0.02 M PBS pH 7.4 aqueous solution as a dialyzed medium, the particle shape was spherical in the size range of 50-70 nm. The percentage of drug encapsulation efficiency (%DE) and the percentage of drug loading (%DL) were  $25.51 \pm 1.06\%$  and  $11.57 \pm 0.76\%$ , respectively.

In case of using the 0.02 M PBS pH 5.5 aqueous solution as a dialyzed medium, the particle shape was spherical with the wide range of particle size 70-800 nm. The %DE and %DL were  $22.55 \pm 3.74\%$  and  $8.85 \pm 0.12\%$ , respectively.

In case of using distilled water as a dialyzed medium, the particle shape was spherical with wide range of particle size 80-250 nm. The %DE and %DL were  $8.08 \pm 0.21\%$  and  $5.06 \pm 0.20\%$ , respectively.

The degree of aggregation observed by TEM was confirmed by the polydispersity index (PI) obtained from PCS. It was found that the degree of aggregation was affected by the presence of the salts in the dialyzed medium at pH 5.5 and the high PI was observed ( $0.55 \pm 0.04$ ). In addition, using 0.02 M PBS pH 7.4 as dialyzed medium showed high PI with  $0.54 \pm 0.03$ . However, the aggregation of particle did not observe. Concerning PI of CLT-loaded nanoparticles prepared by using distilled water as dialyzed medium, it showed the lowest PI with the value of  $0.43 \pm 0.03$ .

2) To investigate the effect of initial drug loading

CLT-loaded nanoparticles were prepared by without stirring and dialysis against distilled water. It was found that the percentage of initial drug loading to the copolymer was varying to 3%, 15%, 50%, and 100%, respectively. The results were found as a following:

The percentage of drug loading (%DL) did relatively increase from  $0.24 \pm 0.06\%$  to  $8.81 \pm 0.44\%$  when the percentage of initial drug loading to the copolymer was increased from 3% to 50%. However, the percentage of drug loading was not significant different between the percentage of initial drug loading from 50%-100%.

The drug encapsulation efficiency (%DE) did not relatively increase with increasing the percentage of initial drug loading to the copolymer. The results

showed that the 50% weight by weight of initial drug loading to the copolymer could be the optimized ratio.

The revealed particle size by TEM was not consistent to the mean particle size by PCS. By TEM, the observing of particle size was not significant different with increasing initial drug loading.

The degree of aggregation by TEM respected to polydispersity index by PCS, it was found that the degree of aggregation was increase with increase the initial drug loading. However, PI of initial drug loading between 15% and 50% was not significant different. So that, the increasing clotrimazole causing the aggregation of nanoparticles.

To investigate the effect of stirring condition, CLT-loaded nanoparticles were prepared by dialysis against stirring time was following :

In case of using without stirring for preparing, it was showed that spherical shape with the mean particle size of 150-300 nm and PI  $0.34 \pm 0.03$  were obtained. The %DE and %DL were  $15.87 \pm 3.99\%$  and  $9.84 \pm 2.51\%$ , respectively

Whereas, using constant stirring showed the lower of %DE ( $8.08 \pm 0.21\%$ ), %DL ( $5.06 \pm 0.20\%$ ), and wide range of the particle size with 80-250 nm causing higher PI  $0.43 \pm 0.33$ .

Additional, the reproducibility and sustained release property of CLT-loaded nanoparticles prepared by non-using stirring and dialysis against distilled water were evaluated by comparison the drug release profiles of different batches. The drug release profiles from three different batches of CLT-loaded nanoparticle showed the sustained release for 5 days (120 hours). All batches of the CLT-loaded nanoparticles showed reproducible of drug release more than 24 hours.

Conclusively, the preparation of CLT-loaded (PLC-g-mPEG) by dialysis method was affected by various parameters of preparation depending on the conditions in the preparation. The simple dialysis against distilled water was suitable for preparing CLT-loaded PLC-g-mPEG which particles in the nanosize range with sustained release property and reproducibility were obtained.

## REFERENCES

1. Lynch DP. Oral candidiasis. History, classification, and clinical presentation. *Oral Surg Oral Med Oral Pathol* 1994 Aug;78(2):189-93.
2. Patton LL, Bonito AJ, DA. S. A systematic review of the effectiveness of antifungal drugs for the prevention and treatment of oropharyngeal candidiasis in HIV-positive patients. *Oral Surg Oral Med Oral Pathol Oral Radiol Endod* 2001 Aug;92(2):170-9.
3. Hai-Quan M, Krishnendu R, L V. Chitosan-DNA nanoparticles as gene carriers: synthesis, characterization and transfection efficiency. *J Contr Rel* 2001;70:399-421.
4. Bravo-Osuna I, Vauthier<sup>a</sup>C, Farabollin A, Palmieri GF, Ponchel G. Mucoadhesion mechanism of chitosan and thiolated chitosan-poly(isobutyl cyanoacrylate) core-shell nanoparticles. *Biomater* 2007 May;28(13):2233-43
5. Pandey R, Ahmad Z, Sharma S. Nano-encapsulation of azole antifungals: potential applications to improve oral drug delivery. *Int J Pharm* 2005 Sep; 14; 301(1-2):268-76.
6. Kim K, Kwon S, Park JH. Physicochemical characterizations of self-assembled nanoparticles of glycol chitosan-deoxycholic acid conjugates. *Biomacromol* 2005;6:1154-1158.
7. Ning M, Guo Y, Pan H. Preparation and characterization of EP-liposomes and Span 40-niosomes. *Pharmazie* 2006 Mar;61(3):208-12.
8. Zhang C, Qineng P, Zhang H. Self-assembly and characterization of paclitaxel-loaded N-octyl-O-sulfate chitosan micellar system. *Colloids Surf B Biointerfaces* 2004 Nov;25;39(1-2):69-75.
9. Memisoglu E, Bochot A, Ozalp M. Direct formation of nanospheres from amphiphilic beta-cyclodextrin inclusion complexes. *Pharm Res* 2003 Jan;20(1):117-25.

10. Ponchel G, Montisci MJ, Dembri C. Mucoadhesion of colloidal particulate system in the gastro-intestinal tract. *Eur J Pharm Biopharm* 1997;44:25-31.
11. Genta I, Colonna C, Perugini P. Evaluation of bioadhesive performance of chitosan derivatives as film for buccal application. *J Drug Del Sci Tech* 2005;15(6):459-63.
12. Kast CE, Valenta C, Leopold M. Design and in vitro evaluation of a novel bioadhesive vaginal drug delivery system for clotrimazole. *J Contr Rel* 2002;81:347-54.
13. Fernandez-Urrusuno R, Calvo P, Remunan-Lopez C, Vila-Jato JL, Alonso MJ. Enhancement of nasal absorption of insulin using chitosan nanoparticles. *Pharm Res* 1999;16(10):1576-81.
14. Haas J, Ravi Kumar MN, Borchard G, Bakowsky U, Lehr CM. Preparation and characterization of chitosan and trimethyl-chitosan-modified poly-(epsilon-caprolactone) nanoparticles as DNA carriers. *AAPS Pharm Sci Tech* 2005;6(1):22-30.
15. Liu WG, Zhang X, Sun SJ, Sun GJ, Yao KD, Liang DC, et al. N-alkylated chitosan as a potential nonviral vector for gene transfection. *Bioconj Chem* 2003;14(4):782-9.
16. Kai E, Ochiya T. A method for oral DNA delivery with N-acetylated chitosan. *Pharm Res* 2004;21(5):838-43.
17. Park IK, Jiang HL, Cook SE, Cho MH, Kim SI, Jeong HJ, et al. Galactosylated chitosan (GC)-graft-poly(vinyl pyrrolidone) (PVP) as hepatocyte-targeting DNA carrier: in vitro transfection. *Arch Pharm Res* 2004;27(12):1284-9.
18. Son YJ, Jang JS, Cho YW, Chung H, Park RW, Kwon IC, et al. Biodistribution and anti-tumor efficacy of doxorubicin loaded glycol-chitosan nanoaggregates by EPR effect. *J Contr Rel* 2003;91(1-2):135-45.

19. Ohya Y, Takei T, Kobayashi H, Ouchi T. Release behaviour of 5-fluorouracil from chitosan-gel microspheres immobilizing 5-fluorouracil derivative coated with polysaccharides and their cell specific recognition. *J Microencapsul* 1993;10(1):1-9.
20. Yoksan R, Matsusaki M, Akashi M. Controlled hydrophobic/hydrophilic chitosan:colloid phenomena and nanosphere formation. *Colloids Polymer Sci.* 2004;282:337-42.
21. Kim JH, Kim YS, Kim S, Park JH, Kim K, Choi K, et al. Hydrophobically modified glycol chitosan nanoparticles as carriers for paclitaxel. *J Contr Rel* 2006;111(1-2):228-34.
22. Opanasopit P, Ngawhirunpat T, Chaidedgumjorn A, Rojanarata T, Apirakaramwong A, Phongying S, et al. Incorporation of camptothecin into N-phthaloyl chitosan-g-mPEG self-assembly micellar system. *Eur J Pharm Biopharm* 2006;64(3):269-76.
23. Mirowski GW, Hilton JF, Greenspan D. Association of cutaneous and oral diseases in HIV-infected men. *Oral Dis.* 1998 Mar;4(1):16-21.
24. Montvale NJ. *Medical Economics . Drug Topics Red Book* Medical Economics Company, Inc; 2000.
25. Speller DCE. *Antifungal chemotherapy*; 1980.
26. Rathbone MJ. *Oral Mucosal Drug Delivery*. Marcel Dekker Inc Newyork 1996.
27. Veuillez F, Kalia YN, Jacques Y. Factors and strategies for improving buccal absorption of peptides. *Eur J Pharm Biopharm* 2001;51(2):93-109.
28. Gandhi RB, JR. R. Oral cavity as a site for bioadhesive drug delivery. *Adv Drug Del Rev.* 1994;13(1-2):43-74.
29. Robinson JR, X. Y. Absorption enhancers. *Encyclopedia of Pharmaceutical Technology*; Marcel Dekker Inc Newyork. 1999;18:1-27.
30. Alur HH, Johnton TP, AK. M. Peptides and proteins: buccal absorption.
  - i. *Encyclopedia of Pharmaceutical Technology*; Marcel Dekker, Inc:
  - ii. New york. 2001;20:193-218.

31. Okamoto H, Taguchi H, K I. Development of polymer film dosage forms of lidocaine for buccal administration -I; Penetrate rate and release rate. *J Contr Rel.* 2001;77(3):253-60.
32. Nielsen HM, MR. R. Nicotine permeability across the buccal TR 146 cell culture model and porcine buccal mucosa in vitro:effect of pH and concentration. *Eur J Pharm Sci.* 2002;16(3):151-7.
33. Henningfield JE, Radzius A, Cooper TM. Drinking coffee and carbonated beverages blocks absorption of nicotine from nicotine polacrilex gum. *Jama.* 1990 Sep;264(12):1560-4.
34. Weatherell JA, Robinson C, BR N. Site-specific variations in the concentrations of substances in the mouth. *Br Dent J.* 1989 Oct;21;167(8):289-92.
35. Khanvilkar K, Donovan MD, DR. F. Drug transfer through mucus. *Adv Drug Deliv Rev.* 2001 Jun;11;48(2-3):173-93.
36. Zambaux MF, Bonneaux F, R G. Influence of experiment parameters on the characteristics of poly(lactic acid) nanoparticles prepared by a double emulsion method. *J Contr Rel* 1998;50: 31-40.
37. Vanthier C, Couvreur P. Development of polysaccharide nanoparticles as drug delivery systems. *Handbook of pharmaceutical controlled release technology*; Wise, Trantolo, Cihon, Inyang, Stottmeister, editors.; Chap. 21. New York: Marcel Dekker 2000:p.413-429.
38. Ibrahim H, Bindschaedler E, Doelker E. Aqueous nanodisperions by a salting-out process. *Int. J. Pharm.* 1992;87:239.
39. Bodmeier R, Chen HG, Paeratakul O. A novel approach to the oral delivery of micro- or nanoparticles. *Pharm Res* 1989;6(5):413-7.
40. Rajaonarivony M, Vauthier C, Couarraze G, Puisieux F, Couvreur P. Development of a new drug carrier made from alginate. *J Pharm Sci* 1993;82(9):912-7.
41. Fessi H, Devissaguet JP, Puisieux F. Procé'de' de préparation des systèmes colloïdaux dispersibles d'une substance sous forme de nanoparticules. *Fr. Patent Appli* 8,618,446 1986.
42. Taegarden DL, Baker DS. Practical aspects of lyophilization using non-aqueous co-solvent systems. *Eur J Pharm Sci* 2002;15:115-133.

43. Fournier E, Durfresne DC, M S. A novel one-step drug-loading procedure for water-soluble amphiphilic nanocarriers. *Pharm Res* 2004;21:962-968.
44. Kim SY, Shin IG, Lee YM, Cho CS, Sung YK. Methoxy poly(ethylene glycol) and epsilon-caprolactone amphiphilic block copolymeric micelle containing indomethacin. II. Micelle formation and drug release behaviours. *J Contr Rel* 1998;51(1):13-22.
45. Shin IG, Kim SY, Lee YM, Cho CS, Sung YK. Methoxy poly(ethylene glycol)/epsilon-caprolactone amphiphilic block copolymeric micelle containing indomethacin. I. Preparation and characterization. *J Contr Rel* 1998;51(1):1-11.
46. Liu SQ, Tong YW, Yang YY. Thermally sensitive micelles self-assembled from poly(N-isopropylacrylamide-co-N,N-dimethylacrylamide)-b-poly(D,L-lactide-c o-glycolide) for controlled delivery of paclitaxel. *Mol Biosyst* 2005;1(2):158-65.
47. Fattal E, Vauthier C. Nanoparticles as drug delivery systems. *Encyclopedia of Pharmaceutical Technology* 2002;p.1867.
48. Berthold A, Cremer K, J K. Preparation and characterization of chitosan microspheres as drug carrier for prednisolone sodium phosphate as model for antiinflammatory drugs. *J Contr Rel* 1996;39:17-25.
49. MacLaughlin FC, Mumper RJ, Wang J, Tagliaferri JM, Gill I, Hinchcliffe M, et al. Chitosan and depolymerized chitosan oligomers as condensing carriers for in vivo plasmid delivery. *J Contr Rel* 1998;56(1-3):259-72.
50. Lee KY, Ha WS, Park WH. Blood compatibility and biodegradability of partially N-acylated chitosan derivatives. *Biomater* 1995;16(16):1211-6.
51. Kurita K. Controlled functionalization of the polysaccharide chitin. *Prog. Polym. Sci.* 2001;26:1921-1971.
52. Van der Lubben IM, Verhoef JC, van Aelst AC, Borchard G, Junginger HE. Chitosan microparticles for oral vaccination: preparation, characterization and preliminary in vivo uptake studies in murine Peyer's patches. *Biomater* 2001;22(7):687-94.

53. Jane K, Alonson MJ. Depolymerized chitosan nanoparticles for protein delivery: preparation and characterization. *J Appl Polym Sci* 2003;88:2769-2766.
54. Jameela SR, Kumary TV, Lal AV, Jayakrishnan A. Progesterone-loaded chitosan microspheres: a long acting biodegradable controlled delivery system. *J Contr Rel* 1998;52(1-2):17-24.
55. Chandy T, Sharma CP. Chitosan--as a biomaterial. *Biomater Artif Cells Artif Organs* 1990;18(1):1-24.
56. David P, Manssur Y, S M. Unusual susceptibility of chitosan to enzymatic hydrolysis. *Carbohydr Res* 1992;237:325-332.
57. Varum KM, Myhr MM, Hjerde RJN. In vitro degradation rates of partially N-acetylated chitosans in human serum. *Carbohydr Res* 1997;299:99-101.
58. Shu XZ, Zhu KJ. A novel approach to prepare tripolyphosphate/chitosan complex beads for controlled release drug delivery. *Int J Pharm* 2000;201(1):51-8.
59. Calvo P, Remunan-Lopez C, Vila-Jato JL. Novel hydrophilic chitosan polyethylene oxide nanoparticles as protein carriers. *J Appl Polym Sci* 1997a;63:125-132.
60. Calvo P, Remunan-Lopez C, Vila-Jato JL. Development of positively charged colloidal drug carriers: chitosan-coated polyester nanocapsules and submicron-emulsions. *Colloids and Polym Sci* 1997b;275:46-53.
61. Fernandez-Urrusuno R, Romani D, Calvo P. Development of a freeze-dried formulation of insulin-loaded chitosan nanoparticles intended for nasal administration, S.T.P. *Pharm Sci* 1999;9:429-436.
62. Janes KA, Fresneau MP, Marazuela A, Fabra A, Alonso MJ. Chitosan nanoparticles as delivery systems for doxorubicin. *J Contr Rel* 2001;73(2-3):255-67.
63. Rosiak JM, Yoshii F. Hydrogels and their medical applications, Nuclear instruments and methods in. *Physics Research B* 1999;151:56-64.
64. Hoffman AS. Hydrogel for biomedical applications. *Adv Drug Del Rev* 2002;43:3-12.

65. Liu LS, Liu SQ, Ng SY. Controlled release of interleukin-2 for the tumor immunotherapy using chitosan/alginate porous microspheres. *J Contr Rel* 1997;43:65-74.
66. Leong KW, Mao HQ, Truong-Le VL, Roy K, Walsh SM, August JT. DNA-polycation nanospheres as non-viral gene delivery vehicles. *J Contr Rel* 1998;53(1-3):183-93.
67. Bartkowiak A, Hunkeler D. Carrageenan-oligochitosan microcapsules: optimization of the formation process(1). *Colloids Surf B Biointerf* 2001;21(4):285-298.
68. Ishii T, Okahata Y, Sato T. Mechanism of cell transfection with plasmid/chitosan complexes. *Biochim Biophys Acta* 2001;1514(1):51-64.
69. Remunan-Lopez C, Bodmeier R. Effect of formulation and process variables on the formation of chitosan-gelatin coacervates. *Int J Pharm* 1996;135:63-72.
70. Cui Z, Mumper RJ. Chitosan-based nanoparticles for topical genetic immunization. *J Contr Rel* 2001;75(3):409-19.
71. Hunter CA. The role of aromatic interactions in molecular recognition. *Chem Soc Rev* 1994;23:101-109.
72. Adams H, Blanco JL, Chessari G, Hunter CA, Low CM, Sanderson JM, et al. Quantitative determination of intermolecular interactions with fluorinated aromatic rings. *Chem* 2001;7(16):3494-503.
73. Sinnokrot MO, Valeev EF, Sherrill CD. Estimates of the ab initio limit for pi-pi interactions: the benzene dimer. *J Am Chem Soc* 2002;124(36):10887-93.
74. Meyer EA, Castellano RK, Diederich F. Interactions with aromatic rings in chemical and biological recognition. *Angew Chem Int Ed Engl* 2003;42(11):1210-50.
75. Cozzi F, Cinquini M, Annunziata R. Polar/ $\pi$  interactions between stacks aryls in 1,8-diarylnaphthalenes. *J Am Chem Soc* 1992;114:5729-5733.
76. Laatikainen R, Ratilainen J, Sebastian R. NMR study of aromatic-aromatic interactions for benzene and some other fundamental aromatic systems using alignment of aromatics in strong magnetic field. *J Am*

Chem Soc 1995;117:11006-11010.

77. Funasaki N, Nomura M, Ishikawa S. NMR chemical shift reference for binding constant determination in aqueous solutions. *J Phys Chem* 2001;105:7361-7365.
78. Atkins PW. *Physical chemistry*. Oxford; 1995.
79. Jung DM, de Ropp JS, Ebeler SE. Study of interactions between food phenolics and aromatic flavors using one- and two-dimensional (1)H NMR spectroscopy. *J Agric Food Chem* 2000;48(2):407-12.
80. Hanna M, Ashbaugh A. Nuclear magnetic resonance study of molecular complexes of 7,7,8,8-tetracyanoquinodimethane and aromatic donors. *J Phys Chem* 1964;68:811-816.
81. Rashkin MJ, Waters ML. Unexpected substituent effects in offset pi-pi stacked interactions in water. *J Am Chem Soc* 2002;124(9):1860-1.
82. Hunter CA, Sanders JK. The nature of  $\pi$ - $\pi$  interactions. *J Am Chem Soc* 1990;112:5525-5534.
83. Hobza P, Selzle HL, Schlag EW. Potential energy surface of the benzene dimer: Ab initio theoretical study. *J Am Chem Soc* 1994;3500-3506.
84. Cubberley MS, Iverson BL. (1)H NMR investigation of solvent effects in aromatic stacking interactions. *J Am Chem Soc* 2001;123(31):7560-3.
85. Battaglia MR, Buckingham AD, Williams JH. The electric quadrupole-moments of benzene and hexafluorobenzene. *Chem Phys Lett* 1981;78:420-423.
86. Nguyen JQ, Iverson BL. An amphiphilic folding molecule that undergoes an irreversible conformational change. *J Am Chem Soc* 1999;121:2639-2640.
87. LeDung P, Milas M, Rinando M. Water soluble derivatives obtained by controlled chemical modification of chitosans. *Charbohydr Polym* 1994;24:209-14.
88. Sieval AB, Thanou M, AF K. Preparation and NMR characterization of highly substituted N - trimethyl chitosan chloride. *Charbohydr Polym* 1998;36:157-65.

89. Muzzarelli RAA, Tanfani F, Emanuelli M. N-(carboxymethylidene) chitosans and N-(carboxymethyl) chitosan: novel chelating polyampholytes obtained from chitosans: novel chelating polyampholytes obtained from chitosan glycoxylyate. *Carbohydr Res.* 1982;107:199-214.
90. Saito H, Wu X, Harris J. Graft copolymer of poly (ethyleneglycol)(PEG) and chitosan. *Macromol Rapid Commun.* 1997;18:547-50.
91. Ohya Y, Cai R, Nishisawa H. Preparation of PEG-grafted chitosan nanoparticles as peptide drug carriers. *STP Pharma Science.* 2000;10:77-82.
92. Vangeyte S, Guatier R, Jerome. About the methods of preparation of poly(ethylene oxide)-b-poly(-capolactone) nanoparticles in water. *Colloids Surf* 2004;242:203-211.
93. Zhang L, Eisenberg A. Multiple morphology of "crew cut" aggregates of polystyrene-b-poly(acrylic acid) block copolymer. *Sci* 1995 ;268:1728-1731.
94. Barratt G. Characterization of colloidal drug carrier systems with zeta potential measurements. *Pharm Tech. Eur* 1999:25-32.
95. Li Y, Kwon GS. Micelle-like structures of poly(ethylene oxide)-*block*-poly(2-hydroxyethyl aspartamide)-methotrexate conjugates. *Colloid Surf B: Biointerfaces* 1999;16:217-226.
96. Li Y, Kwon GS. Methotrexate esters of poly(ethylene oxide)-*block*-poly(2-hydroxyethyl-L-aspartamide). Part I: Effects of the level of methotrexate conjugation on the stability of micelles and on drug release. *Pharm Res* 2000;17(5):607-11.
97. La SB, Okano T, Kataoka K. Preparation and characterization of the micelle-forming polymeric drug indomethacin-incorporated poly(ethylene oxide)-poly(beta-benzyl L-aspartate) block copolymer micelles. *J Pharm Sci* 1996;85(1):85-90.
98. Michelland S, Alonso MJ, Andremont A. Nanoparticles as carrier of antibiotic for intracellular antibiotherapy. *Int J Pharm* 1987.



## APPENDIX A

**Table 46.** Drug release profile of CLT-loaded PLC-g-mPEG batch 1 no.1

Time (hr)	Peak area	drug conc. (µg/ml)	drug content in 0.6 ml	drug content in 11ml	drug cont. existed in receptor (µg)	drug release content (µg)	cumulative content (µg)	%cumulative
0	0.00	0.00	0.00	0.00	0.00	0.00	0.00	0.00
1	0.00	0.00	0.00	0.00	0.00	0.00	0.00	0.00
2	0.00	0.00	0.00	0.00	0.00	0.00	0.00	0.00
3	4457	1.85	1.11	20.30	19.20	20.30	20.30	8.46
6	5349	2.41	1.45	26.55	25.11	7.36	27.66	11.53
12	15062	8.60	5.16	94.61	89.45	69.50	97.16	40.48
24	15556	8.92	5.35	98.07	92.72	8.62	105.78	44.08
48	20861	12.29	7.38	135.24	127.86	42.52	148.30	61.79
72	21026	12.40	7.44	136.39	128.95	8.53	156.84	65.35
120	20580	12.12	7.27	133.27	126.00	4.31	161.15	67.15

**Table 47.** Drug release profile of CLT-loaded PLC-g-mPEG batch 2 no.1

Time (hr)	Peak area	drug conc. (µg/ml)	drug content in 0.6 ml	drug content in 11.0ml	drug cont. existed in receptor(µg)	drug release content (µg)	cumulative content (µg)	%cumulative
0	0.00	0.00	0.00	0.00	0.00	0.00	0.00	0.00
1	0.00	0.00	0.00	0.00	0.00	0.00	0.00	0.00
2	0.00	0.00	0.00	0.00	0.00	0.00	0.00	0.00
3	0.00	0.00	0.00	0.00	0.00	0.00	0.00	0.00
6	1877	2.66	1.60	29.28	27.68	29.28	29.28	13.31
12	8327	7.21	4.33	79.36	75.03	47.35	76.63	34.83
24	11939	9.76	5.86	107.40	101.54	32.37	109.00	49.54
48	17020	13.35	8.01	146.85	138.84	45.31	154.31	70.14
72	16368	12.89	7.73	141.79	134.05	2.95	157.25	71.48
120	16340	12.87	7.72	141.57	133.85	7.52	164.77	74.90

**Table 48.** Drug release profile of CLT-loaded PLC-g-mPEG batch 2 no.2

Time (hr)	Peak area	drug conc. (µg/ml)	drug content in 0.6 ml	drug content in 11.0ml	drug cont. existed in receptor(µg)	drug release content (µg)	cumulative content (µg)	%cumulative
0	0.00	0.00	0.00	0.00	0.00	0.00	0.00	0.00
1	0.00	0.00	0.00	0.00	0.00	0.00	0.00	0.00
2	0.00	0.00	0.00	0.00	0.00	0.00	0.00	0.00
3	0.00	0.00	0.00	0.00	0.00	0.00	0.00	0.00
6	2307	2.97	1.78	32.62	30.84	34.10	34.10	15.50
12	8526	7.35	4.41	80.90	76.49	48.28	82.38	37.45
24	12510	10.17	6.10	111.83	99.69	35.34	117.73	53.51
48	16995	13.33	8.00	146.66	138.66	46.96	164.69	74.86
72	16025	12.65	7.59	139.13	131.54	0.47	165.16	75.07
120	15429	12.23	7.34	134.50	127.16	2.96	168.12	76.42

**Table 49.** Drug release profile of CLT-loaded PLC-g-mPEG batch 3 no.1

Time (hr)	Peak area	drug conc. (µg/ml)	drug content in 0.6 ml	drug content in 11.5 ml	drug cont. existed in receptor(µg)	drug release content (µg)	cumulative content (µg)	%cumulative
0	0.00	0.00	0.00	0.00	0.00	0.00	0.00	0.00
1	0.00	0.00	0.00	0.00	0.00	0.00	0.00	0.00
2	3034	0.94	0.56	10.80	10.24	10.8	10.8	3.27
3	7075	3.51	2.11	40.40	38.30	30.16	40.96	12.41
4	10092	5.44	3.26	62.50	59.24	24.21	65.17	19.75
5	11660	6.43	3.86	73.99	70.13	14.75	79.92	24.22
6	15034	8.58	5.15	98.70	93.55	28.57	108.49	32.88
9	20937	12.34	7.41	141.94	134.54	48.39	156.88	47.54
12	23393	13.91	8.34	159.93	151.59	25.40	182.27	55.23
24	24682	14.73	8.84	169.37	160.54	17.79	200.06	60.62
36	26733	16.03	9.62	184.4	174.77	23.86	223.92	67.85
48	21305	12.58	7.55	144.64	137.09	-30.14	193.78	58.72
72	20085	11.80	7.08	135.7	128.62	-1.39	192.39	58.3
120	20039	11.77	7.06	135.36	128.30	6.74	199.14	60.34

**Table 50.** Drug release profile of CLT-loaded PLC-g-mPEG batch 3 no.2

Time (hr)	Peak area	drug conc. (µg/ml)	drug content in 0.6 ml	drug content in 11.0ml	drug cont. existed in receptor (µg)	drug release content (µg)	cumulative content (µg)	%cumulative
0	0.00	0.00	0.00	0.00	0.00	0.00	0.00	0.00
1	0.00	0.00	0.00	0.00	0.00	0.00	0.00	0.00
2	2557	0.64	6.99	6.61	6.99	6.99	6.99	2.12
3	5948	2.80	30.75	29.07	24.14	31.13	31.13	9.43
4	10659	5.80	63.76	60.28	34.68	65.81	65.81	19.94
5	14864	8.47	93.22	88.14	32.94	98.75	98.75	29.93
6	16263	9.37	103.02	97.40	14.89	113.64	113.64	34.44
9	20861	12.29	135.24	127.86	37.83	151.48	151.48	45.9
12	25579	15.3	168.29	159.11	40.43	191.91	191.91	58.15
24	27100	16.27	178.95	169.19	19.84	211.74	211.74	64.16
36	26251	15.73	173.00	163.56	3.81	215.56	215.56	65.32
48	22113	13.09	144.01	136.15	-19.56	196.00	196.00	59.39
72	23838	14.19	156.09	147.58	19.94	215.94	215.94	65.44
120	20709	12.20	134.17	126.85	-13.41	202.53	202.53	61.37

**Table 51.** Percentage of drug loading (%DL) corresponding to percentage of initial drug loading to the copolymer

Percentage of initial drug loading Peak areas	100%		50%		15%		3%	
	no.1	no.2	no.1	no.2	no.1	no.2	no.1	no.2
Peak area in 1 <sup>st</sup> extract	387856	365070	431017	458214	32538	31586	11574	13704
Peak area in 2 <sup>nd</sup> extract	25377	17514	31064	37664	-	-	-	-
Peak area in 3 <sup>rd</sup> extract	-	-	-	-	-	-	-	-
Sum	413233	382584	465936	500274	32538	31586	11574	13704
Clotrimazole concentration. (µg/ml)	262.21	242.69	295.78	317.65	19.73	19.13	6.38	7.74
Dilution factor	1.00	1.00	0.50	0.50	0.25	0.25	1.00	1.00
Drug content (µg)	262.21	242.69	147.89	158.83	4.93	4.78	6.38	7.74
Wt.of drug load nanoparticles (µg)	2500.00	2750.00	1740.00	1740.00	450.00	410.00	3200.00	2700.00
%DL	10.49	8.83	8.50	9.13	1.10	1.17	0.20	0.29
	average (µg) = 9.66		average (µg) = 8.81		average (µg) = 1.13		average (µg) = 0.24	
	SD = 1.18		SD = 0.44		SD = 0.05		SD = 0.06	

**Table 52.** Percentage of drug encapsulation efficiency (%DE) corresponding to percentage of initial drug loading to the copolymer

Percentage of initial drug loading	100%		50%		15%		3%	
	no.1	no.2	no.1	no.2	no.1	no.2	no.1	no.2
Peak areas								
Peak area in 1 <sup>st</sup> extract	53561	45169	72567	73153	4733	4566	11574	13704
Peak area in 2 <sup>nd</sup> extract	6749	5416	3777	2070	7909	8056	-	-
Peak area in 3 <sup>rd</sup> extract	-	-	-	-	-	-	-	-
Sum	60310	50585	76344	75223	12642	12622	11574	13704
Clotrimazole con. (µg/ml)	37.42	31.23	47.63	46.92	7.06	7.05	6.38	7.74
Dilution factor	50	50	20	20	20	20	4	4
Drug content (µg)	1871.05	1561.34	952.68	938.39	141.18	140.93	25.52	30.94
Initial drug load (µg)	16240.00	16240.00	8120.00	8120.00	2420.00	2420.00	410.00	410.00
%DE	11.52	9.61	11.73	11.56	5.83	5.82	6.22	7.55
	average (µg) = 10.57		average (µg) = 11.64		average (µg) = 5.83		average (µg) = 6.89	
	SD = 1.35		SD = 0.12		SD = 0.01		SD = 0.94	

**Table 53.** Percentage of drug encapsulation efficiency (%DE) of CLT-loaded nanoparticles which were prepared by dialysis against distilled water with constant stirring

Sample	Batch 1 no.1	Batch 1 no.2	Batch 2 no.1	Batch 2 no.2
Peak area				
Peak area in 1 <sup>st</sup> extract	29112	27969	70474	72500
Peak area in 2 <sup>nd</sup> extract	-	-	-	-
Peak area in 3 <sup>rd</sup> extract	-	-	-	-
Sum	29112	27969	70474	72500
Clotrimazolecon.(µg/ml)	17.55	16.82	43.89	45.19
Dilution factor	35	35	15	15
Drug content (µg)	614.24	588.76	658.42	677.78
Initial drug loaded(µg)	7610	7610	8120	8120
%DE	8.07	7.74	8.11	8.35
	Average (µg) = 7.90		Average (µg) = 8.23	
	SD = 0.24		SD = 0.17	

**Table 54.** Percentage of drug encapsulation efficiency (%DE) of CLT-loaded nanoparticles which were prepared dialysis against 0.02 M PBS pH 5.5 aqueous solution with constant stirring

Sample	Batch 1 no.1	Batch 1 no.2	Batch 2 no.1	Batch 2 no.2
Peak area				
Peak area in 1 <sup>st</sup> extract	306645	312542	232031	Nd
Peak area in 2 <sup>nd</sup> extract	-	-	268677	Nd
Peak area in 3 <sup>rd</sup> extract	-	-	204670	Nd
Sum	306645	312542	705378	Nd
Clotrimazole concentration.(µg/ml)	194.32	198.08	448.29	Nd
Dilution factor	8.33	8.33	5	Nd
Drug content (µg)	1619.35	1649.99	2241.46	Nd
Initial drug loaded(µg)	8020	8020	8350	Nd
%DE	Average (µg) = 8.85			
	SD = 0.89			

**Table 55.** Percentage of drug encapsulation efficiency (%DE) of CLT-loaded nanoparticles which were prepared dialysis against 0.02 M PBS pH 7.4 aqueous solution with constant stirring.

Sample	Batch 1 no.1	Batch 1 no.2	Batch 2 no.1	Batch 2 no.2
Peak area				
Peak area in 1 <sup>st</sup> extract	123046	113780	84635	110322
Peak area in 2 <sup>nd</sup> extract	22280	38789	72241	36371
Peak area in 3 <sup>rd</sup> extract	-	-	-	-
Sum	145326	152569	156876	146693
Clotrimazole con.(µg/ml)	91.57	96.18	98.93	92.44
Dilution factor	20	20	20	20
Drug content (µg)	1831.43	1923.69	1978.56	1848.84
Initial drug loaded(µg)	7430	7430	7430	7430
%DE	24.65	25.89	26.63	24.88
	Average = 25.27			
	SD = 0.88			
	Average = 25.76			SD = 1.23

**Table 56.** Percentage of drug loading (%DL) of CLT-loaded nanoparticles which were prepared dialysis against distilled water with constant stirring

Sample	Batch 1 no.1	Batch 1 no.2	Batch 2 no.1	Batch 2 no.2
Peak area				
Peak area in 1 <sup>st</sup> extract	29112	27969	70474	72500
Peak area in 2 <sup>nd</sup> extract	-	-	-	-
Peak area in 3 <sup>rd</sup> extract	-	-	-	-
Sum	29112	27969	70474	72500
Clotrimazole con.(µg/ml)	17.55	16.82	43.89	45.19
Dilution factor	5	5	3	3
Drug content (µg)	87.75	84.11	131.68	135.56
Wt. of drug-loaded nanoparticles (µg)	2000	2000	2200	2400
%DL	4.39	4.21	5.99	5.65
	Average = 4.30			
	SD = 0.13			
				Average = 5.82
				SD = 0.24

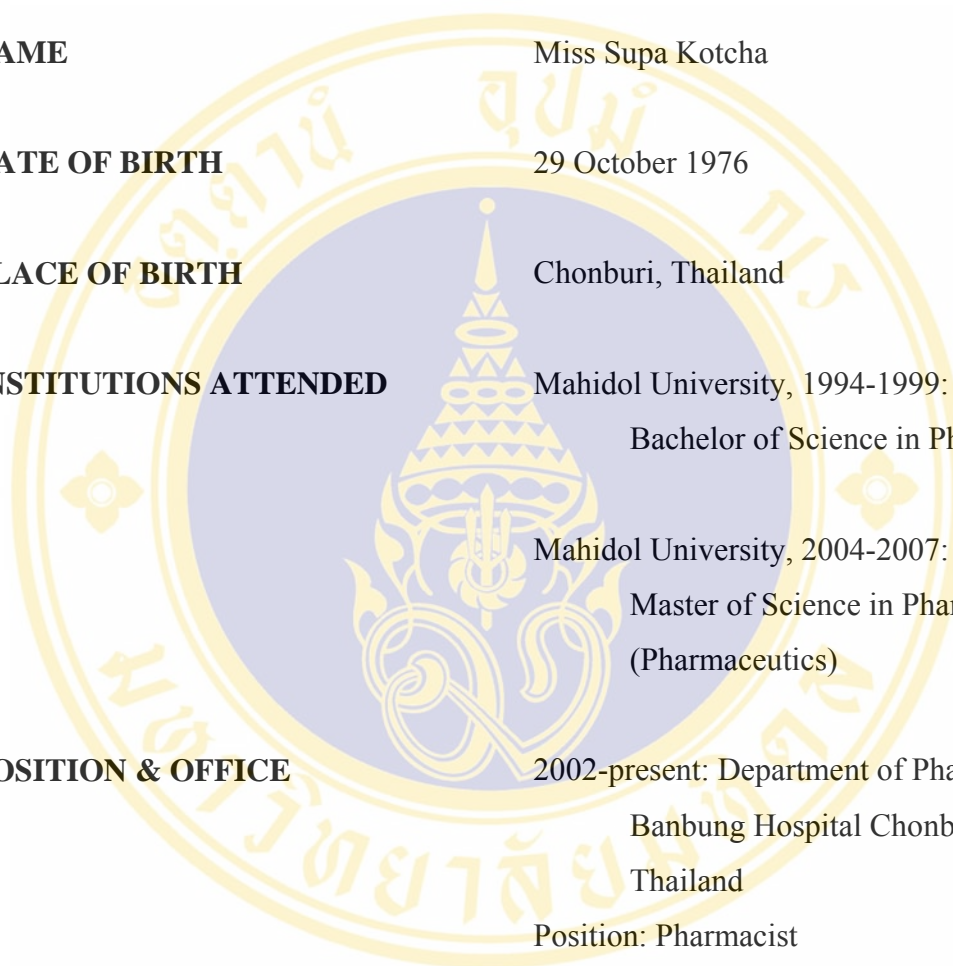
**Table 57.** Percentage of drug loading (%DL) of CLT-loaded nanoparticles which were prepared dialysis against 0.02 M PBS pH 5.5 aqueous with constant stirring

Sample	Batch 1 no.1	Batch 1 no.2	Batch 2 no.1	Batch 2 no.2
Peak area				
Peak area in 1 <sup>st</sup> extract	306645	312542	276583	265782
Peak area in 2 <sup>nd</sup> extract	-	-	-	-
Peak area in 3 <sup>rd</sup> extract	-	-	-	-
Sum	306645	312542	276583	265782
Clotrimazole con.(µg/ml)	194.32	198.08	175.17	168.29
Dilution factor	1	1	1	1
Drug content (µg)	194.32	198.08	175.17	168.29
Wt. of 1 drug-loaded nanoparticles(µg)	2040	2040	2150	2100
%DL	9.53	9.71	8.15	8.01
	Average = 9.62			
	SD = 0.13			
	Average = 8.08			
	SD = 0.09			

**Table 58.** Percentage of drug loading (%DL) of CLT-loaded nanoparticles which were prepared dialysis against 0.02 M PBS pH 7.4 aqueous with constant stirring

Sample	Batch 1 no.1	Batch 1 no.2	Batch 2 no.1	Batch 2 no.2
Peak area				
Peak area in 1 <sup>st</sup> extract	411658	424017	581360	463703
Peak area in 2 <sup>nd</sup> extract	12743	13502	24205	18322
Peak area in 3 <sup>rd</sup> extract	-	-	-	-
Sum	424401	437519	605565	482025
Clotrimazole con.(µg/ml)	269.33	277.68	384.72	306.03
Dilution factor	1	1	1	1
Drug content (µg)	269.33	277.68	384.72	306.03
Wt of drug loaded-nanoparticles (µg)	2520	2540	2900	2690
%DL	10.69	10.93	13.27	11.38
	Average = 10.81		Average = 12.32	
	SD = 0.17		SD = 1.34	

## BIOGRAPHY



<b>NAME</b>	Miss Supa Kotcha
<b>DATE OF BIRTH</b>	29 October 1976
<b>PLACE OF BIRTH</b>	Chonburi, Thailand
<b>INSTITUTIONS ATTENDED</b>	Mahidol University, 1994-1999: Bachelor of Science in Pharmacy  Mahidol University, 2004-2007: Master of Science in Pharmacy (Pharmaceutics)
<b>POSITION &amp; OFFICE</b>	2002-present: Department of Pharmacy, Banbung Hospital Chonburi, Thailand Position: Pharmacist
<b>HOME ADDRESS</b>	159/13 Sukumvit Rd., Soi 2, Tumbon Bansai, Ampur Muang, Chonburi, Thailand 41000 E-mail: Supa_95@hotmail.com